From the Institut für Klinische Molekularbiologie

(Directors: Prof. Dr. med. Stefan Schreiber, Prof. Dr. med. Philip Rosenstiel, Prof. Dr. rer. nat. Andre Franke)

at the University Medical Center Schleswig-Holstein, Campus Kiel

at Christian-Albrechts-Universität zu Kiel - Kiel University

Epithelial endoplasmic reticulum stress predisposes for CMV infection by suppression of cGAS/STING/type I interferon - signalling

Dissertation

to acquire the doctoral degree (Dr. med.)

at the Faculty of Medicine

at Kiel University

presented by

Felix Wottawa

from **Kiel**

Kiel, 2023

1st examiner: Prof. Dr. med. Konrad Aden

2nd examiner: Prof. Dr. rer. nat. Robert Häsler

Date of oral examination: 10.01.2023

Approved for printing: Kiel, 23.08.2022

Signed:

_____

(Chair of examination committee)

Parts of this doctoral thesis are published in the following publications:

1. **Wottawa, F.**; Bordoni, D.; Baran, N.; Rosenstiel, P.; Aden, K. The role of cGAS/STING in intestinal immunity. *European Journal of Immunology* **2021**, 51 (4), 785–797. https://doi.org/10.1002/eji.202048777.
2. Stengel, S. T.; Fazio, A.; Lipinski, S.; Jahn, M. T.; Aden, K.; Ito, G.; **Wottawa, F.**; Kuiper, J. W. P.; Coleman, O. I.; Tran, F.; Bordoni, D.; Bernardes, J. P.; Jentzsch, M.; Luzius, A.; Bierwirth, S.; Messner, B.; Henning, A.; Welz, L.; Kakavand, N.; Falk-Paulsen, M.; Imm, S.; Hinrichsen, F.; Zilbauer, M.; Schreiber, S.; Kaser, A.; Blumberg, R.; Haller, D.; Rosenstiel, P. Activating Transcription Factor 6 Mediates Inflammatory Signals in Intestinal Epithelial Cells Upon Endoplasmic Reticulum Stress. *Gastroenterology* **2020**, S0016508520349246. https://doi.org/10.1053/j.gastro.2020.06.088.

Table of contents

List of abbreviations

AGS ..... Aicardi - Gourtières syndrome
AIM2 ..... Absent in melanoma 2
AMPs ..... Anti - microbial peptides
ATF4 ..... Activating transcription factor 4
ATF6α ..... activating transcription factor 6α, activating transcription factor 6α
ATG ..... Autophagy - related protein
ATG16L1 ..... Autophagy-related 16-like 1
BafA, BafA1 ..... Bafilomycin A1
Bax ..... B-cell lymphome 2 – associated X protein
BiP ..... Binding immunoglobulin protein
BSA ..... Bovine serum albumin
CD ..... Crohn's disease
cDNA ..... complementary DNA
cGAMP ..... cyclic guanosine monophosphate adenosine monophosphate
cGAS ..... Cyclic GMP-AMP synthase
CHOP ..... C/EBP homologous protein
CMV ..... Cytomegalovirus
CR ..... conventionally - raised
CXCL10 ..... C-X-C motif chemokine 10
DAMP ..... danger – associated molecular pattern
DMSO ..... Dimethylsulfoxid
DNAJC3 ..... DnaJ homolog subfamily C member 3, syn: p58
dsDNA ..... double - stranded DNA
DSS ..... Dextransodiumsulfate
DTT ..... Dithiothreitol
E. coli ..... *Escherichia coli*
EGF ..... Epidermal growth factor
eIF2α ..... Eukaryotic translation initiation factor 2α
ENR ..... EGF - Noggin - R-Spondin 1
ER ..... Endoplasmic reticulum
ER - stress ..... Endoplasmic reticulum stress
ERAD ..... ER - associated degradation
GF ..... Germ -free
GRP78 ..... Glucose-Regulated Protein, 78kDa
GRP94 ..... Glucose-regulated protein 94, syn.: HSP90B1
GWAS ..... Genome wide association study
HSPA5 ..... Heat - shock protein family A member 5
IBD ..... Inflammatory bowel disease
IFIT1 ..... Interferon Induced Protein With Tetratricopeptide Repeats 1
IFIT3 ..... Interferon Induced Protein With Tetratricopeptide Repeats 3
IFN ..... Interferon
IFNAR1 ..... Interferon alpha and beta receptor subunit 1

IFNAR2 ..... Interferon alpha and beta receptor subunit 2
IFNβ ..... Interferon β
IL ..... Interleukin
IRE1α ..... inositol-requiring enzyme 1α
IRF3 ..... Interferon regulatory factor 3, Interferon regulatory factor 3
IRF7 ..... Interferon-regulating factor 7
ISC ..... Intestinal stem cell
ISG ..... Interferon - stimulated gene
JAK ..... Janus kinase
L. monocytogenes ..... *Listeria monocytogenes*
LC3 ..... Microtubule-associated protein 1 light chain 3
LPS ..... Lipopolysaccharide
mCMV ..... murine cytomegalovirus
MEF ..... Mouse embryonic fibroblast
MLKL ..... *Mixed lineage kinase domain-like protein*
NBR1 ..... Neighbor of BRCA1 gene 1 protein
NDP52 ..... Nuclear dot protein 52
NFDM ..... Non-fat dry mild
NFκB ..... nuclear factor 'kappa-light-chain-enhancer' of activated B-cells
NOD2 ..... Nucleotide Binding Oligomerization Domain Containing 2
OMM ..... Oligo - mouse - microbiota
p62 ..... Sequestome 1, protein 62
PAMP ..... pathogen – associated molecular pattern
PBS ..... Phosphate - buffered saline
PERK ..... PKR-like ER kinase
PI ..... Propidiumiodide
PI3 ..... phosphatidylinositol-3-phosphate
PI3K ..... class III phosphatidylinositol-3-OH kinase
PRR ..... Pattern - recognition - receptor
q-RT-PCR ..... quantitative real-time PCR
RIDD ..... Regulated IRE1α-dependent decay of mRNA
RIPK3 ..... Receptor-interacting serine/threonine-protein kinase 3
S1P ..... Site 1 protease
S2P ..... Site 2 protease
SAR ..... Selective autophagy receptor
SAVI ..... STING - associated vasculopathy with onset in infancy
SDS ..... Sodiumdodecylsulfate
SI ..... Small intestine
siRNA ..... Small interfering RNA
STAT ..... Signal transducer and activator of transcription
STING ..... Stimulator of Interferon Genes
T300A ..... Threonine to alanine at position 300
Tax1BP1 ..... Tax1 Binding Protein 1
TBK1 ..... Tank-binding-kinase 1
TEMED ..... Tetramethylethylenediamine

TFF3.....trefoil factor 3
TLR.....Toll - like receptor
TLR9.....Toll - like - receptor 9
TNFα.....Tumor necrosis factor alpha
TRAPβ..... translocon – associated protein β
TRIF ..... TIR-domain containing adapter inducing interferon β
UC.....Ulcerative Colitis
ULK1 ..... Unc-51 like autophagy activating kinase
UPR.....Unfolded protein response
XBP1 ..... X-box binding protein 1
*XBP1*s .....XBP1 spliced
*XBP1*u ..... XBP1 unspliced

List of figures

List of tables

1 Introduction

This study was designed to investigate the function and regulation of a specific innate immune pathway, cGAS/STING, in the intestinal epithelium. In detail the aim of the study was to test the hypothesis that endoplasmic reticulum stress, a molecular hallmark of IBD, is crucially interconnected with cGAS/STING function and that a dysregulation of these two pathways critically contributes to the pathophysiology of inflammatory bowel disease. With this in mind, all experiments were designed in order to work towards its role in gastrointestinal immunity with a focus on intestinal inflammation.

The introduction will first cover basic features of inflammatory bowel disease and the biology of the intestinal epithelium necessary to understand the experimental approach later on, and then proceed to introducing the current understanding of the above mentioned signalling pathway in order to depict the rationale behind this study.

1.1 Inflammatory bowel disease

Inflammatory bowel disease (IBD), comprising Ulcerative Colitis (UC) and Crohn's Disease (CD) as the two main entities, are chronic-relapsing inflammatory diseases affecting mainly the gastrointestinal tract, but also presenting with extraintestinal manifestations. IBD usually progress as an alternation of acute episodes and symptom-free intervals[1,2].

1.1.1 Clinical features

Common features of acute episodes can include abdominal pain, diarrhoea, gastrointestinal bleedings, anaemia, fever and immunosuppression. The individual clinical phenotype is very heterogeneous though[3]. Both forms have a progressive-destructive character, eventually leading to severe complications such as stenoses, abscesses, fistulas or colitis-associated neoplasia, frequently resulting in necessity for surgical treatment[1,2]. CD involves discontinuous transmural inflammation which can occur throughout the entire gastrointestinal tract, however typically affecting the terminal ileum and the perianal region[3]. UC on the other hand manifests into a continuous, mucosal inflammation restricted to the colon, occasionally including inflammation extending to the terminal ileum too[3].

1.1.2 Epidemiology

Although IBD prevalence varies considerably around the globe with highest prevalence among the Western countries such as Canada or Northern Europe, IBD affects roughly 0,5 % of the general population[4]. The incidence of IBD in newly industrialized nations is however still steeply rising[4]. It is

estimated that by 2025, IBD prevalence in those countries might have a reached a similar level as in Western countries[5]. In addition, IBD affects patients mainly from the second to fourth decade of life, having an impact on one's most productive years, and despite remarkable advances in therapy, IBD still remains a severe disease that comes with great morbidity[6], emphasizing the huge cost of IBD not only to the individual, but also to society and health care[4,7].

1.1.3 Pathophysiology

IBD pathophysiology is characterized by a complex interaction of genetic predisposition, environmental risk factors, disturbed microbial ecology and immune dysregulation[8], which still remains to be fully understood. A common way to think of IBD pathophysiology is as a dysregulated, overshooting **immune response**, i.e. inflammation, in response to commensal or pathogenic **microbes**

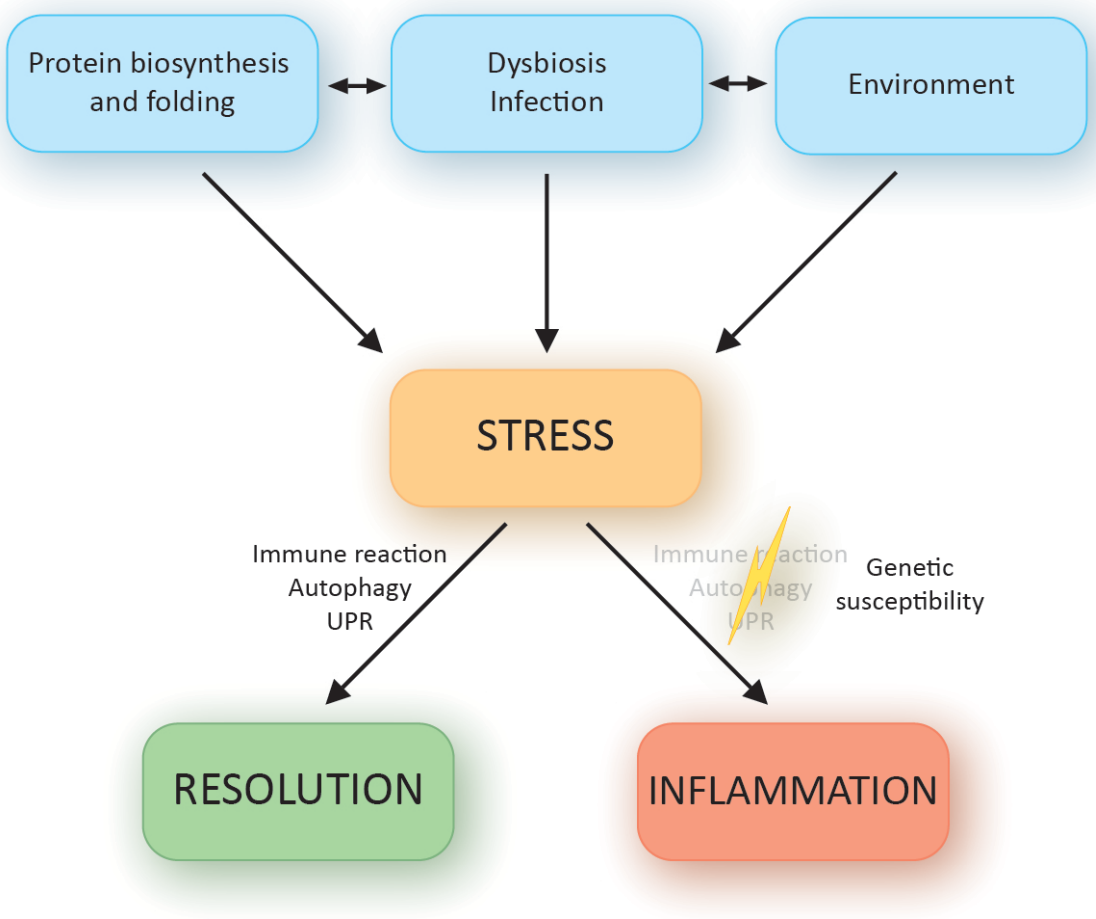

Figure 1-1: Model of IBD pathophysiology

Various highly co-dependent stressors induce intestinal inflammation if stress resolution fails due to individual genetic susceptibility. Otherwise, i.e. in a healthy state, stress would be eased via pathways such as the unfolded protein response (UPR), autophagy or immune reactions.

enabled by individual **genetic susceptibility** leading to defective stress resolution, thus lower resilience, triggered and exacerbated by **environmental** stress factors[9] (Figure 1-1).

1.1.3.1 Genetic susceptibility and heritability

IBD is a polygenetic disease. High disease concordance rates in monozygotic twins suggest that genetic susceptibility accounts for up to 50 % of disease risk for CD, while for UC the heritable risk is lower and estimated to be around 16 %[10]. Early-onset IBD shows high rates of family history and has additionally shaped the idea of a strong genetic contribution to IBD[11]. This has led to large-scale genome wide association studies (GWAS) attempting to identify gene variants responsible for such heritability phenomenons.

In 2001, the first gene variant conferring risk for IBD has been described with the discovery of a mutation in the *Nucleotide Binding Oligomerization Domain Containing 2* (*NOD2)* gene which is associated with CD[12]. *NOD2* encodes for a pattern - recognition-receptor that recognizes bacterial and viral components and is involved in mucosal immune defense[13]. Since then, a broad number of 163 IBD-associated loci has been identified, of which a vast majority is shared between CD and UC with roughly a third being specific for either one, such as *Autophagy - related 16 - like 1* (*ATG16L1*) or *NOD2*[14]. Of those 163 loci, associations with other inflammatory conditions point towards a possible mechanism how those gene variants result in heightened disease risk. For example, a remarkable number of IBD loci is shared with genes known to be causative for primary immunodeficiencies, characterized by severe infections, or genes predisposing for mycobacterial infection[14].

Mechanistically, gene ontology analysis has shown enrichment of IBD loci in gene ontology terms involved in immune reactions, such as regulation of cytokine production, response to molecules of bacterial origin or the JAK-STAT (Janus kinase-signal transducer and activator of transcription) signalling pathway, which is a key signal transduction pathway for e.g. cytokine induction and release[14].

The discovery of *NOD2* has highlighted the implication of microbe sensing and epithelial defence in IBD pathophysiology. Disease susceptibility conferred by *NOD2* variants is higher than of any other risk gene[15]. Thus, a lot of effort has been put into research on loci linked to antimicrobial defence. When GWAS additionally identified novel, previously unsuspected disease-associated pathways such as autophagy[16–18] or the unfolded protein response (UPR)[19–22], many studies followed investigating the interplay of autophagy, the UPR and bacterial sensing pathways.

Autophagy (from the ancient greek word “autóphagos”, “self-devouring”) refers to cellular pathways involved in delivering cytosolic components or organelles to the lysosome and subsequent degradation or recycling[23] (for more detailed information, also see 1.2.3, p. 11, on autophagy in general). Among a variety of conditions of cellular stress, autophagy is also engaged upon intracellular infection (a process termed xenophagy, from the greek word “xénos“ for “strange, foreign”) and helps to trap and kill intracellular pathogens, which is explicitly important for antibacterial defence in the gut mucosa[24–27],

suggesting a possible pathomechanism explaining the association of autophagy to IBD. *NOD2* for example recruits the autophagy protein ATG16L1 to localize to the site of microbe invasion in order to eliminate intracellular bacteria[28]. ATG16L1 is part of the ATG12-5-16L1-complex that functions as an ubiquitin-like enzyme and is required for the lipidation of microtubule-associated protein 1 light chain 3 (LC3-I) with phosphatidylethanolamine to form LC3-II, which in turn enables formation and closure of the autophagosome[29]. Various SNPs have been identified in the *ATG16L1* gene, of which the rs2241880 SNP is the most common disease-associated polymorphism and encodes for a missense mutation in ATG16L1, the T300A version of ATG16L1 ($ATG16L1^{T300A}$)[16].

The T300A (Threonine to alanine at position 300) version is, unlike the normal ATG16L1 protein, subjected to increased caspase-mediated cleavage, thus lower protein levels are available for formation of the ATG12-5-16L1 complex, resulting in impaired autophagy and xenophagy[30–33]. As a consequence, defective autophagy in patients carrying the T300A polymorphism of ATG16L1 fails to restrict proinflammatory NOD2 signalling upon bacterial infection, which sheds light on how microbe sensing and autophagy synergize to maintain mucosal homeostasis and thus prevent IBD susceptibility[32,34] (also see 1.2.5.2, p. 20).

Another possible pathomechanism explaining the implication of autophagy in IBD pathophysiology is endoplasmic reticulum stress (ER - stress). ER-stress refers to the accumulation of unfolded or misfolded proteins in the endoplasmic reticulum (for more detailed information, also see 1.2.4, p. 15 on the unfolded protein response).

ER-stress can be triggered by both environmental factors, e.g. smoking[35] or infection[36–39], and internal factors, e.g. defects in the UPR or autophagy themselves[19,39–42], and specifically impairs cell types with high secretory activity[42–44]. Likewise, cells with high secretory activity such as for example Paneth cells or Goblet cells (also see 1.2.1, p. 8, on cell types within the intestinal epithelium) are more prone to suffer from accumulating proteins[42,45–48]. Unresolved ER-stress can result in inflammation via proinflammatory cytokine release, impaired antimicrobial defence or induction of cell death[19,40,41,44].

Heightened chaperone expression is found in the mucosa of IBD patients, indicative of a stressed ER[19,46,49]. Correspondingly, disorganized secretory granules and elevated chaperone levels in Paneth cells in context of IBD or crippled autophagy are in line with the identified risk genes and suggest a causative involvement of ER-stress and the UPR in IBD pathophysiology[39,50–53].

Various polymorphisms in genes involved in ER-stress responses (i.e. the UPR) have been identified to mediate risk for IBD development[19–22]. Both the UPR and autophagy are engaged upon such accumulation to resolve ER - stress via a broad variety of mechanisms, altogether aiming to relieve the

ER from accumulated proteins and further protein biosynthesis[40,54,55]. Most prominently, rare variants of *X-box binding protein 1* (*XBP1*) have been associated to both UC and CD[19].

However, these gene variants do not satisfyingly account for the observed heritable proportion of IBD, which raised the possibility that the remaining heritability could rather be caused by the functional interaction of the previously identified risk gene variants[56]. Additionally, studies on adult-onset IBD imply that only a small proportion of the identified risk gene variants is likely to actually account for the pathophysiology of the majority of IBD patients[57,58]. As a consequence, the interest has shifted more towards regulation of gene expression and interplay of genetics with the environment rather than focussing on genetic predisposition only[59].

1.1.3.2 Environmental factors

Although GWAS have identified a plethora or IBD risk genes, they still do not sufficiently explain the dramatically rising incidence in westernized countries. Hence, it is obvious that the environment takes part in influencing disease risk[10,60]. A broad set of environmental factors has been identified to contribute to IBD risk or modify disease severity, such as for example tobacco smoke, diet, exercise, infections and the microbiota[61].

1.1.3.3 Host-microbe interaction

The microbiota itself varies between individuals and in individuals over time. It is known to be influenced by both environmental (e.g. diet[62]) and host factors[63,64]. On the other hand, the gut microbiota also drives changes in host gene expression[65] and strongly affects the immune system[66]. Due to this reciprocal relationship, dissecting cause and consequence in IBD is challenging as IBD itself is associated with a dysbiotic microbiota[64,67,68].

Dysbiosis refers to a state of altered microbial composition or function in the gut[64]. In IBD, the microbiota is typically characterized by a reduced diversity, which is supposed to render the host more prone to colonization and infection by pathogens or opportunistic bacteria[69], but also for example influences therapy outcome[70]. Manipulation of the gut microbiota might offer an opportunity for disease management of IBD in the near future. Currently, the exact molecular mechanism on how the intestinal microbiome shapes mucosal immunity is not yet fully unraveled[71–73].

1.1.3.4 Infection

Experimental studies have demonstrated how variants of IBD risk genes such as *ATG16L1* or *XBP1* reduce the host's ability to cope with commensal or pathogenic bacteria, resulting in intestinal inflammation[19,74,75]. Conversely, the presence of such risk variants resulting in impaired antimicrobial

defence gives rise to changes in the microbial flora[76,77]. Correspondingly, pathogen infection in IBD is more frequent than in healthy individuals as a consequence of either dysbiosis and/or genetic susceptibility, such as for example *Listeria monocytogenes* (*L. monocytogenes*) infection[78–80].

Besides commensal bacteria, there are also IBD-associated pathogens conferring risk for IBD development. Certain *E. coli* strains, i.e. adherent-invasive *E. coli* such as *E. coli* LF82, associate to the mucus layer, invade epithelial cells and replicate within macrophages or induce CD-like granulomas[69,81–83]. Strikingly, genetic susceptibility, i.e. defective autophagy caused by the *ATG16L1* risk variant, has been shown to promote colonization and infection with strains such as *E. coli* LF82[41,84]. On the contrary, presence of some bacteria such as *Faecalibacterium prausnitzii* can also offer protection against IBD development[85].

1.1.4 Therapeutic approach

IBD treatment comprises anti-inflammatory drugs (e.g. 5-Aminosalicylate), immunosuppressive drugs (e.g. Azathioprine, Methotrexate), corticosteroids and biologics. Biologics, a relatively novel generation of pharmacological drugs, are antibodies designed to specifically interfere with cytokine pathways or inhibit immune cell migration. Therefore, they are also referred to as "targetted therapy".

Within the last years an increasing battery of targetted therapies has been approved for the treatment of IBD. The major drug classes of targetted therapy are i) anti-TNF (anti-Tumor necrosis factor alpha (TNFα) agents, ii) anti-$\alpha_4\beta_7$-integrin antagonist (Vedolizumab)[86] and iii) anti-IL12/IL23 antibodies (Ustekinumab).

The introduction of biological therapies in the past years has markedly extended the available arsenal of treatment options. Biologics have not only enabled clinicians to reduce the use of systemic corticosteroids and thus minimize their severe and stigmatising long-term side-effects (e.g. moon face, acne, immunosuppression, diabetes, osteoporosis[87]), but also proven themselves to improve efficacy of immunosuppressive drugs (e.g. Azathioprine, Methotrexate)[88,89].

Ultimately the advances in the in pharmacological management of IBD have provided substantial improvement in the long-term care of IBD patients, reducing disease associated complications such as recurrent flares, stenosis, surgery and proctocolectomies. However, there is still a huge unmet need for novel therapeutic strategies as still many patients do not respond to e.g. TNFα - blockage or integrin antagonists[88,90]. Also, though current IBD treatment is able to suppress symptoms, it fails to actually reverse the underlying predisposing conditions, i.e. to reinstate a healthy microbial ecology, restore intestinal immune homeostasis, improve epithelial barrier function or eventually identify and remove the individual cause of the disease. Therefore, current IBD therapy still cannot provide ultimate disease

resolution nor protection from disease associated complications [91]. On the other hand, there is a scope for new therapeutical strategies in targetting basic pathophysiology features (e.g. immune homeostasis, barrier function, dysbiosis). Currently, drugs aiming to modulate mucosal fibrosis, immune cell homing and cytokine release, epithelial barrier function or microbial dysbiosis are being developed and tested[86].

1.1.4.1 CMV-colitis

Therapy-refractory colitis in IBD patients is a common complication, and continues to resemble a clinical challenge, despite improved therapeutic strategies. Cytomegalovirus (CMV) presence is frequently found in IBD patients, specifically in ulcerative colitis patients, and a well-recognised phenomenon since the 1960s[92,93]. Nevertheless, evidence on how to manage CMV in UC patients is rare, as the clinical significance remains to be determined[94].

Although CMV-reactivation, that is, replication of the virus, is well described in severe or steroid-refractory ulcerative colitis, the pathophysiological origin on the interplay of chronic inflammation and CMV-reactivation are not entirely understood.

In essence, there is a lack of understanding whether viral replication merely occurs as a consequence of severe inflammation, not resulting in aggravation of inflammation; or whether the reactivation of the virus underlies the severity of disease or the disease being refractory to e.g. steroids. Additionally, distinguishing between replication of the virus and actual CMV-mediated colitis resembles a diagnostic challenge[94].

Seroprevalence rates of CMV in IBD patients are high (for both UC and CD estimated around 70 %), just as in the general population, depending on the respective population tested[95,96]. CMV-colitis does not seem to occur more frequently in patients with inactive or mild to moderate UC, compared to the general population[95,97,98]. In severe or steroid-refractory UC however, studies suggest by far higher rates of CMV-colitis, estimated between 20 % and 40 %[99–102]. Pathophysiologically, this could be attributed both to IBD-inherent impaired innate immune activity in such patients, but also to immunosuppressive drug specimens[95,99,103–105]. Again, reliable data is rare, as it is difficult to distinguish between causative and associated factors, e.g. the use of steroid as an indicator of disease severity, versus the use of steroids as a cause of immunosuppression and thus CMV-colitis[106].

Although it is difficult to decipher whether CMV reactivation actually underlies an aggravated disease course in IBD in general[107,108], for UC patients studies suggest that CMV-reactivation, respectively colitis, could be attributable for steroid-refractory episodes[99,109,110]. Consequences are a poorer

prognosis due to elongated disease duration, impaired therapy efficacy, coinfection with bacteria, toxic megacolon development and necessity for surgical intervention[109,111–119].

On a molecular level, latent CMV is localized in monocytes and is then delivered to the mucosa in form of inflammation-associated invading monocytes. Upon monocyte invasion CMV subsequently starts to replicate and infect enterocytes[120–122]. Interestingly, CMV not only seems to cause worsened disease due to immunosuppression, but also seems to be specifically attracted by inflamed tissue[122–124], as proinflammatory cytokines such as IFNγ and TNFα have been proposed to attract CMV. On the other hand, CMV seems to be perfectly capable to avoid clearance by innate immune cells such as macrophages[122].

1.2 The intestinal epithelium in health & disease

Given the different tasks that the many parts of the gut have to fulfil, the epithelial layer differs strongly in architecture, cellular composition and function. As the research presented in this study has overall focussed on the small intestine (SI), in the following also mainly the small intestinal epithelium shall be addressed and referred to as “the intestinal epithelium” hereafter.

First, the general architecture of the intestinal epithelium and its homeostatic mechanisms (namely autophagy, microbe sensing and the UPR) will be introduced. Subsequently, in 1.2.5, p. 19, the implication and interaction of those pathways in IBD and intestinal inflammation will be addressed.

1.2.1 Specialized cell types ensure barrier integrity and protect from microbes

The intestinal epithelium consists of a subset of specialized epithelial cells with very specific tasks and functions, altogether working in concert towards maintenance of an intact barrier, segregation from the luminal outside and nutrient absorption (see Figure 1-2). Homeostasis and regeneration is guaranteed by constant replenishment and renewal of the epithelial layer, which is estimated to undergo complete replacement every four to five days[125].

In the small intestine, the epithelium is organized in crypts and villi in order to maximize surface. While nutrient absorption takes place mainly in between and on top of the villi and is carried out by enterocytes, within the crypts a distinct microenvironment is formed in order to keep microbes at distance from the crypt base, where stem cells reside[126].

All cell types of the epithelium derive from the pluripotent intestinal stem cell (ISC) and are continuously renewed. The ISCs dwell at the crypt base and are nurtured and safeguarded by Paneth cells and mesenchymal cells altogether constituting the stem cell niche[127]. ISCs constitutively divide into lineage-progenitors, which rapidly proliferate, migrate upwards and differentiate in order to

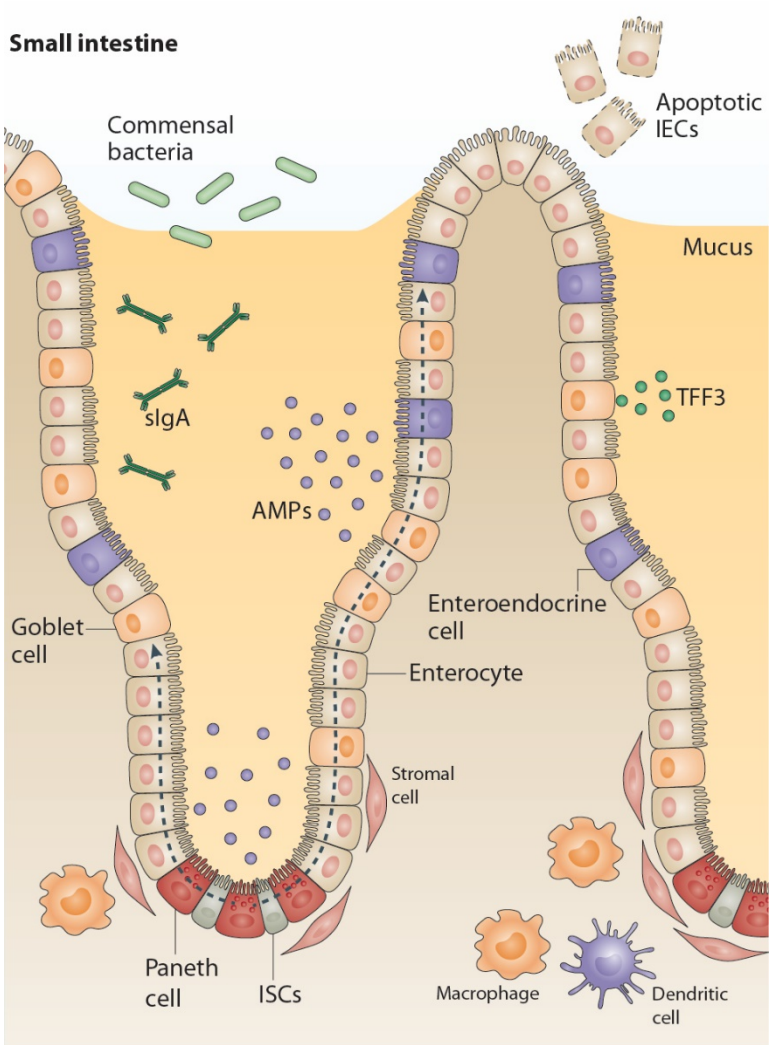

Figure 1-2: Architecture of the intestinal epithelium.

Paneth cells are located at the crypt base and constitute the stem cell niche, together with stromal cells. ISCs are embedded in between Paneth cells and divide into lineage – progenitors to replenish the pool of IECs (i.e. enterocytes, Goblet cells, enteroendocrine cells, Paneth cells). Paneth cells secrete AMPs such as lysozyme to prevent microbes from entering the crypts. A protective mucus layer is secreted by Goblet cells in order to create a physical barrier limiting exposure of the epithelium to bacteria. Additionally, Goblet cells stabilize the mucus and regulate epithelial barrier integrity by release of additional factors such as TFF3. Transcytosis of soluble IgA (sIgA) further contributes to keeping microbes at distance from the crypt base. The intestinal epithelium primes and recruits adaptive and innate immunity via cytokines and is vice versa dependent on cytokines released by immune cells. With permission from Springer Nature modified from Peterson & Artis, *Nat Rev Immunol* (2014)[130].

IECs: intestinal epithelial cells; AMPs: antimicrobial peptides; TFF3: Trefoil-factor 3

replace apoptotic, shredded IECs[127]. This process both allows a fast epithelial turnover and protects genomic integrity of stem cells from hazards within the lumen.

The most abundant cell types in the epithelium are enterocytes which are both responsible for nutrient absorption and forming a tight physical barrier. Therefore, tight junctions seal up the space in between adjacent IECs in order to limit epithelial permeability[128]. Paneth cells are located in the base of crypts next to ISCs and secrete anti - microbial peptides (AMPs) such as α-defensin or lysozyme to shape microbial composition, protect against pathogens and restrain bacterial entry to the crypts[128,129]. The mucus layer is produced by Goblet cells, consists of strongly glycosylated proteins and keeps bacteria at distance from the epithelium, thereby limiting epithelial exposure to microbes[129]. Additional factors

supporting epithelial barrier integrity and stabilizing the mucus layer such as trefoil factor 3 (TFF3) are released by Goblet cells[130]. Enteroendocrine cells are a very specialized epithelial cell subset and rather involved in connecting central and enteric neuroendocrine systems through the secretion of numerous hormone regulators of digestive function (e.g. serotonin, somatostatin, gastrin) than in contributing to barrier function and defense[131].

1.2.2 Microbe sensing

Except from merely keeping microbes at distance, the intestinal epithelium also actively engages in microbe sensing and forms a vital part of the innate immune system by conducting danger signals to immune cells in the lamina propria. IECs express a variety of innate immune Pattern-recognition-receptors (PRRs) such as NOD2 (also see 1.1.3.1, p. 3), Toll-like-receptors (TLRs) or, subject of this study, the cGAS/STING-signalling pathway (see 1.3, p. 23). Those PRRs enable dynamic sensing of the microbial environment and danger signals[132].

PRRs specifically recognize pathogen-associated molecular patterns (PAMPs) or danger-associated molecular patterns (DAMPs) and subsequently initiate signalling cascades cumulating in the expression and secretion of various cytokines and chemokines such as e.g. TNFα to recrute and prime immune cells, but also leading to increased secretion of AMPs[133]. Additionally, bacterial sensing by PRRs and their downstream signalling have also been shown to be essential for epithelial repair, stem cell proliferation, Paneth cell function and thus overall barrier function[132,134].

PRRs can also collaborate with antibacterial autophagy to remove pathogens. Autophagy is not only engaged by PRRs to eliminate pathogens, but also serves to limit detrimental immune responses caused by PRRs as described in the next chapter (especially see 1.2.3.2, p. 13 and 1.2.3.3, p. 14).

1.2.3 Autophagy

Autophagy is an essential homeostatic process executed by a complex molecular machinery consisting of multiple autophagy proteins with the task of directing cellular components to the lysosome for degradation in order to respond to cellular stress and thus adapt to harsh conditions[23]. While there are at least three types of autophagy, namely macro-, micro- and chaperone-mediated autophagy, the term "autophagy" is generally used to simply refer to macroautophagy[23], which different function shall be addressed hereafter.

A variety of stressful conditions has been found to activate autophagy including for example starvation, ER-stress, infection and bacterial sensing[23–25,28,34,37,39–42,54,55,135–137]. Based on the respective inducer, cargo and the mechanism of cargo engulfment and delivery, autophagy can be further classified: xenophagy removes intracellular pathogens[24,25,137], ER-phagy or reticulophagy specifically removes

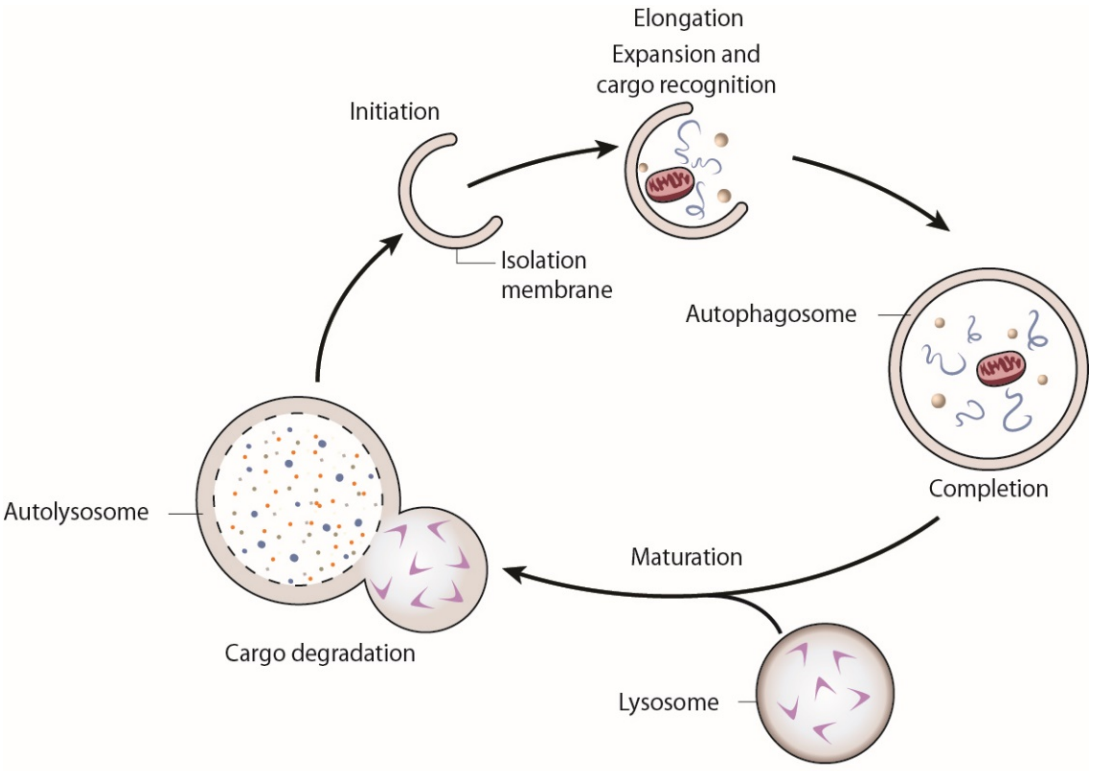

Figure 1-3: Autophagy engulfs and delivers cellular components for lysosomal degradation

Cellular components such as bacteria, organelles or proteins are trapped in the autophagosome by initiation and expansion of an isolation membrane closing around the cargo, which is identified for degradation via interaction of membrane – bound LC3-II and selective autophagy receptors labelling the cargo. The autophagosome subsequently fuses with the lysosome to form the autolysosome, where final degradation and recycling take place. With permission from Springer Nature adapted from Levine, Mizushima, Virgin, *Nature* (2011)[23].

stressed or damaged ER parts and regulates ER quantity and size[138,139], and in innate immunity for example selective autophagy removes specific targets, both to restrain or activate immune responses, requiring additional selective autophagy receptors labelling the cargo for degradation[140,141].

1.2.3.1 The canonical autophagy machinery

Autophagy works by sequestration of its cargo (organelles, large protein complexes or intracellular pathogens) into double-membrane structures called autophagosome, which then fuse with the lysosome (autolysosome), where proteolytic degradation takes place (see Figure 1-3). In a first step, the initiation, several autophagy-related proteins (ATGs) orchestrate the formation of a cup-shaped isolation membrane derived from the ER around the respective cargo. In the elongation phase the isolation membrane expands, forming the phagophore and cargo recognition takes place. Next, the isolation membrane fuses around the target and thereby traps the cargo inside, forming the autophagosome. After merging with the lysosome, in the autolysosome the cargo is degraded and eventually recycled[23,142].

A more detailed view on the initiation and completion of the autophagosome is of interest in order to understand the data shown later on (see Figure 1-4). Upon stress, the ULK1 (Unc-51 like autophagy activating kinase)-complex (again consisting of multiple autophagy proteins) translocates from the cytosol to the ER, which serves as a membrane source for the isolation membrane[143,144]. Of note, other membrane sources have been proposed. ATG9 for example, a multispanning membrane protein trafficking between Golgi, endosomes and autophagosome precursors, is essential for autophagy[145,146], indicating the involvement of the Golgi network.

Following the activation of the ULK1-complex, the PI3K (class III phosphatidylinositol-3-OH kinase)-complex is recruited to the site of membrane formation and produces phosphatidylinositol-3-phosphate (PI3), leading to the engagement of further effector proteins[147,148]. Elongation and final closure of the autophagosome then require additional ubiquitin-like-conjugation systems.

First, LC3, which is synthesized as a precursor protein, is cleaved and further activated to form the active LC3-I version. Cleavage and activation is facilitated by the autophagy proteins ATG3, ATG3 and ATG7[149].

Next, the ATG12-5-16L1 conjugate, which is assembled by the autophagy proteins ATG7 and ATG10[150,151], acts as an E3 ubiquitin ligase-like enzyme and promotes the lipidation of LC3-I with phosphatidylethanolamine, converting it to LC3-II and enabling its binding to the phagosomal membrane, where it remains and is degraded along with the autophagy target[152,153].

Thus, in order to experimentally monitor autophagic activity, LC3-I to LC3-II turnover can be analyzed[154]. For instance, defects in the ATG12-5-16L1 complex impair LC3-I lipidation, resulting in the accumulation of LC-I. Conversely, a high autophagic flux can be documented by observing LC3-II accumulation if final lysosomal degradation is blocked experimentally[154].

1.2.3.2 Xenophagy & selective autophagy

Although originally considered a mainly unspecific process of bulk degradation, autophagy can in fact degrade targets in a very selective manner[155].

Autophagy of intracellular pathogens, named xenophagy, is a process used by IECs to get rid of bacteria that have breached prior defence layers, i.e. mucus or AMPs. The autophagy machinery is then engaged to remove such invasive bacteria by PRRs[24–28,34], as briefly described above (see 1.1.3.1, p. 3). Basically, xenophagy works the same way as canonical autophagy (see Figure 1-3 and Figure 1-4), once the pathogen is engulfed in the autophagosome.

A more complex issue is the precise mechanism of trapping the pathogen in a membrane vacuole. While bacteria can simply be targeted by fusion or envelopment of bacteria-containing vacuoles (i.e. phagosome, endosome) with the autophagosome or lysosome, the xenophagic capture of bacteria that have escaped into the cytoplasm requires selective autophagy receptors (SARs) such as p62 (Sequestome 1, SQSTM1), NDP52 (Nuclear dot protein 52) or NBR1 (Neighbour of BRCA1 gene 1

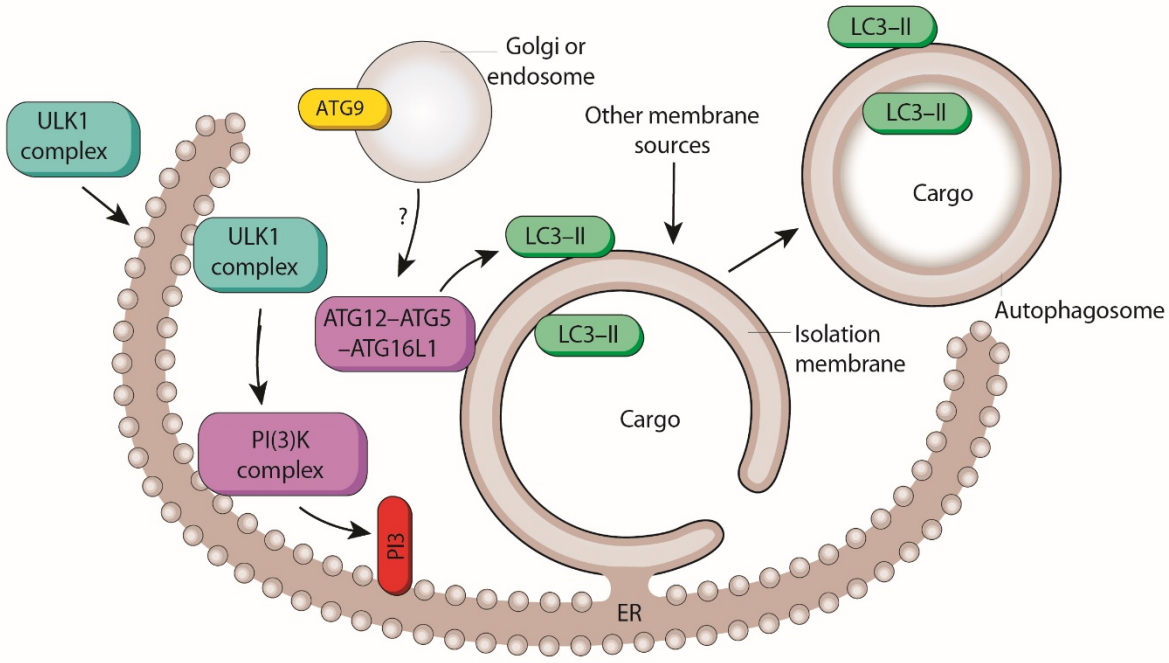

Figure 1-4: The autophagy machinery

Upon a broad variety of cellular stress, including infection, ER – stress or starvation, the ULK1 – complex initiates the process of autophagosome formation. The ER serves as an initiation platform and membrane donator. At the site of membrane isolation, the PI3K – complex generates PI3, which recruits further effector proteins required for membrane formation. The ATG12-ATG5-ATG16L1 complex is generated by ubiquitin – like conjugation systems and promotes the lipidation of LC3-I with phosphatidylethanolamine, generating the membrane bound LC3-II. In selective autophagy, LC3 serves as an adapter binding the LC3 – binding domain of selective autophagy receptors, which capture and deliver the respective target to autophagic degradation. With permission from Springer Nature modified from Levine, Mizushima, Virgin, *Nature* (2011)[23].

protein)[155,156]. SARs have binding domains for both molecular tags labelling cargo for degradation (i.e.

ubiquitin) and LC3, thereby mediating recognition of the respective cargo for engulfment in the autophagosome (see Figure 1-3, cargo recognition, and Figure 1-4)[140,157–161].

Just like LC3-II, p62 remains within the autophagosome until lysosomal degradation, thus p62 protein levels can also be used to study autophagy defects or induction[162].

1.2.3.3 Regulation of innate immune signalling by (selective) autophagy

Autophagy is not only engaged and extensively regulated by infection and immune pathways as briefly outlined above (see 1.1.3.1, p. 3; 1.1.3.3, p. 5; 1.2.3.2, p. 13), but also balances and modulates immune activity to avoid excessive signalling and subsequent inflammation[23,163]. Likewise, defective autophagy can result in inflammation as a consequence of uncontrolled immune signalling[32–34,135,141,164]. While autophagy finetunes a broad spectrum of innate immune responses such as inflammasome activation or type I and type II IFN (interferon) inducing pathways[165], for this work mainly the regulation of type I IFN induction will be of interest.

Autophagy can both directly suppress activation of protein complexes involved in interferon induction, thus interrupting the signalling cascade, and remove substrates stimulating interferon induction, thus preventing or abrogating initial activation[165]. For example, ATG9A (involved in autophagy initiation, see Figure 1-4) negatively regulates trafficking of STING (Stimulator of Interferon Genes), which mediates interferon induction in response to cytosolic double-stranded DNA (dsDNA)[146]. Additionally, the upstream activator of STING, the dsDNA sensor cGAS (Cyclic GMP-AMP synthase) is a direct substrate for p62-dependent autophagic removal[166] (also see 1.3.6, p. 27, on regulation of STING-signalling by autophagy).

Likewise, MAVS (Mitochondrial antiviral-signalling protein), involved in RNA-sensing, is removed by NDP52-dependent selective autophagy[167], illustrating how defective autophagy may result in amplified interferon-inducing signalling. TRIM21 (Tripartite motif-containing protein 21) has been found to directly target both parts of the NFκB (nuclear factor 'kappa-light-chain-enhancer' of activated B-cells) - signalling pathway and IRF3 (Interferon regulatory factor 3), a downstream transcription factor of type I IFN-inducing pathways, for autophagic removal[168]. The adaptor TRIF (TIR-domain-containing adapter-inducing interferon-β) is targeted by the selective autophagy receptors p62 and Tax1BP1 (Tax1 Binding Protein 1) for ATG16L1-dependent autophagy, giving rise to uncontrolled type I IFN secretion in case of defective autophagy[141].

In turn, the substrates for interferon-inducing pathways themselves such as dsDNA can be removed via autophagy, thereby limiting access of PRRs to it. During DNA-damage, dsDNA leaks from the nucleus and gains access to the cytosol in form of micronuclei, where it associates with cGAS, which

subsequently triggers type I IFN induction via STING[169,170]. In order to limit such proinflammatory cGAS activity, autophagy engages to remove leaked dsDNA and thereby counterbalances type I IFN induction[171].

1.2.4 Endoplasmic reticulum homeostasis: the unfolded protein response

All secretory or membrane proteins are directly translated into the ER, where correct folding, posttranslational modification and processing take place. Accordingly, secretory highly active cells such as Paneth cells or Goblet cells (see 1.2.1, p. 8) are especially prone to accumulate unfolded or misfolded proteins within the ER if the fragile balance between ER folding capacity and protein load is disturbed[42,46–48]. The accumulation of proteins exceeding the current folding capacity is commonly referred to as "ER-stress".

ER-stress in the epithelium may occur as a consequence of either environmental forces demanding high secretory activity (e.g. infection or dysbiosis, see 1.1.3.3, p. 5) or resulting from genetic variants causing functional defects in important homeostatic pathways (e.g. autophagy or UPR, see 1.1.3.1, p. 3)[19,40,41,45,135].

As a consequence, aggregates of un- or misfolded proteins in the ER render the cell incapable of carrying out its function (with regard to secretory cells, resulting in e.g. dampened AMP or mucus secretion[19,41,45,46,50,51]). This can result in inflammatory responses and eventually cell death induction, pointing towards its association to inflammatory disease[19,40,45,47]. Thus, it is crucial for general cell function and survival to maintain ER homeostasis.

Accordingly, the ER has evolved various protein-folding mechanisms such as chaperones and protein-modifying enzymes to ensure proper folding, preventing capacity exhaustion. If however proteins do accumulate, numerous ER-stress response pathways aiming to lower protein load and eliminate excess protein stand by to allow the cell to cope with ER-stress and fulfil the secretory demands, most prominently the ERAD (ER-associated degradation), the unfolded protein response and autophagy.

While the ER-associated degradation (ERAD) simply marks and removes protein aggregates from the ER to the cytosol for subsequent proteolytic degradation by the ubiquitin-proteasome system[172], the UPR consists of a sophisticated collection of closely interconnected pathways sensing protein accumulation and initiating appropriate responses to alleviate ER-stress.

Initiation of the UPR takes place by the coordinated dissociation of the chaperone BiP (binding immunoglobulin protein[173], synonymous for GRP78 or HSPA5), owing to its higher affinity to un- or misfolded proteins, of three ER transmembrane stress sensors, namely inositol-requiring enzyme 1α (IRE1α)[174], PKR-like ER kinase (PERK)[175,176] and activating transcription factor 6α (ATF6α)[177].

Additionally, unfolded proteins can also directly bind IRE1α and activate this branch of the UPR[178] (see Figure 1-5).

Together, the three UPR pathways aim to restore ER homeostasis by mainly four different approaches[173]. While PERK mainly works through downregulating mRNA translation, thereby reducing the amount of protein newly synthesized into the ER, IRE1α degrades ER membrane-associated mRNA,

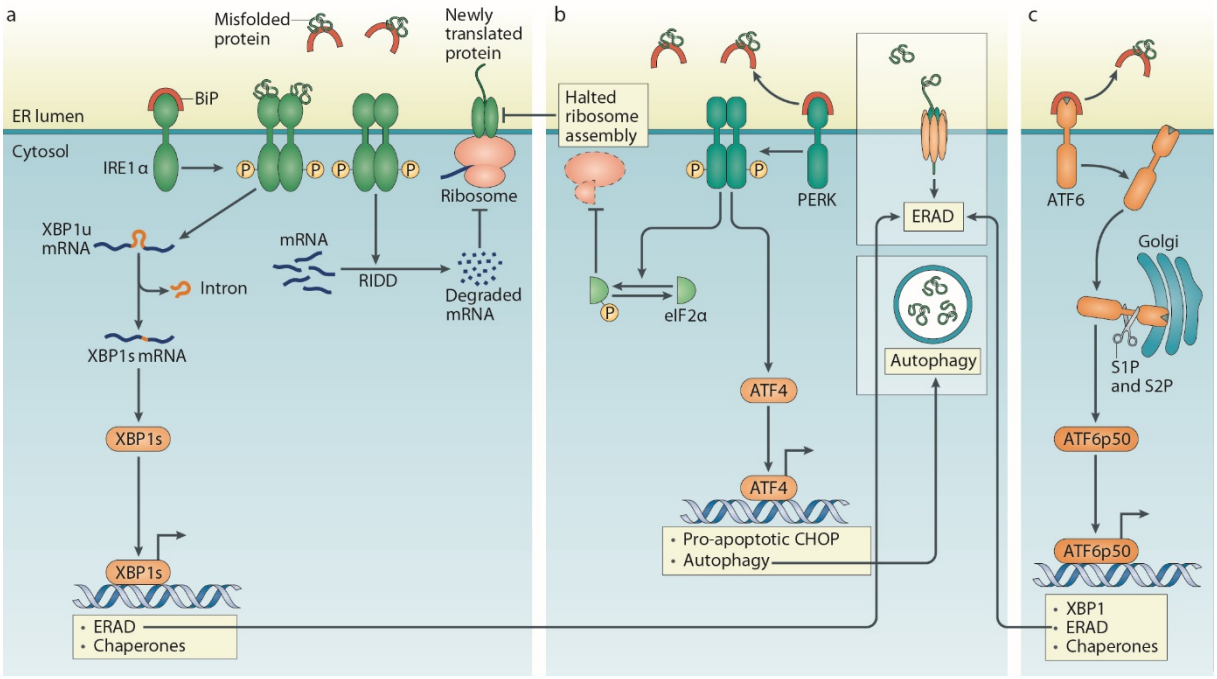

Figure 1-5: The unfolded protein response (UPR)

The UPR consists of three main branches, named according to the respective ER transmembrane stress sensor: the IRE1α branch (A) cleaves XBP1u mRNA ("u" for unspliced) to XBP1s ("s" for spliced), leading to translation of the active transcription factor XBP1. XBP1 initiates translation of proteins involved in the ERAD and chaperones strengthening ER folding capacity. Additionally, IRE1α activates RIDD (regulated IRE1α-dependent decay of mRNA) to degrade mRNAs that would otherwise be translated into the ER, further increasing protein load. PERK (B) phosphorylates eIF2α to block further translation and activates the transcription factor ATF4, resulting in translation of the proapoptotic protein CHOP, stress response gene induction and expression of autophagy – related genes. ATF6 (C) traffics from the ER to the Golgi network, where its cleavage by site 1 and site 2 proteases (S1P, S2P) results in the active transcription factor ATF6p50, which targets ERAD and chaperone genes, of note also *XBP1*, thus synergizing with the IRE1α pathway. With permission from Springer Nature modified from Grootjans et al., *Nat Rev Immunol* (2016)[173].

thus also lowering protein biosynthesis[175,176,179]. Next, compensatory mechanisms eliminating unfolded proteins (such as ERAD or autophagy) are strengthened by increasing transcription of ERAD- or autophagy-related proteins. Lastly, genes directly increasing ER protein-folding capacity are induced and the ER itself is expanded by biogenesis of ER and membrane components[173,180].

As a last resort, if even after stress responses have engaged, the cell is still unable to overcome ER-stress, the UPR can lead to cell death, a process named terminal UPR[181,182].

1.2.4.1 The IRE1α/*XBP1* pathway

Once activated by dissociation of BiP from its ER-luminal end, IRE1α elicits ER-protective effects via two different mechanisms (Figure 1-5a) using the two enzymatic activities of its cytosolic domain[183].

First, an endoribonuclease (RNase) domain splices a single mRNA that encodes *XBP1* (*XBP1*u, "u" for unspliced), removing an intron and resulting in a frameshift enabling translation of the transcription factor *XBP1*s ("s" for spliced)[184,185]. XBP1 then translocates to the nucleus and induces a subset of ERAD proteins, chaperones and protein-folding enzymes that aim to boost ER-size and function[180,186].

Second, the cytosolic part of IRE1α contains a serine/threonine kinase domain activating regulated IRE1α-dependent decay of mRNA (RIDD), which cleaves ER-membrane-associated mRNA and thus lowers the translational burden of the already stressed ER[187].

Prolonged and unresolved activation of IRE1α may however turn out to have detrimental effects on cell survival. If IRE1α is increasingly oligomerized, its RNase activity also applies to many other RNAs in addition to *XBP1*u, including for example apoptosis-inhibitory microRNAs, which then renders the cell susceptible to apoptosis[181,188,189], again pointing towards a mechanistic explanation for associations of UPR genes with intestinal inflammation. Likewise, IRE1α has been proposed to drive inflammatory responses during prolonged ER-stress if not appropriately removed via autophagy (also see 1.2.5, p. 19)[135].

1.2.4.2 PERK/ATF4/CHOP-signalling

Just like IRE1α, PKR-like ER kinase is an ER-resident kinase activated by release of BiP from its ER-luminal domain upon accumulation of unfolded proteins (Figure 1-5b). PERK subsequently dimerizes and autophosphorylates to activate its cytosolic kinase function. Activated PERK phosphorylates the translation factor eIF2α (eukaryotic translation initiation factor 2α), which inhibits global mRNA translation and thereby provides a translational break giving the cell time to manage the accumulated proteins[173]. Although overall mRNA translation is inhibited by PERK activation, the translation of ATF4 mRNA (activating transcription factor 4) is increased[190]. ATF4 in turn induces the transcription of various genes involved in stress responses, noteworthy also autophagy-related genes[176]. Additionally ATF4 initiates the translation of CHOP (C/EBP homologous protein), which is partly responsible for ER-stress-mediated apoptosis[191,192]. Because the UPR is meant to enable the cell to overcome ER-stress, stable levels of CHOP sufficient to induce cell death are only achieved by strong and sustained PERK-signalling[193]. If however ER-stress is too great, ATF4 also acts together with CHOP to induce terminal UPR[194].

1.2.4.3 ATF6-signalling

Activating transcription factor 6α (ATF6α) is a transcription factor which is activated by trafficking from the ER to the Golgi network upon release from BiP (Figure 1-5c). At the Golgi network, ATF6 is further processed by two proteases (site 1 and site 2 protease, S1P and S2P), resulting in a cytosolic p50 leftover (ATF6p50), which forms the active transcription factor[173]. ATF6p50 then translocates to the nucleus and initiates expression of genes improving ER folding capacity (among them BiP or chaperones such as GRP94, DNAJC3, but also *XBP1* for example) as well as genes involved in the ERAD[173,185,195].

There is also compelling evidence pointing towards ATF6 being critically involved in gastrointestinal homeostasis. In contrast to *XBP1*, where variants with impaired activity mediate risk, elevated ATF6 activity has been associated with reduced time of disease-free survival in colorectal carcinoma patients[196]. Mechanistically, ATF6 overexpression gives rise to microbial dysbiosis and barrier dysfunction, which essentially enables colorectal adenoma formation and paves the road for carcinogenesis. Interestingly, this was dependent on the PRR MyD88 and downstream signalling via TRIF[196]. Presumably, barrier dysfunction in ATF6 overexpressing IECs results from ER-stress based on overactive ATF6[196].

Apart from carcinogenesis, in a study of our own group we shed light on the role of ATF6 mediating inflammatory signals via NFκB in context of *Xbp1* or *Atg16l1* deficiency[197]. By identifying various suppressors and activators of ATF6 signalling and respective chemicals serving to modulate such repressors and activators, we could show that inhibition of ATF6 signalling, which is overactive during *Xbp1* or *Atg16l1* deficiency, alleviates the proinflammatory phenotype in the *Xbp1* or *Atg16l1* deficient situation. Importantly, this also translated to a reduction of the proinflammatory phenotype of CD patient derived human organoids.

1.2.4.4 Autophagy as a branch of the unfolded protein response

The UPR also relies on autophagy as the professional cellular recycling machinery to restore ER homeostasis (Figure 1-5b). The mechanisms by which autophagy acts to ease ER-stress is however incompletely understood. In the intestinal epithelium, autophagy most likely works through selectively removing stressed ER membranes, a process named ER - phagy[37,198,199]. Also, just like the UPR, ER-stress-induced autophagy can both serve to support cell survival or result in cell death[54,200].

While the respective downstream result of UPR-induced autophagy remains to be further characterized, it is known through which mechanisms the UPR acts to recruit the autophagy machinery upon ER-stress. PERK and IRE1α pathways have for example been found to mediate autophagy

induction at the level of gene expression[201]. Similarly, ATF4 and CHOP both induce expression of autophagy-related genes[55,202].

With regard to the intestinal epithelium, it is known that autophagy is engaged to compensate genetic defects in the UPR resulting in ER - stress[40,135]. Accordingly, defective autophagy even potentiates ER-stress induced inflammation[40,135], which shall be further addressed in the next chapter.

1.2.5 ER-stress, microbe sensing and defective autophagy converge in intestinal inflammation

Since GWAS have identified IBD - associated genes involved in the unfolded protein response, autophagy and microbe sensing (see 1.1.3.1, p. 3), numerous studies have followed up those findings providing insides to how such risk variants result in inflammation. Increasing evidence has mounted that especially the interplay of defects in more than one pathway rather than the presence of a single risk gene variant can cause inflammation, which shall be pictured hereafter (also see Figure 1-1).

1.2.5.1 The interplay of ER-stress and infection results in intestinal inflammation

Rare variants of *XBP1* confer risk for both UC and CD[19]. Besides a possible role of XBP1 in immune cells, mice with a conditional deletion of *Xbp1* in the intestinal epithelium (*Xbp1*$^{\Delta IEC}$ mice) show increased ER-stress in the epithelium. As a consequence, *Xbp1*$^{\Delta IEC}$ mice suffer from spontaneous mild intestinal inflammation and increased susceptibility to inflammatory triggers such as infection[19].

Mechanistically, *Xbp1*-deficiency induced ER-stress gives rise to IRE1-dependent NFκB and JNK (c-Jun N-terminal kinase) activation, leading to expression of proinflammatory cytokines predisposing for intestinal inflammation. Noteworthy, due to insufficient function of the IRE1α branch of the UPR (see 1.2.4.1, p. 17), the secretory function of Paneth and Goblet cells is significantly impaired by *Xbp1*-deficiency, leading to disruption of AMP secretion such as lysozyme. Consistently, *Xbp1*-deficiency results in dysbiosis, heightened susceptibility to *L. monocytogenes* infection and dextransodiumsulfate (DSS)-induced colitis[19].

In turn, ER-stress has not only been shown to result in impaired antimicrobial defence as being the case for *XBP1*-deficiency, but infection vice versa also induces ER-stress and subsequently the UPR[37,39], illustrating how an environmental trigger might result in inflammation if the respective stress response is unable to respond properly. Although performed on phagocytes, a recent interesting study has found the intracellular pathogen *L. monocytogenes* to induce ER-stress, which is then resolved via STING-dependent autophagy of stressed ER-membranes to promote cell survival[37], emphasizing the close link between ER-stress and autophagy as a compensatory mechanism.

Another recent report has found the intracellular pathogen *Salmonella enterica* serovar Typhimurium to disrupt the Golgi network specifically in Paneth cells and thereby block the AMP secretion machinery, resulting in ER-stress and impaired antibacterial defence. The UPR then recruits autophagy via PERK/eIF2α as a compensatory mechanism to deliver AMP-filled vacuoles to the apical membrane for exocytosis[39]. Additional defects in autophagy such as the CD-associated T300A version of ATG16L1[16] even impair this compensatory AMP secretion pathway[39], underscoring the co-dependency of autophagy and UPR.

1.2.5.2 Defective autophagy predisposes to intestinal inflammation by impaired pathogen defence, heightened cytokine secretion and altered epithelial function

Since the SNP encoding for the missense variant ATG16L1^{T300A} has been first associated to CD[16] (also see 1.1.3.1, p. 3), a plethora of studies has followed up this finding confirming the genetic association[203] and dissecting the underlying mechanisms.

Defective autophagy might even be involved in IBD pathophysiology beyond genetic susceptibility. For example, CD-associated adherent invasive *E. coli* are able to specifically downregulate ATG16L1 expression and thereby compromise antibacterial autophagy[204]. While ATG16L1 deficiency results in abolished ability to form the autophagosome (Figure 1-4)[33], it has also been demonstrated that indeed the actual CD - linked missense variant of ATG16L1 has functional consequences as it significantly impairs autophagy by predisposing ATG16L1^{T300A} to cleavage by caspase 3[30,32]. Interestingly, ATG16L1^{T300A} cleavage is predominantly induced upon cellular stress such as nutrient starvation or *Yersinia enterocolica* infection[30]. As suggested by other studies[32,75,84,136,137,203,205], knock - in mice carrying ATG16L1^{T316A} (the respective murine equivalent of T300A) showed impaired clearance of *Yersinia enterocolica*, confirming the critical role of ATG16L1 in intestinal pathogen defense[30]. In addition, ATG16L1 has been found to be essential to prevent intracellular replication of the CD-associated adherent invasive *E. coli* strain LF82[84], suggesting that patients carrying ATG16L1^{T300A} might be more prone to *E. coli* LF82 colonization. Using a *Salmonella enterica* serovar Typhimurium infection model, Conway et al. showed that *Salmonella* infection in context of epithelial deletion of *Atg16l1* lead to increased inflammation and sepsis, providing evidence for a crucial role of ATG16L1 in IECs[137]. Mechanistically, ATG16L1 is required for autophagic capture of intracellular *Salmonella*, which is impaired in cells harbouring the defective ATG16L1^{T300A} [75]. Consistently, in another study using *ATG16L1^{T300A}* mouse embryonic fibroblasts (MEFs), *Shigella flexneri* was found to replicate more easily intracellularly[32].

ATG16L1 deficiency, or the defective T300A variant respectively, also directly enables proinflammatory cytokine release[32,33,141]. Following exposure to lipopolysaccharide (LPS), ATG16L1-deficient

macrophages produce immense amounts of IL1ß and IL18, both mediating strong inflammatory signals[33]. Accordingly, mice lacking ATG16L1 in myeloid cells are highly susceptible to DSS-induced colitis, demonstrating how defective ATG16L1 might result in intestinal inflammation[33]. This finding was replicated using the *Salmonella* infection model[32].

With regard to selective autophagy, Samie et al. have demonstrated that in myeloid cells, ATG16L1-dependent selective autophagy of the adaptor TRIF (TIR-domain-containing adapter-inducing interferon-β) regulating type I IFN production is mediated by the SARs p62 and Tax1BP1 (Tax1 Binding Protein 1)[141]. As a consequence, in case of defective autophagy, TRIF was found to accumulate and result in elevated type I IFN secretion. Additionally, epithelial ATG16L1 was found to govern the response to the usually protective cytokine IL22. ATG16L1-deficient IECs respond to IL22 with elevated type I IFN production, which then mediates susceptibility to TNFα-induced necroptosis[164].

ATG16L1 is also critical for intact basic epithelial function, most particularly Paneth cell function. Mice hypomorphic for expression of ATG16L1 display morphological defects in Paneth cells, based on a disrupted granule exocytosis pathway, indicative of reduced AMP secretory activity[53]. The same applies for mice harbouring the T300A variant of *ATG16L1*[32]. Moreover, a proinflammatory transcriptional profile was observed in *ATG16L1*^{T300A} Paneth cells[53]. Consequently, mice with a conditional knock-out in the intestinal epithelium (*ATG16L1*$^{\Delta IEC}$) develop spontaneous transmural ileitis in an age-dependent manner, phenocopying human ileal CD[135]. Notably, this depends on the accumulation of activated IRE1α, pointing towards a compensatory engagement of the UPR following defective autophagy[135].

In line with this finding, a more recent study has found intact ATG16L1 to be essential for autophagy-mediated lysozyme exocytosis in Paneth cells if the standard secretory pathway is disrupted by ER-stress due to *Salmonella enterica* Serovar Typhimurium infection[39]. Interestingly, the role of ATG16L1 is not only limited to the secretory pathway, but also extends to the stem cell niche constituting function of Paneth cells as illustrated by organoid formation experiments: when cocultured with *ATG16L1*^{T300A} Paneth cells, Lgr5 (+) stem cells[206] are remarkably impaired in their ability to form organoids compared to coculture with wildtype Paneth cells[32].

Importantly, the essential role of ATG16L1 for proper Paneth cell function has been validated *in vivo* in several studies examining CD patients. If homozygous for the T300A allele, CD patients display characteristic Paneth cell abnormalities similar to Paneth cells observed in mice with hypomorphic ATG16L1[53]. *ATG16L1*^{T300A} homozygous patients also show accumulation of IRE1α, supporting the idea that Paneth cell alterations indeed result from ER-stress induction[135]. In untreated paediatric CD patients, activation of autophagy was observed in Paneth cells independently of the presence of risk

variants[50]. This was accompanied by decreased and disorganized secretory granules. In another study, Paneth cells from CD patients were categorized according to secretory granule morphology. Strikingly, patients with a high proportion of altered Paneth cells also showed signs of immune activation in their transcriptional signature and were more likely to suffer a more fulminant clinical course[51].

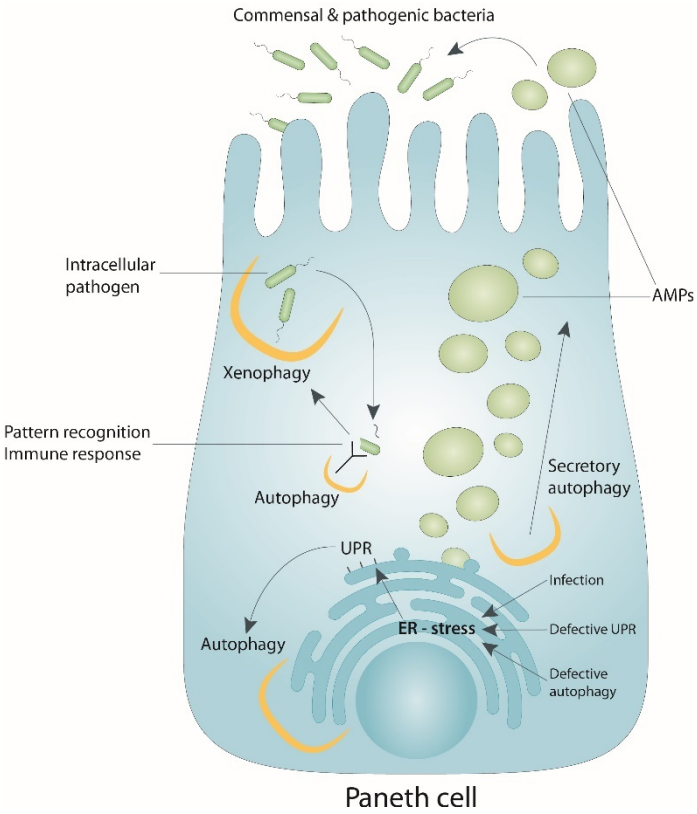

Figure 1-6: Paneth cells rely on intact autophagy for antibacterial defence, immune responses and secretory function

Commensal or pathogenic bacteria trigger secretion of AMPs, which eventually results in ER - stress due to a high secretory burden. Unresolved ER - stress results in proinflammatory signalling and cell death. The ER engages the UPR to ease ER - stress and activate autophagy to further alleviate ER -stress. Additionally, autophagy is engaged as a compensatory mechanism for AMP secretion in case of intracellular infection disrupting the ER – Golgi – secretory pathway. Intracellular pathogens are sensed by PRRs, which rely on signalling cascades to induce proinflammatory responses. Autophagy removes intracellular pathogens, but also selectively targets parts of innate immune signalling cascades to prevent excessive inflammatory signalling. Defective IBD risk gene variants (e.g. in *XBP1*; *ATG16L1*) or environmental stressors such as infection result in ER - stress, which in turn prevents proper secretory function of Paneth cells enabling microbial dysbiosis and giving rise to infection susceptibility.

1.2.5.3 Defective autophagy fails to alleviate ER-stress mediated inflammation

Paneth cells from patients with quiescent CD with homo- or heterozygosity for *ATG16L1*^{T300A} display elevated markers of ER-stress, suggesting that ER-stress occurs following defective autophagy[41]. Clinically, alterations in Paneth cells go hand in hand with increased risk for fistulizing disease course and the need for intestinal surgery, i.e. a more fulminant clinical course[41].

Strikingly, dysfunctional autophagy in Paneth cells was found to directly disrupt ER-homeostasis as shown by ER-stress spontaneously occurring in case of defective autophagy[40,135]. Likewise, in Paneth cells autophagy is directly activated as a compensatory mechanism for (genetically induced) ER-stress via PERK - eIF2α signalling (see 1.2.4.2, p. 17 and Figure 1-5), and additional defects in autophagy fail to alleviate ER-stress, resulting in severe spontaneous transmural inflammation, reminiscent of ileal CD[40]. Notably, the compensatory engagement of autophagy via PERK-eIF2α signalling was also observed using a *Salmonella enterica* Serovar Typhimurium infection model to induce ER - stress[39].

In case of sufficient autophagy, ER-stress engages ATG16L1-dependent autophagy to restrain IRE1α-dependent proinflammatory signalling by selectively removing IRE1α[40,135]. In line with this, accumulating IRE1α can be found in crypts of patients carrying the T300A version, presumably due to a defective resolution of ER-stress by autophagy[135].

1.3 The Stimulator of Interferon Genes pathway

The recognition of foreign (but also self) nucleic acids has emerged as a key feature of innate immunity[207]. Such nucleic acids involve single- or double-stranded RNA or DNA, RNA-DNA hybrids and cyclic dinucleotides[207]. Of note, as a second important homeostatic function, nucleic acid sensing pathway can also detect nucleus-leaked self-DNA in order to register genomic damage and initiate senescence[169–171,208].

For DNA sensing, three major pathways have been described that are engaged by self- or foreign DNA. Toll-like receptor 9 (TLR9) is located at endosomal membranes and recognizes DNA that has entered the cell via phagocytosis, resulting in NFκB and IRF7 (Interferon-regulating factor 7) activation[209,210]. TLR9 is mainly important for pathogen defence. AIM2 (Absent in melanoma 2), mainly involved in defence against DNA viruses and cytosolic bacteria, senses dsDNA encountered in the cytosol and subsequently triggers formation of the AIM2 inflammasome, which results in activation of caspase 1, Il1ß and IL18 production and pyroptotic cell death[211,212]. However, the most prominent response to cytosolic dsDNA is the production and release of type I IFNs and subsequent induction of an array of interferon-stimulated genes (ISGs)[213,214]. This is initiated by the cytosolic dsDNA sensor cGAS and further mediated by the adaptor STING, hereafter collectively referred to as the STING pathway, respectively STING-signalling.

1.3.1 Canonical STING - signalling

STING (Stimulator of Interferon Genes) is an ER-resident adaptor protein facilitating the induction of type I IFNs following detection of cytosolic dsDNA by cGAS[215–217]. cGAS is a cytosolic sensor of dsDNA which catalyses the subsequent production of the second messenger 2'3'-cGAMP (2'3' linked cyclic guanosine monophosphate–adenosine monophosphate, cyclic GMP-AMP)[218–220]. Upon cGAMP binding, STING dimers complexed with TBK1 (Tank-binding kinase 1) translocate from the ER to the perinuclear Golgi network in an autophagy-like manner[146,216,221–224]. TBK1 subsequently autophosphorylates and phosphorylates STING, which enables docking of IRF3 (Interferon regulatory factor 3), which is in turn also phosphorylated by TBK1, promoting its dimerization and translocation to the nucleus, finally resulting in expression of type I IFNs, most prominently Interferon β (IFNβ) (see

Figure 1-7)[216,225,226]. Once having completed this translocation and activation process, STING is rapidly degraded by autophagy to avoid sustained cytokine production[146,227,228].

Type I IFNs signal through binding to the type I IFN receptor (consisting of a heterodimer of IFNAR1 and IFNAR2; Interferon Alpha And Beta Receptor Subunit 1 and 2) in an auto- and paracrine manner and promote expression of a broad subset of ISGs via JAK-STAT signalling, involved in antiviral

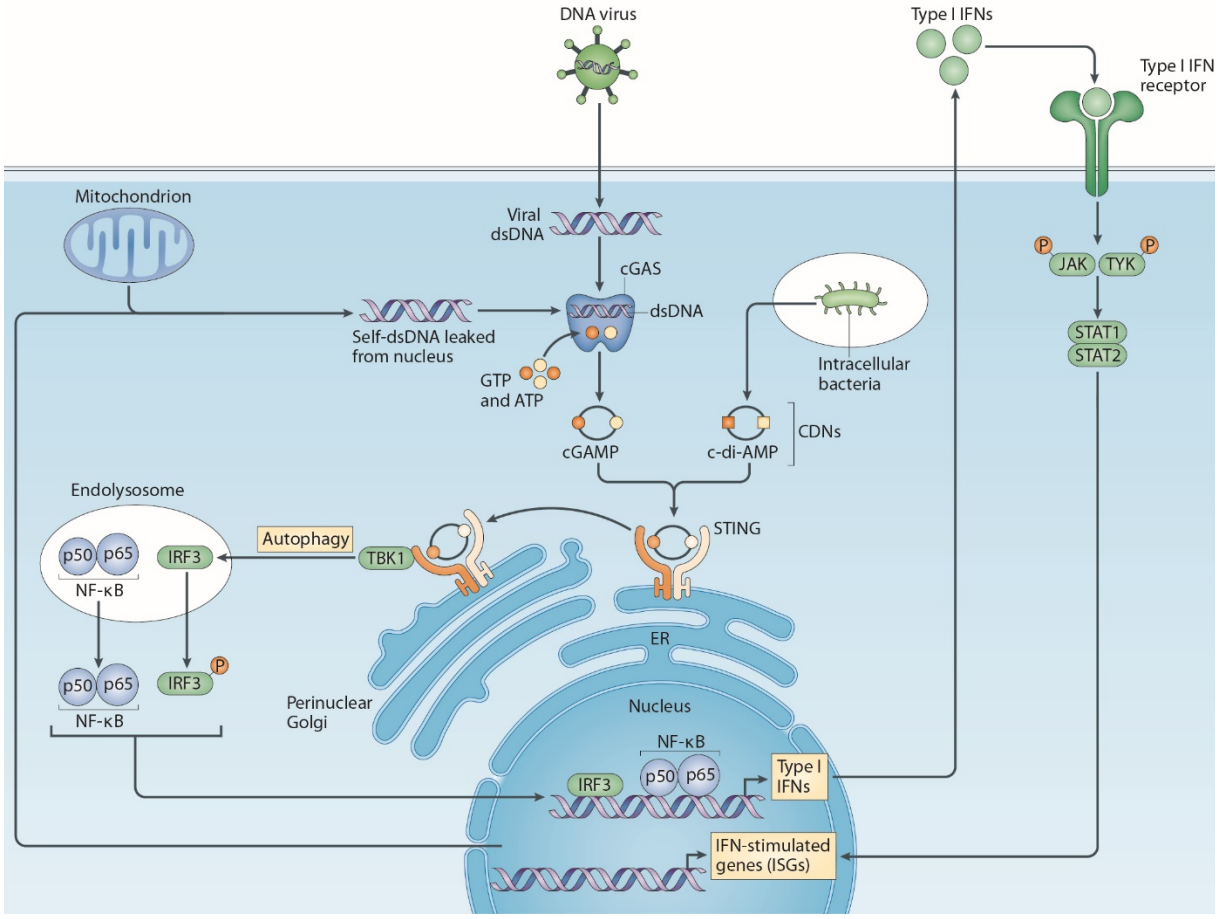

Figure 1-7: The Stimulator of Interferon Genes (STING) pathway

STING is an ER – resident adaptor protein involved in type I IFN induction following dsDNA or CDN detection. Cytosolic dsDNA, derived from dsDNA viruses or DNA – damage, is sensed by cGAS, which catalyses 2'3' cGAMP synthesis. cGAMP functions as a second messenger and is bound by STING, initiating STING activation. Likewise, STING also directly binds bacteria – derived CDNs (e.g. c-di-AMP). STING dimers subsequently translocate from the ER to the perinuclear Golgi and the endolysosome in an autophagy – reminiscent manner, where the transcription factors IRF3 and NFκB are activated via phosphorylation by TBK1. Following translocation and activation, STING is rapidly degraded by autophagy involving e.g. ATG9A, p62 and ULK1 to prevent sustained immune signalling. Type I IFNs are induced mainly as a consequence of IRF3 activation and signal in a para- and autocrine manner binding to the type I IFN receptor, which in turn induces ISGs via JAK-STAT signalling. With permission from Springer Nature modified from Barber et al., *Nat Rev Immunol* (2015)[217].

immunity, such as for example IFIT1 (Interferon Induced Protein With Tetratricopeptide Repeats 1), IFIT3 (Interferon Induced Protein With Tetratricopeptide Repeats 3) or CXCL10 (C-X-C motif chemokine 10)[229–231].

As a second class of cytokines besides IRF3-dependent type I IFNs, STING also mediates NFκB (comprised of a p50 and p65 subunit)-dependent release of proinflammatory cytokines, most prominently TNFα and IL6, in a process involving TBK1, but also other parts of the NFκB-signalling cascade[232–234]. Conversely, NFκB-signalling has been reported to form a vital part of the IRF3-dependent branch of STING - signalling[233,234].

1.3.2 Regulation of STING signalling

Since excessive innate immune activity can lead to inflammation and tissue damage, STING signalling is tightly controlled by a variety of mechanisms. Such mechanisms include regulation of ligand availability, a multitude of posttranslational modifications of STING itself and protein-protein interactions modulating STING stability, activity and trafficking. As to ligand availability, cytosolic DNA presence is limited by numerous Dnases distributed over the cellular compartments[235]. Additionally, DNA is usually sequestered in nucleus or mitochondria, where it is inaccessible to cGAS. With regard to posttranslational modifications and protein interactions, a plethora of mechanisms has been identified both negatively and positively regulating both cGAS and STING[229].

1.3.3 STING in bacterial and viral infection

DNA virus sensing by cGAS/STING signalling is essential for proper type I IFN response and subsequent ISG induction, which in turn prevents viral replication, assembly and release[230]. Such a critical role for STING in viral infection has been described for a broad number of viruses, among them herpes simplex virus 1 and 2, adenoviruses, murine gamma herpesvirus 68, papillomavirus and cytomegalovirus, but also retroviruses such as human immunodeficiency virus[207,216,236–239]. Thus, mice deficient for cGAS or STING show severely impaired ability to induce a proper type I IFN response and thereby suffer from heightened infection susceptibility and aggravated disease course.

STING is also a direct sensor for foreign nucleic acids, i.e. bacteria-derived CDNs such as cyclic diAMP or cyclic diGMP[240–244]. Such CDNs are derived from intracellular bacteria that escape into the cytosol, such as *L. monocytogenes*, and type I IFN production is a hallmark of *L. monocytogenes* infection[241,244,245]. *L. monocytogenes* replicates in the cytosol, where it releases cyclic diAMP via multidrug resistance efflux pumps[241,244]. Besides cyclic diAMP, *Listeria* DNA additionally activates the cGAS/STING pathway via DNA sensing by cGAS[245]. STING is however essential for *L. monocytogenes* mediated type I IFN induction both *in vitro* and *in vivo*[216,245,246].

1.3.4 STING-dependent cell death

Beyond cytokine induction, STING signalling is also involved in cell death pathways such as apoptosis, pyroptosis and necroptosis. Given that classically STING is involved in antiviral immunity, induction of cell death might resemble the last option to prevent viral replication when the viral burden is overwhelming. In monocytes, STING has been found to initiate proinflammatory pyroptotic cell death via activation of the NLRP3 inflammasome[247]. Unlike monocytes, in adaptive immune cells, i.e. T cells and B cells, STING activation can result in apoptosis[248–251]. A more recent study investigating STING function in T cells revealed that STING disrupts calcium homeostasis, thereby predisposing T cells to receptor-activation-induced ER-stress, in turn leading to apoptotic cell death[252].

Besides apoptosis and pyroptosis, STING and type I IFNs have recently been linked to necroptosis, another highly proinflammatory form of cell death. In macrophages, DNA sensing by cGAS/STING lead to RIPK3 (Receptor-interacting serine/threonine-protein kinase 3)-dependent necroptosis. This required both type I IFN and TNFα signalling[253]. Additionally, STING-dependent type I IFNs have also been found to be critical for maintaining MLKL (Mixed lineage kinase domain-like protein) expression, which is essential for necroptosis[254].

A recent study of our own group has provided further evidence supporting a role for STING signalling in necroptotic cell death induction[164]. In case of defective autophagy in IECs, the usually protective cytokine IL22 induced excessive STING-dependent type I IFNs, thereby predisposing to TNFα-induced necroptosis. Necroptotic cell death in turn lead to intestinal inflammation as a result of immune signalling in response to cell debris[164].

1.3.5 Regulation of STING signalling by endoplasmic reticulum stress

Given that STING is an ER-resident protein, one would assume that STING signalling and ER-stress responses, respectively the UPR, are somewhat interconnected. Accordingly, type I IFN production in response to LPS is enhanced if additionally ER-stress is induced[255]. This is mediated by the IRE1α/XBP1 branch of the UPR, as active XBP1 was found to bind an enhancer element upstream of the *Ifnb1* (coding for IFNβ) promotor[255]. Likewise, IRF3 recruitment to the *Ifnb1* promotor is enhanced by combining ER-stress and LPS stimulation[255]. Strikingly, in MEFs even without LPS exposure, ER-stress is able to engage IRF3 to induce a type I IFN response[256]. This is, however, dependent on the mode of ER-stress induction, only in part mediated by STING activation.

With regard to the implication of STING in cell death induction, in a model of alcoholic liver disease, STING was found to mediate apoptosis in response to ethanol induced ER-stress via association with IRF3 and the proapoptotic protein Bax (B-cell lymphoma 2-associated X protein), suggesting that ER-

stress, respectively the UPR, might engage STING to carry out apoptosis under unresolved ER-stress conditions[257].

STING activation in turn can also lead to ER-stress. As mentioned above (1.3.4, p. 26), STING activation due to a gain-of-function mutation in T cells results in an altered calcium homeostasis, which renders such T cells prone to ER-stress as a consequence of T cell receptor activation[252]. In another study on macrophages, intracellular infection with *L. monocytogenes* was found to result in ER-stress induction via STING activation by *Listeria*-derived cyclic diAMP[37]. As a consequence, autophagy is engaged to alleviate STING-induced ER-stress by removing stressed parts of the ER, thereby preventing macrophage death[37].

1.3.6 Interplay of STING signalling and autophagy

Besides posttranslational modifications and direct protein-interactions, STING signalling is also tightly controlled by (selective) autophagy. As mentioned above (1.3.1, p. 23), STING activation requires trafficking from ER to the perinuclear Golgi in an autophagy-like manner. Additionally, STING is degraded following activation to prevent excessive type I IFN signalling.

Conversely, STING is also directly involved in inducing antimicrobial autophagy. STING-containing ER-Golgi intermediate membranes for example have been found to serve as a membrane donator for LC3 lipidation (see 1.2.3.1, p. 12)[258]. Moreover, antibacterial autophagy responses rely on STING and are further involved in *Mycobacterium* and *Listeria* infection[37,259,260].

STING translocation from ER to the perinuclear Golgi and assembly with TBK1 and IRF3 are essential steps for STING activation and downstream type I IFN induction[224]. Autophagy-like processes are involved to facilitate this trafficking[227]. After activation, STING associates with TRAPβ, a member of the translocon-associated protein (TRAP) complex, which facilitates protein translocation from ER to perinuclear membrane structures[215], where STING colocalizes with SEC5[216]. Reminiscent of non-canonical autophagy necessary for TLR9 trafficking to interferon-signalling compartments[261], STING trafficking via autophagosomal membrane structures, together with TBK1, results in assembly of STING, TBK1 and IRF3, thus enabling downstream cytokine induction[227]. After autophagosome formation and completing trafficking through the Golgi, STING is then phosphorylated by ULK1, which in turn is activated by cGAMP to serve as a negative feedback loop, leading to subsequent degradation of STING[227], presumably to avoid excessive immune signalling.

STING was found to colocalize with ATG9A, an autophagy protein traveling between ER and Golgi (see 1.2.3.1, p. 12), but also with LC3 in autophagosome-like vesicles[146]. ATG9A-deficiency however lead to increased assembly of STING with TBK1, and accordingly to enhanced cytokine induction[146], altogether

suggesting that STING signalling, or at least assembly with TBK1 is abrogated by ATG9A-dependent autophagy to prevent sustained signalling.

In another study investigating STING degradation, STING was found to be sorted to endolysosomes for degradation, which was dependent on previous ER-exit of STING[262], in line with other results indicating that STING trafficking is essential for both activation and degradation[224]. Of note, blockage of lysosome acidification using Bafilomycin A1 (BafA) resulted in heightened type I IFN induction in response to cGAMP, indicating that impaired autophagy might give rise to excessive STING-dependent type I IFN induction. A more recent report demonstrated that STING is not only eliminated via autophagy, but also targeted by the selective autophagy receptor p62 for removal following activation[228]. This required previous phosphorylation of p62 by TBK1, thereby initiating a negative feedback loop. Consistent with Bafilomycin A1 treatment[262], p62 deficiency and thus impaired removal of STING also resulted in increased type I IFN production[228].

1.3.7 STING-dependent inflammation in autoimmunity

Uncontrolled STING activation and downstream type I IFN production results in severe inflammation, requiring strict regulation of induction and resolution of type I IFN production (1.3.2, p. 25, 1.3.6, p. 27). Accordingly, gain-of-function mutations in *TMEM173* promoting constitutive STING activation yield severe type I IFN mediated inflammatory disorders belonging to the field of interferonopathies[263–268]. Additionally, monogenic IFN-related diseases show a phenotypic overlap with non-monogenic diseases such as systemic lupus erythematosus or dermatomyositis, suggesting that nucleic acid sensing and type I IFNs contribute to inflammation in these autoinflammatory disorders, highlighting the proinflammatory potential of type I IFNs[263,269].

As to interferonopathies, the cGAS/STING pathway has been linked mechanistically to the pathophysiology of the monogenic disease Aicardi-Goutières syndrome (AGS)[236,270–273]. Among multiple mutations causing AGS, loss-of-function mutations in *TREX1* or *RNASEH2A* result in dsDNA sensing by cGAS and consequently proinflammatory type I IFN induction by STING activation[270,272–274]. Accordingly, additional deletion of either *Cgas* or *Tmem173* rescues *Trex1*-deficient mice from a lethal autoimmune phenotype[270,271,274], and RNase H2-deficiency mediated perinatal death is alleviated by additional *Tmem173* knockout[273].

Multiple dominant gain-of-function mutations in *TMEM173* have been identified as the underlying cause in patients suffering from SAVI (STING-associated vasculopathy with onset in infancy)[264,265,275]. SAVI-associated *TMEM173* mutations result in constitutive STING activation without presence of any ligands, leading to permanent STING ER-exit, trafficking and activation[224]. Hyperactivation of STING as a consequence of these gain-of-function mutations and subsequent type I IFN production then results

in sterile inflammation, mainly affecting the skin and the lungs[265,267]. SAVI patients commonly present with ulcera of the skin and pulmonary fibrosis, eventually leading to respiratory failure[265,267].

1.3.8 Role of STING signalling in intestinal homeostasis

While STING variants leading to excessive STING activity have been linked to autoinflammatory disorders, GWAS have not found *TMEM173* variants associated to IBD. Type I IFNs however seem to be critical for intestinal homeostasis, indicating that STING, as a central upstream regulator of type I IFNs, might likewise inherit a central role in balancing immunity and inflammation in the gut. Physiologically, type I IFNs fulfil antiviral, antiproliferative and immunomodulatory functions[276–278]. Identification of variants in the type I IFN receptor gene *IFNAR1* linked to IBD thus suggests a causal implication of type I IFN signalling for development of inflammation and IBD[279]. Furthermore, ISG expression in IBD patients correlates with disease activity and impaired therapy response[141], suggesting that uncontrolled IFN production underlies therapy-refractory intestinal inflammation. While abrogation of type I IFN signalling in *Ifnar1* -/- mice impairs disease course in DSS-induced colitis, *Ifnar1*$^{\Delta IEC}$ mice however do not suffer more from DSS-treatment than IFNAR1-proficient mice[279,280]. Instead, abrogation of epithelial IFNAR1 signalling results in epithelial hyperproliferation, leading to increased Paneth cell and Goblet cell numbers, and, ultimately, to increased intestinal carcinogenesis[279], in line with the antiproliferative function of type I IFNs[277]. Of note, disruption of type I IFN signalling in *Ifnar1*$^{\Delta IEC}$ mice also lead to an altered microbial composition, suggesting a crucial role of type I IFNs in shaping the microbial environment[279].

The association of *IFNAR1* to IBD suggests a crucial role for STING as it resembles a main coordinator of type I IFN production. Notably, a recent study on paediatric IBD patients has found *TMEM173* to be hypomethylated in IECs and human intestinal organoids of these patients, suggesting a functional implication of STING signalling in intestinal inflammation[281]. Although to date there is no data available investigating STING function specifically in the intestinal epithelium (i.e. employing *Tmem173*$^{\Delta IEC}$ mice), multiple studies on *Tmem173* -/- mice support a critical role for STING in maintaining intestinal homeostasis as well as in induction of inflammation. According to the dual role of type I IFNs, i.e. on the one hand mediating destructive inflammation[264–270,272–275], on the other hand essential for proper epithelial development and microbe interaction[279], also STING carries out both favourable and detrimental functions.

In a model of IL10 induced colitis, STING was found to sense microbial presence and subsequently transmit proinflammatory signals[282], suggesting that STING might rather promote than restrict intestinal inflammation. In line with this, STING can be activated by faecal content, thus directly sense the microbial environment[283]. In turn, *Tmem173* -/- mice also present with a microbial composition

altered towards a more inflammatory profile, suggesting that transmission of microbial signals via STING is key for proper microbial ecology shaping by the epithelium[283]. In line with a more proinflammatory role for STING, in a model of intestinal injury-induced sepsis, STING was found to promote microbial translocation, gut permeability and intestinal apoptosis. *Tmem173* knockout accordingly alleviated sepsis symptoms, while additional pharmaceutical stimulation of STING with a STING agonist further aggravated the inflammatory response[284].

On the other hand, in DSS-induced colitis and *Salmonella* infection, *Tmem173* -/- mice suffered more compared to wildtype mice[283], demonstrating a protective role of STING signalling in intestinal inflammation. In both DSS-colitis and *Salmonella* infection, inflammation is however the consequence of a disrupted epithelial barrier function, promoting microbial tissue invasion, or direct infection.

Conversely, in a recent study of our own group, unleashed STING signalling due to defective autophagy was found to mediate potent inflammatory signals in response to the usually protective cytokine IL22, supporting a role of STING as a protective PRR, but also potent proinflammatory type I IFN inducer in response to other stimuli, or in case of failing negative regulatory mechanisms (i.e. autophagy) respectively[164].

In conclusion, both studies on human autoinflammatory disease involving STING and studies employing mouse models of intestinal injury or barrier disruption have revealed an important role for STING in maintaining gut homeostasis. STING can either give rise to infection and inflammation susceptibility, or protect from e.g. microbially induced inflammation. However, STING function in specific cell types remains to be determined.

2 Aims & hypothesis of the study

While STING signalling in immune cells has been extensively studied, little is known about its role in intestinal epithelial cells. Thus, the overall aim of this study is to investigate function and regulation of STING in the intestinal epithelium.

Additionally, there is mounting evidence that STING signalling might be critically regulated by ER-stress-dependent mechanisms, such as the UPR and autophagy. Likewise, the role of ER-stress and defective autophagy in IECs in IBD is well characterized, suggesting shared mechanisms for both. Finally, type I IFNs have been linked to IBD. This might result from disturbed STING - regulatory mechanisms due to ER-stress or defective autophagy. Accordingly, the interplay of STING signalling and IBD risk genes such as *XBP1* or *ATG16L1* shall be addressed to provide data on a possible implication for STING signalling in IBD pathophysiology.

Altogether, the goals of this study are to answer the following questions:

(1) Is STING expressed in the intestinal epithelium?
(2) What regulatory mechanisms control STING, respectively *TMEM173*, expression and function in intestinal epithelial cells?
(3) Given such regulations, how is STING signalling affected by IBD risk genes such as *XBP1* or *ATG16L1* and what are possible clinical consequences?

Based on previous research, the following hypotheses are proposed and will be tested:

(1) STING is expressed in the intestinal epithelium and fulfils a role mainly centred around pathogen defence.
(2) STING in IECs is regulated by microbial signals and ER-stress and controlled by autophagy once activated.
(3) Presence or absence of IBD risk genes involved in ER-stress responses and autophagy critically determines, i.e. exacerbates or suppresses STING signalling.

3 Methods and materials

3.1 Materials

A detailed list of all materials used in this study (buffers, solutions, chemicals, reagents, kits, plasmids, antibodies, devices and consumables) can be found in the appendix (9, p. 96).

3.2 Cell biological methods

3.2.1 Cell lines

In this study, the SV40 large T-antigen-immortalized murine small intestinal epithelial cell line MODE-K[285] was employed as an *in vitro* model for the intestinal epithelium. MODE-K cells harbouring an RNA interference (RNAi) based knockdown of *Xbp1* and a control RNA interference (i*Xbp1*, iCtrl) were kindly gifted by Artur Kaser, University of Cambridge[19]. In brief, RNA interference was achieved by stable introduction of a small hairpin RNA specific for *Xbp1* and a control small hairpin RNA identical to Lee et al. (2013)[286], except that SFGΔU3hygro was used. Knockdown of *Xbp1* was confirmed by qPCR.

Table 1: Components for 565ml MODE-K culture medium

Medium component	amount	concentration	Supplier
DMEM GlutaMAX	500 ml	-	Gibco/Life Technologies, Darmstadt, Germany
Fecal calf serum	50 ml	-	Gibco/Life Technologies, Darmstadt, Germany
HEPES	5 ml	1 M	Gibco/Life Technologies, Darmstadt, Germany
MEM Non-Essential Amino Acids Solution	5 ml	100 x	Gibco/Life Technologies, Darmstadt, Germany
Penicillin/Streptomycin	5 ml	10000 U/ml	Gibco/Life Technologies, Darmstadt, Germany

Cells were cultured in the respective media (Table 1) and incubated at 37 °C with 5 % (v/v) carbon dioxide. For splitting, cells were first washed with PBS and then treated with a trypsin/EDTA solution (Life Technologies, Darmstadt, Germany) for 5 min at 37 °, enabling dissociation. After complete detachment, trypsin was antagonized by adding full culture media to prevent cell digestion. Cells were centrifuged at 300 g for 5 min, resuspended in fresh media and plated out at the desired concentration (see Table 2). Cell culture work was generally run in a laminar flow hood providing semi-sterile conditions (Thermo Scientific, Bremen, Germany).

Table 2: Cell seeding numbers

Culture dish	Cells per well (for transfection experiment)	Cells per well (for stimulation experiment)	Medium per well	Used for
25 ml flask	$5x10^6$	-	25 ml	
10 ml flask	$1,5x10^6$	$2,5x10^6$	10 ml	Protein isolation
6 - well plate	$2x10^5$	$3x10^5$	2 ml	Protein isolation
12 - well plate	$1x10^5$	$1,5x10^5$	1 ml	Protein isolation
24 - well plate	$0,5x10^5$	$0,75x10^5$	500 µL	Cell death assay, RNA isolation

3.2.2 Isolation of crypts and murine small intestinal organoid cultures

Isolation of crypts from mouse small intestine was achieved by EDTA-based Ca^{2+}/Mg^{2+} chelation. Small intestinal organoid cultures were established and maintained as first described by Sato et al. (2009)[287]. In brief, isolated crypts form 3D organoids if provided with a 3D growing matrix and a special medium containing growth and stem cell niche factors. Organoids resemble epithelial crypt growth *in vitro*, growing in a three-dimensional manner, forming a central lumen that is surrounded by a polarized epithelial layer. Just like the intestinal epithelium *in vivo*, organoids continuously renew the epithelium and differentiate into the respective epithelial cell lines (e.g. Paneth cells, stem cells, enterocytes, Goblet cells). Multiple crypt-like structures project outward. The basal side of the epithelial cells is oriented towards the outside, whereas the apical side is orientated towards the lumen[288].

In brief, the small intestine was removed and cut longitudinally. The intestine was then cut in small pieces of approximately 5 mm. After thorough washing to remove most contamination, the pieces were incubated in cold PBS with 10 nM EDTA for 10 min with vigorous shaking. Supernatant was removed and the PBS - EDTA solution was added again. This procedure was repeated four times. The resulting crypt suspension was passed through a 100 µm strainer and centrifuged at 1200 rpm at 4 °C for five minutes. Supernatant was removed and epithelial crypts were resuspended in a 2:1 Matrigel-PBS suspension (5-10 crypts/1 µl Matrigel) (BD Bioscience, Heidelberg, Germany), if crypts were not directly used or stored at -80 °C for protein or RNA harvesting. Matrigel provides a 3D laminin- and collagen-rich matrix resembling the basal lamina. 40 µl of the crypt-Matrigel-PBS-suspension was embedded in pre-cooled 24 well plates and incubated at 37 °C for 15 min to let the gel polymerize. Organoids were cultivated in ENR medium as described before[289].

In essence, a medium consisting of accordingly diluted 2x basal culture medium (Table 3, Advanced DMEM/F12 containing 10 % fetal bovine serum (Gibco/Life Technologies, Darmstadt, Germany), 10 mM HEPES (Gibco/Life Technologies, Darmstadt, Germany), 1 % penicillin/streptomycin (Gibco/Life Technologies, Darmstadt, Germany)) and murine EGF (epidermal growth factor), murine Noggin and human R-Spondin 1 was used (hereafter named ENR medium according to the components EGF, Noggin and R-Spondin 1). Medium was changed every two to three days, organoids were passaged every five to seven days and experiments were carried out after four days of cultivation.

Table 3: 2x basal culture medium composition

Component	Amount (for 25ml)	stock concentration	Supplier
Advanced DMEM/F12	23,4 ml	-	Gibco/Life Technologies, Darmstadt, Germany
Penicillin/Streptomycin	500 µl	10000 U/ml	Gibco/Life Technologies, Darmstadt, Germany
HEPES	500 µl	1 M	Gibco/Life Technologies, Darmstadt, Germany
GlutaMAX supplement	500 µl	100x	Gibco/Life Technologies, Darmstadt, Germany

For passaging organoids, medium was removed and the well was flushed with 1 ml of ice-cold PBS. After pipetting up and down for five to ten times the organoid - containing gel dissociated from the well and suspensions were collected in a 15 ml falcon. After centrifugation at 500 g for three minutes, the supernatant and excessive Matrigel were removed, leaving a loose pellet of organoids which was then vigorously resuspended in 100 µl of cold PBS to break down organoids to single crypt structures. Afterwards, crypts were again seeded out in 2:1 Matrigel - PBS suspension.

Cryopreservation and thawing of organoids was performed according to manufacturer's protocol of StemCell Technologies using CryoStor™ CS10.

3.2.2.1 Organoid enrichment for specific epithelial lineages

To study cell-type-specific effects, murine small intestinal organoids were enriched for specific epithelial lineages as described before (Table 4)[289]. Briefly, organoids were enriched for stem cells using ENR medium supplemented with 3 µM CHIR99021 (Stemgent, Cambridge, USA) and 1 mM Valproic acid (Sigma-Aldrich, St. Louis, USA) (ENR-CV) for two days. Next, stem cell-enriched organoids were subjected to enrichment for either Paneth cells, enterocytes or goblet cells, or further cultivated in stem-cell enriching medium (ENR-CV). For Paneth cell enrichment, 3 µM CHIR99021 and 10 µM DAPT (Stemgent, Cambridge, USA) was added to ENR medium. Enterocyte differentiation was induced

adding 2 µM IWP-2 (Stemgent, Cambridge, USA) and 1 mM Valproic acid to the ENR medium (ENR-IV), and Goblet cell enrichment was induced by adding 2 µM IWP-2 and 10 µM DAPT (ENR-ID).

Table 4: Organoid enrichment for specific epithelial lineages

Medium	Predominant cell type	Special components
ENR	All cell types of the intestinal epithelium	EGF, Noggin, R-Spondin 1
ENR-CV	Stem cells	CHIR99021, Valproic acid
ENR-CD	Paneth cells	CHIR99021, DAPT
ENR-IV	Enterocytes	IWP-2, Valproic acid
ENR-ID	Goblet cells	IWP-2, DAPT

3.2.2.2 Tamoxifen-inducible n*Atf6* overexpressing small intestinal organoids

Small intestinal organoids with a Tamoxifen inducible overexpression of active ATF6 (nATF6) were derived from Tamoxifen-inducible Villin-Cre nAtf6^{IEC} tg/tg mice and kindly provided by Dr. Olivia Coleman and Prof. Dr. Dirk Haller, Technische Universität München. Mice were generated as described previously[196]. Organoids were cultures as described above (3.2.2) and overexpression was induced by adding 500 nM Tamoxifen to the medium for the respective time course.

3.2.3 Isolation of crypts and human small intestinal organoid cultures

Human intestinal biopsy specimens were obtained from patients who underwent endoscopic examination for the diagnosis of digestive symptoms or the evaluation of diseases such as CD or UC. Ileal biopsies were taken from macroscopically non-inflamed and inflamed mucosa of IBD patients. Isolation of crypts and subsequent establishment of intestinal organoids were performed as previously described[290]. Briefly, crypts were collected by rigorously shaking biopsy specimens in 2.5 mM EDTA. Isolated crypts were embedded in 40 µl of 2:1 Matrigel at a density of 100-200 crypts per well and placed in a 24 well culture dish. Crypts were maintained conditioned medium consisting of 50 % L-WRN and accordingly diluted 2x basal culture medium (Table 3), supplemented with recombinant human EGF (50 ng/ml, PeproTech, Hamburg, Germany), Y-27632 (10 µM, Sigma-Aldrich, St.Louis, USA), A83-01 (500 nM, Tocris, Bristol,UK), Nicotinamide (10 mM, Sigma-Aldrich, St.Louis, USA), N2 supplement and B12 supplement (ThermoFisher Scientific, Waltham, USA), SB202190 (10 µM, Enzo Lörrach, Germany), human Gastrin I (10 nM, Sigma-Aldrich, St. Louis, USA), A8301 (500 nM, Tocris Bioscience, Bristol, UK) and CHIR99021 (10 µM). 50 % L-WRN conditioned media was generated as previously described using a L-WRN producing cell line[291]. Human organoids were passaged every 6-7 days as described above (3.2.2, p. 33).

The study was approved by the Ethics Committee of B231/98 and written informed consent was obtained from each patient.

3.2.4 Transfection of plasmid DNA

For transfection of plasmid DNA into cultured cells, Lipofectamine™ 3000 Transfection Reagent (ThermoFisher Scientific, Waltham, USA) was used according to the manufacturer's protocol. MODE-K cells were transfected with plasmid DNA-lipid complex the day following cell seeding. MODE-K cells were therefore plated out at lower density in order to reach a 70-90 % confluency at timepoint of plasmid DNA transfection.

In brief, Lipofectamine™ 3000 Reagent was diluted in Opti-MEM™ medium (Gibco/Life Technologies, Darmstadt, Germany) and briefly mixed. Plasmid DNA was diluted in Opti-MEM™ medium, then the P3000™ reagent mix was added. Diluted DNA was then transferred to the prepared tube of Lipofectamine™ 3000 at a 1:1 ratio and incubated for 15 min to allow for DNA-lipid complex formation. Next, the DNA-lipid complex was added to the cells according to well size. Experiments were carried out 48 h after plasmid transfection.

For a 6 well plate well containing 2 ml of media, 250 µL DNA-lipid complex, a total DNA amount of 2500 µg, 5 µl of P3000™ reagent and 3,75 µg of Lipofectamine™ 3000 reagent was used, and scaled up or down according to well size.

3.2.5 Transfection of siRNA

Small interfering RNA (siRNA) was transfected using Viromer® Blue (Lipocalyx, Halle, Germany) according to the manufacturer's protocol. MODE-K cells were seeded at lower cell number (Table 2) and transfected the following day. Briefly, siRNA was diluted in Viromer® Blue buffer to a concentration of 2,75 µM. Viromer® Blue was diluted in Viromer® Blue buffer in a 1:100 ratio. After brief mixing, the Viromer® Blue-buffer mix was transferred to the tube containing the siRNA-buffer mix in a 10:1 ratio, followed by 15 min incubation at room temperature to allow for complexation. Afterwards, the complexed siRNA was added to the cells in a 1:10 siRNA-medium ratio. Experiments were carried out one or two days following siRNA transfection.

3.3 Molecular biological methods

3.3.1 RNA isolation

RNA extraction was performed using the RNeasy Mini Kit (Qiagen, Hilden, Germany) according to the manufacturer's instruction. Samples were disrupted and homogenized using the TissueLyser II (Qiagen, Hilden, Germany) and 350 µL RLT buffer with 1 % β-mercaptoethanol. Cells were usually lysed directly in the cell-culture plate and lysates were subsequently transferred into a tube. To minimize

contaminations by DNA, DNase digestion using the RNase-Free DNase Set (Qiagen, Hilden, Germany) was performed. RNA was eluted in 10-15 µl RNase-free water and RNA concentration was determined using the NanoDrop ND-1000 spectrophotometer (PeqLab Biotechnologie GmbH, Erlangen, Germany). Finally, RNA was stored at -80 °C or directly used for cDNA synthesis, respectively.

3.3.2 cDNA synthesis

To generate cDNA, 100-1000 ng total RNA (depending on the amount of previously extraced RNA) was transcribed into complementary DNA (cDNA) by reverse transcription using the Maxima H Minus First Strand cDNA Synthesis Kit (Thermo Scientific, Bremen, Germany). Reverse transcription was performed following the manufacturer´s instruction (Table 5). The synthesized cDNA was stored at -20 °C or -80 °C.

Table 5: Reverse transcription with the Maxima H Minus First Strand cDNA synthesis kit

Step	Component	Quantity	Temperature	Time
1	RNA	100-1000ng	65 °C	5 min
	Oligo(dt)18 oligonucleotide	0,125 µl		
	dNTP mix (10 Mm each)	0,5 µl		
2	nuclease-free water	to 7,5 µl	25 °C	10 min
	5x RT buffer	2 µl	50 °C	15 min
	Maxima H Minus RT	0,5 µl	85 °C	5 min

3.3.3 Quantitative real-time polymerase chain reaction

Quantitative real-time PCRs (q-RT-PCR) was used to amplify and simultaneously quantify mRNA levels using target-specific oligonucleotides. Predesigned TaqMan probes (Applied Biosystems, Carlsbad, USA were purchased and used. TaqMan probes are listed in the supplementary material (Table 23). The 7900HT Fast Real Time PCR System (Applied Biosystems, Darmstadt, Germany) was used for qPCR experiments. Samples were run in duplicates on 384-well plates.

For the PCR reaction, 5-10 ng cDNA and 0,5 µl of the respective TaqMan gene expression assay were used. The PCR program was carried out following the manufacturer's recommendation (TaqMan Gene Expression Master Mix protocol, Applied Biosystems, Darmstadt, Germany). To standardize and compare gene expression of the respective target gene, cycle threshold (Ct) values of the target genes were compared to the respective mRNA levels of housekeeping genes (usually *actinb*, if not otherwise stated).

3.3.4 Plasmid DNA isolation

After multiplication of genetically modified plasmids in *E. coli* cultures, plasmids were isolated by alkaline lysis. The PureLink® HiPure Plasmid Filter Midiprep Kit (Life Technologies, Darmstadt, Germany) was used and plasmids were isolated following the manufacturer's recommendation. DNA concentration was determined using the NanoDrop ND-1000 spectrophotometer (PeqLab Biotechnologie GmbH, Erlangen, Germany). Plasmid DNA was frozen and stored at -20 °C or -80° C.

3.3.5 Quantification of cell death in organoids & cell lines

Organoids and cell lines were cultivated in 24 well plates as described above. After carrying out the experiment, medium was removed and the organoids/cells washed once with PBS.

Organoids were then resuspended in 1 ml of cold PBS, transferred to a 1,5 ml tube and pelleted after centrifugation at 4 °C, 400 g for 5 min. Supernatants were removed. Next, organoids were incubated in TrypLE Express (ThermoFisher Scientific, Waltham, USA) for 5 min at 37 °C to dissociate cells, followed by washing with cold PBS. Cells were then incubated 1 h in staining solution containing 2 µl Propidiumiodide (PI) (BD, Franklin Lakes, USA) and 98 µl PBS. Next, flow cytometry analysis using BD FACSCalibur™ (BD, Franklin Lakes, USA) was performed. Data was analysed using the free flow cytometry analysis software Flowing Software[292]. The gating strategy involved plotting FL-2H for PI fluorescence intensity against forward scatter (FSC) to distinguish PI_{high} vs PI_{low} populations which are assumed to be dead vs living cells. These gates excluded cellular clumps with did not dissociate well after TrypLE Express treatment. Dead cells were then first quantified as fraction of dead cells (= dead cells/total single cells).

For analysis of cell death in MODE-K cells, 150 µl of trypsin/EDTA solution (Gibco/Life Technologies, Darmstadt, Germany) was added to each well. Cells were incubated at 37 °C for 10 to 15 min until cells lost adhesion. Next, 300 µl DMEM with 10 % fetal calf serum (Gibco/Life Technologies, Darmstadt, Germany) was added to each well to neutralize the trypsin. Cells were then transferred to 1,5 ml tubes and centrifuged at 3000 g for 2 min. After discarding supernatants, the staining solution was applied (see above).

To visualise dead cells, 1 µl of PI was added to 500 µl medium for 4 hours beforehand flow cytometry analysis. Medium was then removed and replaced by PBS. Merged images with a bright-field image overlaid by a RFP-filtered fluorescence channel capture (red fluorescent cells indicate PI^+ dead cells) or only RFP-filtered fluorescence channel images were generated using Zeiss Axio Vert.A1 observer (Jena, Germany) and Zeiss AxioVision LE software. Images are shown at indicated magnification.

3.4 Protein biochemical methods

3.4.1 Protein lysate preparation

Cells and tissues were lysed using 40-100 µl SDS-based DLB buffer + 1 % Halt™ Protease inhibitor cocktail (ThermoFisher Scientific, Waltham, USA) before incubation for 5 minutes at 95°C followed by sonification for 2x 5 seconds. To remove cell remnants, lysates were centrifuged at 16.000 x *g* for 15 minutes at 4°C and supernatants were transferred into a new tube. For protein extraction of organoids, Matrigel™ was removed by incubation of organoids in Corning™ Cell Recovery Solution (Corning, New York, USA) for 45-60 min at ice after transferring organoids to tubes, centrifugation at 3000 g for 2 min and discarding supernatants. Next, the lysis buffer as described above was added.

3.4.2 Protein concentration determination

The protein concentration was determined applying the copper-based DC Protein Assay (Bio-Rad, Munich, Germany) according to the manufacturer´s protocol. This is a colorimetric assay (adapted from Lowry[293]) based on the biuret reaction. In brief, in an alkaline environment copper ions react with peptide bonds, resulting in monovalent copper ions. Such monovalent copper ions subsequently react with the Folin reagent, reducing the Folin to a blue colored substance. This can be quantified measuring absorbance at 750 nm.

According to the manufacturer's instruction, 5 µl of protein lysate was diluted with 5 µl of aqua bidest. and the assay reagents were added. After 15 min of incubation at room temperature with slight shaking, the absorbance was measured. A microplate reader Infinite M200 Pro (Tecan, Männedorf, Switzerland) and its associated software i-control 1.9 (Tecan, Männedorf, Switzerland) were used. Absorbance of the sample was correlated with protein concentrations of a bovine serum albumin (BSA) standard curve.

3.4.3 Gel electrophoresis of proteins

Proteins were separated by their molecular weight using self-prepared polyacrylamide gels or precast gradient polyacrylamide gels for improved separation of a wide range of proteins (NuPAGE® 4-12 % Bis-Tris gels, Life Technologies, Darmstadt, Germany). Self-prepared gels consisted of a 12 or 15 % acrylamide separation gel and a 3 % stacking gel (Table 6).

Table 6: Components of self - prepared acrylamide gels

Components	12 % acrylamide gel	15 % acrylamide gel	3 % stacking gel
Distilled water	3,5 ml	2,5 ml	1,95 ml
Buffer	2,5 ml (separation)	2,5 ml (separation)	0,75 ml (stacking)
30% bisacrylamide (35,7:1)	4 ml	5 ml	0,3 ml
TEMED	10 µl	10 µl	10 µl
10 % APS	100 µl	100 µl	30 µl

For using commercially available NuPAGE gels, protein lysates were prepared by supplementation with the corresponding NuPAGE LDS Sample Buffer (Thermo Scientific, Bremen, Germany), followed by incubation at 70 °C for 70 min. SDS-PAGE electrophoresis was run at 160 V and a maximum current of 300 mA for 1 to 2 h in the XCell SureLock Mini Cell system (Life Technologies, Darmstadt, Germany). NuPAGE MOPS SDS running buffer was used to run the gels and Prestained PageRuler plus protein ladder 10-250 K (Thermo Scientific, Bremen, Germany) served to estimate protein size.

Electrophoresis of self-prepared polyacrylamide gels was performed in 1x Tris/Glycine/SDS (TGS) buffer at 75V (maximum current of 300mA) for 15 min followed by 150V (maximum current of 300mA) for 60 to 90 min.

3.4.4 Western blot analysis & immunodetection

To detect proteins using immunodetection by specific antibodies, separated proteins were transferred onto polyvinylidene difluoride (PVDF) membranes. PVDF membranes (Bio-Rad, Munich, Germany) were activated under mild agitation using methanol for 10 s, followed by 5 min of washing in A. bidest. and then transferred for 5 min to anode buffer 1. Separated proteins were transferred from the gel onto the membrane by semi-dry blotting using the Trans-Blot Turbo™ Transfer System (Bio-Rad, Munich, Germany) with a discontinuous buffer system consisting of one cathode buffer and two anode buffers. Proteins were blotted onto the membrane at 0,3 A, 25 V for 60 min.

In order to prevent unspecific binding of antibodies, after the transfer membranes were blocked with 5 % (w/v) blotting grade blocker (non-fat dry milk) in Tris - buffered saline (TBS) supplemented with 0.1 % (v/v) Tween 20 (TBS - T) for 1 h. For specific protein detection, membranes were probed with the appropriate primary and secondary antibody (see Table 21 and Table 22). The primary antibody was applied in 5 % (w/v) blotting grade blocker (non-fat dry milk) or bovine serum albumin (BSA) in Tris-buffered saline (TBS) supplemented with 0.1 % (v/v) Tween 20 according to the manufacturer's instruction and incubated overnight at 4 °C under mild shaking. Next, the membrane was washed three times with TBS - T for 15 min to remove excess antibody. To detect primary antibody bound to membrane-bound proteins, a horseradish peroxidase (HRP) conjugated secondary antibody

recognizing the Fc region of the primary antibody was diluted in 5 % (w/v) blotting grade blocker (non-fat dry milk) in TBS-T according to the manufacturer's recommendation and incubated for 1 h at room temperature. Binding of the secondary antibody was detected using a chemiluminescent substrate kit (Thermo Scientific) and recorded with an automated developer machine (Agfa, Mortsel, Belgium).

If required, quantification of Western blot results was performed using GelAnalyzer 19.1 (www.gelanalyzer.com) by Istvan Lazar Jr., PhD and Istvan Lazar Sr., PhD, CSc according to the developer's recommendation (http://www.gelanalyzer.com/gelanalyzer-19.1-user-manual.pdf).

3.5 Microbiological methods

3.5.1 Bacterial infection of MODE-K cells

MODE-K cells were infected with *Listeria monocytogenes* to test type I IFN induction in response to live bacteria. Therefore, MODE-K were cultured as described above (3.2.1, p. 32), but with medium lacking antibiotics to allow for bacterial infection.

Listeria monocytogenes serotype 1/2a strain EGD was used to test type I IFN induction in MODE-K cells. Bacteria were plated out from glycerol stocks onto brain-heart infusion (BHI; BD Biosciences, Franklin Lakes, USA) agar plates overnight. *Listeria* colonies were then transferred into 1 ml BHI medium and incubated overnight at 37 °C to allow for bacterial replication. Next, bacteria were diluted and reincubated at 37 °C to induce a log - phase growth until OD600 = 0.6 was reached. After washing with PBS, bacteria were diluted in MODE-K medium without antibiotics and added to the cells according to multiciply of infection (MOI). As described above[294], MODE-K cells were infected at a MOI of 50. After allowing bacterial invasion for 1 h, the bacteria-containing medium was removed, cells were washed once with PBS and then treated with gentamicin (50 µg/ml) for 1 h to kill extracellular bacteria. The gentamicin-containing medium was then replaced with medium containing a lower concentration of Gentamicin (5 µg/ml), and cells were lysed after another 23 h as described above (3.3.1, p. 36).

3.5.2 Virus infection & replication assay

Infection experiments with murine CMV were carried out by Samuel Windross and Prof. Søren Riis Paludan, Department of Biomedicine, Aarhus University. mCMV was prepared as described previously[295] and infection of MODE-K cells was performed at a MOI of 10. Fold induction of mCMV was quantified by RT-PCR using the following primer sequence:

Table 7: Primer sequence used to assess mCMV virus load.

Target	Species	Used primers (forward, reverse)
mCMV M54 gene	virus	ATCATCCGTTGCATCTCGTTG CGCCATCTGTATCCGTCCAT

3.5.3 Oligo - Mouse-Microbiota

The oligo-mouse-microbiota (OMM)[296] consists of 12 bacterial strains representing members of the major bacterial phyla of the mouse gastrointestinal tract. Gnotobiotic mice colonized with an OMM have a stable OMM microbial community over several mouse generations, which provides colonization resistance against pathogens such as *Salmonella* Serovar *Typhimurium*. Accordingly, the OMM flora can be used to model a simplified gastrointestinal microbial ecology.

To test for microbe-dependent gene regulation, the OMM strains were cultivated as described previously[296] and subsequently centrifuged in order to separate live bacteria and supernatant. Only supernatants (containing e.g. bacterial metabolites) were used to stimulate cells. OMM supernatants were kindly provided by Dr. Felix Sommer and Kenneth Klischies.

3.6 Generation, handling & treatment of mice

3.6.1 Generation of mouselines

For this study, the following mouse lines were used:

Table 8: Mouselines used in this study

Mouse line	Genotype
Xbp1$^{\Delta IEC}$	*Xbp1*$^{fl/fl}$;VillinCre$^{+/-}$
Xbp1$^{fl/fl}$	*Xbp1*$^{fl/fl}$;VillinCre$^{-/-}$
Atg16l1$^{\Delta IEC}$	*Atg16l1* $^{fl/fl}$;VillinCre$^{+/-}$
Xbp1/Atg16l1$^{\Delta IEC}$	*Xbp1/Atg16l1*fl/fl;VillinCre$^{+/-}$
Tmem173 -/-	*Tmem173* -/-
n*Atf6* Vil-Cre$^{ERT2\ Tg}$	n*Atf6*$^{tg/tg}$;VillinCre^{ERT2}
n*Atf6*^{IEC} tg/tg, n*Atf6*^{IEC} fl/tg, n*Atf6*^{IEC} fl/fl	n*Atf6*^{IEC} tg/tg, n*Atf6*^{IEC} fl/tg, n*Atf6*^{IEC} fl/fl
Wildtype	C57BL/6J

Atg16l1$^{\Delta IEC}$, *Xbp1*$^{\Delta IEC}$ and *Xbp1/Atg16l1* $^{\Delta IEC}$ mice have been described previously[19,40]. In brief, *Atg16l1*$^{fl/fl}$ mice were generated by insertion of LoxP sites flanking the exon 1 of the *Atg16l1* gene (Genoway, Lyon, France). *Xbp1*$^{fl/fl}$ mice were generated by targeted insertion of LoxP sites flanking the exon 2 of the *Xbp1* gene. VillinCre$^{+/-}$ mice (strain: B6.SJL-Tg (Vil-cre)997Gum/J) were purchased from Jackson Laboratory.

Conditional knockout of *Atg16l1* and *Xbp1* in the intestinal epithelium was then established by crossing VillinCre$^{+/-}$ mice with *Atg16l1*$^{fl/fl}$ or *Xbp1*$^{fl/fl}$ mice, resulting in specific deletion of *Atg16l1* (*Atg16l1*$^{\Delta IEC}$) and *Xbp1* (*Xbp1*$^{\Delta IEC}$) in the intestinal epithelium. *Xbp1/Atg16l1*$^{\Delta IEC}$ double knockout mice were created by crossing *Xbp1*$^{\Delta IEC}$ mice with *Atg16l1*$^{\Delta IEC}$.

Homo- and heterozygous nATF6-HA-overexpressing mice (n*Atf6*^{IEC} tg/tg and tg/wt) and floxed controls (n*Atf6*^{IEC} fl/fl) were generated as described previously as well as Tamoxifen-inducible Villin-Cre nAtf6^{IEC} mice (nATF6 Vil-Cre$^{ERT2\ Tg}$)[196]. Small intestinal sections of those mouse lines were kindly gifted by Dr. Olivia Coleman and Prof. Dr. Dirk Haller, Technische Universität München.

3.6.2 Germ-free mice

Xbp1$^{\Delta IEC}$ and *Xbp1*$^{fl/fl}$ germ-free mouse (described previously[40]) small intestinal sections were kindly gifted by A. Kaser, University of Cambridge.

3.6.3 Animal housing & animal care

Xbp1$^{\Delta IEC}$, *Xbp1*$^{fl/fl}$, *Atg16l1*$^{\Delta IEC}$, *Tmem173* -/- and wildtype mice were housed under specific pathogen-free (SPF) conditions in individually ventilated cages (IVCs) at the Central Animal Facility, Germany and Victor Hensen Animal Facility of the University Hospital Schleswig-Holstein, Campus Kiel. Animals were held in a 12 h light-dark cycle at 21 °C ± 2 °C and 60 % ± 5 % humidity. Food and water were available *ad libitum*. All animal experiments were approved by the Animal Investigation Committee of the University Hospital Schleswig-Holstein and all acceptance numbers are listed in Table 9.

Table 9: Animal experiments approved by the Animal Investigation Commitee of the University Hospital Schleswig-Holstein.

Title	Acceptance number
Studien zum Einfluss von IBD Risikogenen auf die experimentelle Darmentzündung und die entzündungsassoziierte Karzinogenese	V 242-17696/2016 (32-3/16)
Studien zum Einfluss des Autophagie Gens ATG16l1 und des ER-Stress Regulators XBP-1 und des Zellzyklusregulators p53 auf genetisch induzierten DNA Schaden	V 242-29834/2016 (52-5/16)
Zucht von belasteten Phänotypen bei Mäusen mit IBD Risikogenen	V 241 - 61544/2017 (69-5/17)
Untersuchung der protektiven Wirkung gegen Tunicamycin-induzierten ER Stress durch pharmakologische Inhibition des ATF6 Signalweges in IBD-Risiko Mäusen	V 242 - 32647/2018 (59-7/18)
Rolle der epithelialen Glykolyse für die intestinale entzündungsunabhängige Karzinogenese	V 242 - 56302/2018 (100-11/18)

Xbp1/Atg16l1$^{\Delta IEC}$ mouse small intestinal sections were kindly gifted by A. Kaser, University of Cambridge.

3.6.4 Genotyping of mice

Genotyping strategies for each transgenic mice strain have previously been established and were carried out as described before[19,40,297].

In brief, genotyping was conducted by polymerase chain reaction (PCR) using the primers listed in Table 10. Genomic DNA from mice was aquired from tail biopsies by boiling tails with 100 µl of 50 mM NaOH for 1 h. Next, samples were centrifuged and the supernatant containing the DNA was subjected to two independent touch - down PCRs per mouse line applying the GoTaq DNA polymerase (Promega, Mannheim, Germany). Details of the PCR reaction and profile are shown in Table 11 and Table 12. Size of the amplified PCR products was determined by agarose gel electrophoresis (3.6.5, p. 45).

Table 10: Oligonucleotides for genotyping applied in this study

Target	Species	Used primers (forward, reverse)
Xbp1	murine	CCTGTGGGACAGAATTGGACCCAG, CGCATACACACGCTGCTTTCTATCC
Atg16l1	murine	CAGAATAATTTCCGGCAGAGACCGG, GTCTTATTAAAGGCCGTCTCTGGCC
Tmem173	murine	CCTCTCCTAGACAGGTGCTG, TGATTTGGTGGATCCTTTGC
Villin Cre	murine	GTGTGGGACAGAGAACAAACC, ACATCTTCAGGTTCTGCGGG

Table 11: PCR components for genotyping

loxP-Site PCR		**Cre-PCR**	
5 x Green GoTaq® Reaction Buffer	5 µl	5 x Green GoTaq® Reaction Buffer	4 µl
dNTPs (10 mM)	0,5 µl	dNTPs (10 mM)	0,5 µl
Primer forward & reverse (0,8 µM)	4 µl	Primer forward & reverse (10 µM)	0,5 µl
DreamTaq DNA polymerase (5 U/µl)	0,5 µl	DreamTaq DNA polymerase (5 U/µl)	0,5 µl
DNA (diluted 1: 10)	1 µl	DNA (diluted 1: 10)	3 µl
A. bidest	14 µl	A. bidest	11,5 µl

Table 12: PCR profile for genotyping

number of cycles	temp [°C]	time
1	95	2 min
10	95	30 s
	65 to 55 (-1 °C/cycle)	5 s
	72	4 min
33	95	10 s
	55	5 s
	72	4 min
1	72	7 min
1	4	∞

3.6.5 Agarose Gel Electrophoresis

To separate DNA fragments and determine fragment size, agarose gel electrophoresis was performed. Therefore, 0,5 % TAE gels containing 1 % (w/v) agarose were used and run at a constant voltage of 120 V with a maximum current of 300 mA for 30-60 min using Bio-Rad Power Pac 300 power supply (Bio-Rad, Munich, Germany). Fragments were visualized adding SYBR Safe DNA gel stain to the gel, enabling visualization by UV light excitation. Images were taken using Molecular Imager ChemiDoc XRS Imaging System (Bio-Rad, Munich, Germany). SmartLadder MW-1700-10 (Eurogentec, Cologne, Germany) was used as a molecular weight standard.

3.6.6 Dextransodiumsulfate-induced colitis

Dextransodiumsulfate (DSS) was used as a model of intestinal inflammation and disrupted epithelial barrier function as described before[298]. 10 to 12-week-old wildtype mice received 1,5 % (weight/volume) dextransodiumsulfate (DSS, MP Biomedicals, Santa Ana, USA) in drinking water for seven days. After sacrifice, colonic tissue was collected and subjected to *Lamina propria* dissection kit (Miltenyi Biotec, Bergisch-Gladbach, Germany) in order to isolate the epithelial fraction according to the manufacturer's instruction.

This animal experiment was approved by the Animal Investigation Committee of the University Hospital Schleswig-Holstein (acceptance no.: V 242 - 56302/2018 (100-11/18), also see Table 9).

3.6.7 Intraperitoneal Tunicamycin injection

Mice were treated with 1 mg/kg bodyweight Tunicamyccin or DMSO as a control intraperitoneally for 24 h before being sacrificed. This animal experiment was approved by the Animal Investigation Committee of the University Hospital Schleswig-Holstein (acceptance no.: V242-32647/2018 (59-7/18), also see Table 9).

3.7 Imaging

3.7.1 Immunofluorescence

After cells were cultured on a cover slip overnight, cells were first washed with PBS and fixed in 4 % (w/v) paraformaldehyde for 20 minutes at room temperature. Next, permeabilization of the cell membrane was achieved applying 1 % (v/v) Triton X-100 in PBS supplemented with 5 % (w/v) BSA for 3 minutes at room temperature. The primary antibody (usually at a 1:100 dilution, see Table 20) was added and the specimen incubated overnight at 4 °C. The secondary antibody coupled to a fluorophore was added the next day for 45 minutes at room temperature, after the primary antibody was removed and cells were washed three times with PBS, respectively. After another three washing steps, the fluorescent stain DAPI (strongly binding A-T rich regions in the DNA) was added for 10 min. The specimen was again washed once with PBS and once with H_2O and then mounted onto glass slides covered with mounting medium (Roth, Karlsruhe, Germany). A Zeiss AxioImager.Z1 apotome fluorescence microscope and AxioVision Rel 4.9 software (ZEISS, Oberkochen, Germany) was used for analysis and image generation.

3.7.2 Immunohistochemistry

3.7.2.1 Tissue processing

After sacrifice, the respective tissue was removed and immediately fixed in 10 % (w/v) formalin for 24 h at 4 °C. The tissue was then immersed in a series of ethanol solutions of increasing concentrations until 100 %. Next, the ethanol was gradually replaced with xylene, which is then replaced by paraffin. Paraffin embedded tissue was cut into 3.5-4.5 µm thin sections using the RM2255 microtome (Leica, Wetzlar, Germany).

3.7.2.2 Haematoxylin & Eosin (HE) staining

Paraffin embedded tissue sections were stained for 2-5 min in haematoxylin. Haematoxylin in complex with aluminium salts reacts with negatively charged, i.e. basophilic, cell compartments including e.g. nucleic acids, which are then stained blue. The cytoplasm was counterstained with 1 % (v/v) eosin solution for 2 min. Eosin on the other hand is negatively charged and therefore binds to positively charged, i.e. acidophilic, compartments such as amino groups of cytoplasmic proteins. Eosin treatment results in pink staining.

Stained slides were then dehydrated and embedded in Roti-Histo-Kit mounting medium (Roth, Karlsruhe, Germany) and examined with a Zeiss AxioImager.Z1 apotome microscope and the AxioVision Rel 4.9 software (Zeiss, Oberkochen, Germany).

3.7.2.3 3,3'-Diaminobenizidine staining

To visualize specific proteins, 3,3'-Diaminobenizidine staining was performed. Slides were rehydrated and boiled for 20 min in citrate buffer (pH 6.0) for antigen retrieval. Unspecific binding sites were blocked by incubating slides with 5 % (v/v) goat serum in phosphate-buffered saline (PBS). Naturally occurring peroxidases were inactivated by applying 3 % hydrogen peroxide. Antibody binding and 3,3'-diaminobenzidine staining was performed according to the manufacturer's instruction (Vectastain Elite ABC Kit, Vector Labs, Peterborough, United Kingdom). In brief, after primary antibody binding, the signal was amplified by adding a horseradish peroxidase-conjugated streptavidin antibody. 3,3'-diaminobenzidine is then oxidized by the horseradish peroxide which finally results in the deposition of a brown precipitate. Primary antibodies are listed in Table 21.

3.8 Transcriptomics analysis

RNA sequencing (RNAseq) was used to analyse the colonic epithelial fraction of DSS-treated mice. Samples were sequenced on HiSeq3000 (Illumina, San Diego, United States) using Illumina total RNA stranded TruSeq protocol. An average of ~28 million 150-nt paired-end reads was sequenced for each sample. Raw reads were pre-processed using cutadapt[299] to remove adapter and low quality sequences. RNAseq reads were aligned to the mm10/Ensemble (GrCm38) reference genome with TopHat2[300]. Gene expression values of the transcripts were computed by HTSeq[301]. Differential gene expression levels were analysed and visualised by the Bioconductor package DESeq2[302].

3.9 Statistical analysis

The GraphPad Prism 5 software package (GraphPad Software Inc., La Jolla, USA) was used for statistical analysis. If not otherwise specified, the Student's unpaired t-test was performed. Data is visualized as mean ± standard error of the mean (SEM), if not otherwise stated. A significance threshold of a p-value ≤ 0.05 (*) was used, a p-value of ≤ 0.01, respectively ≤ 0.001, were considered as strongly significant (**) and highly significant (***), if not otherwise specified.

4 Results

4.1 STING is expressed in the intestinal epithelium and most prominently in Paneth cells

The role of STING has been so far described in various innate and adaptive immunity cell types, such as e.g. T cells[252] and B cells[250], macrophages[247] and monocytes[253]. Whether STING is expressed in the intestinal epithelium has not been fully addressed. We therefore investigated the expression of STING

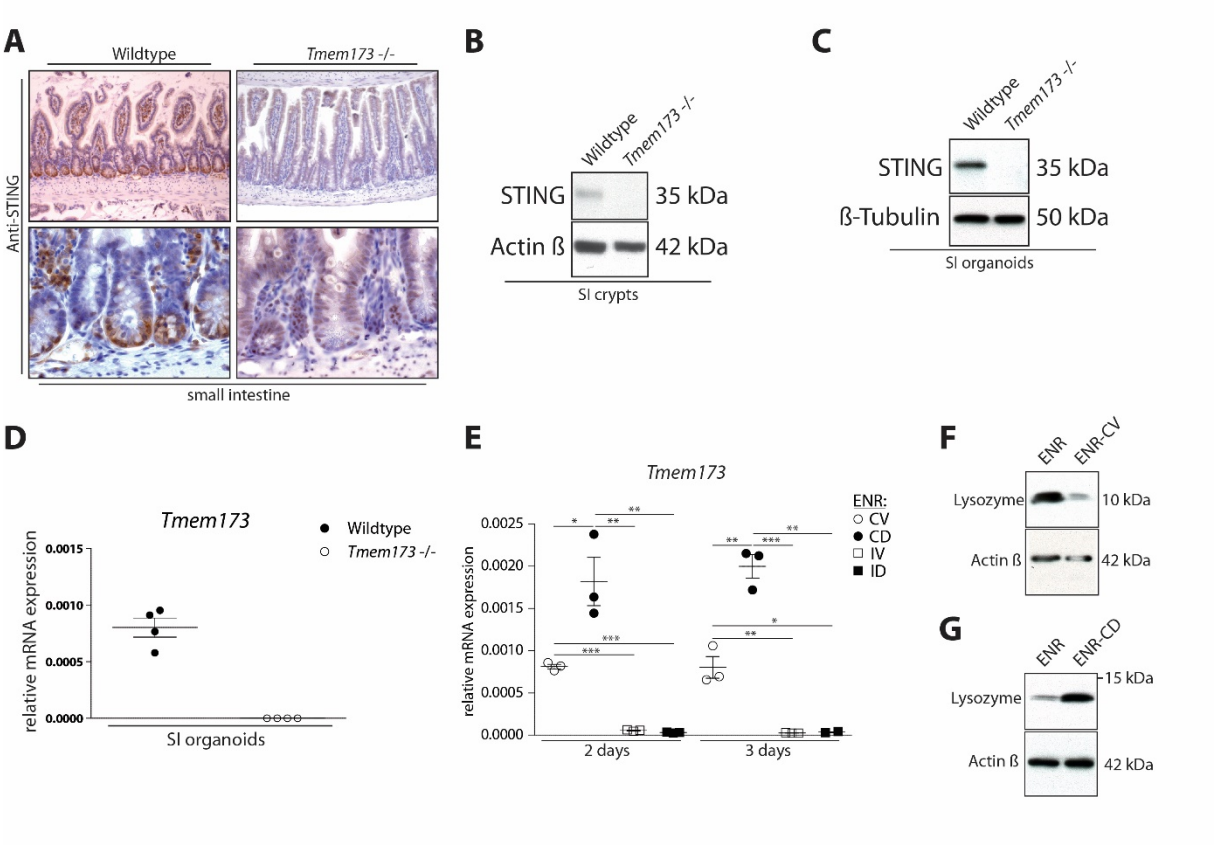

Figure 4-1: STING is expressed in the intestinal epithelium and predominantly in Paneth cells

(A) Immunohistochemistry staining of murine small intestine sections for STING.
(B) Western blot analysing STING expression in small intestinal crypts derived from wildtype and *Tmem173* -/- mice.
(C) Western blot analysing STING expression in small intestinal organoids derived from wildtype and *Tmem173* -/- mice.
(D) Taqman assay for *Tmem173* expression in small intestinal organoids derived from wildtype and *Tmem173* -/- mice.
(E) Murine small intestinal organoids were enriched for stem cells using ENR – CV medium for 3 days, then specific epithelial lineages were induced for 2, resp. 3 days using ENR – CD (Paneth cells), - IV (enterocytes) and – ID (Goblet cells). Taqman assay for *Tmem173* expression. Experiment kindly performed by Simon Imm.
(F) Western blot for Lysozyme of small intestinal organoids enriched for stem cells.
(G) Western blot for Lysozyme of small intestinal organoids enriched for Paneth cells.

SI: small intestine

in the intestinal epithelium using immunohistochemistry of wildtype and *Tmem173* -/- mice. We observed strong STING expression in immune cells within the lamina propria (Figure 4-1A), however in the intestinal epithelium, STING was most expressed in the crypt base (Figure 4-1A). Specificity of the

staining was confirmed using *Tmem173* -/- mouse small intestinal sections as a negative control. To validate expression of STING in the intestinal epithelium, we isolated small intestinal crypts from wildtype and *Tmem173* -/- mice. Accordingly, STING could only be detected in crypts from wildtype mice (Figure 4-1B). Likewise, in small intestinal organoids derived from the same genotypes, STING was only present in the wildtype organoids as well as *Tmem173* expression (Figure 1-7C, D).

As found in the immunohistochemistry staining, STING expression was limited to the crypt base. To reveal which specific cell type predominantly expresses STING in the small intestinal epithelium, we subjected small intestinal organoids to different conditioned media in order to enrich for specific epithelial lineages, i.e. stem cells, Paneth cells, Goblet cells and enterocytes (Figure 4-1E - G)[289]. Notably, *Tmem173* expression was most pronounced when organoids were enriched for Paneth cells (-CD) (Figure 4-1E). *Tmem173* was also induced when organoids were enriched for stem cells (-CV), while enrichment for enterocytes or goblet cells did not result in *Tmem173* induction (Figure 4-1E), but rather abolished *Tmem173* expression compared to stem cell or Paneth cell enrichment. To determine whether lineage differentiation with the respective conditioned media did work appropriately, we assessed lysozyme expression as measured by Western blot. As expected ENR-CV-treated organoids showed decreased lysozyme, while ENR-CD-treated organoids showed increased lysozyme expression (Figure 4-1F, G).

4.2 Epithelial STING expression is regulated by the microbiota

Physiological bacterial stimuli are key for proper development of intestine-protective mechanisms, especially in the intestinal epithelium[65,283]. Our finding that STING expression in intestinal epithelial cells (IECs) is most pronounced in Paneth cells suggests that epithelial STING inherits a predominantly antimicrobial function. Additionally, STING has been shown to be activated by fecal contents such as bacterial DNA, and *Tmem173* -/- mice show an altered microbial composition towards a more inflammatory profile[283], indicating a tight reciprocal interplay of STING and luminal microbes. Thus, we hypothesized that physiological stimuli of the microbiota are key for STING expression in IECs.

To test our hypothesis, we analysed small intestinal sections of germ-free (GF) and conventionally raised (CR) mice (Figure 4-2A). Indeed, we observed drastically reduced STING expression in crypts of GF mice compared to CR mice, providing evidence for a close reciprocal regulation of STING by the microbiota and vice versa (Figure 4-2B). To further support this, we analysed data from a previously published study investigating epithelial gene expression in response to microbial colonization[65]. The authors used laser capture microdissection to gather ileal and colonic tip and crypt epithelial fractions from GF and CR mice, analysed gene expression and validated their results in a separate experiments where GF mice were colonized with a conventional microbiota[65].

In line with the immunohistochemistry results, *Tmem173* expression was highest in ileal crypts of CR mice and drastically reduced in ileal crypts of GF mice, while there was in general much lower expression and no difference in the tips (Figure 4-2C). *Tmem173* expression in colonic crypts was also found to be regulated by the microbiota, however less pronounced than in the ileum (Figure 4-2C). Again, there was no increase in *Tmem173* expression in the tips of the colon. Accordingly, when GF mice were colonized with a conventional microbiota, *Tmem173* expression was rapidly induced in GF

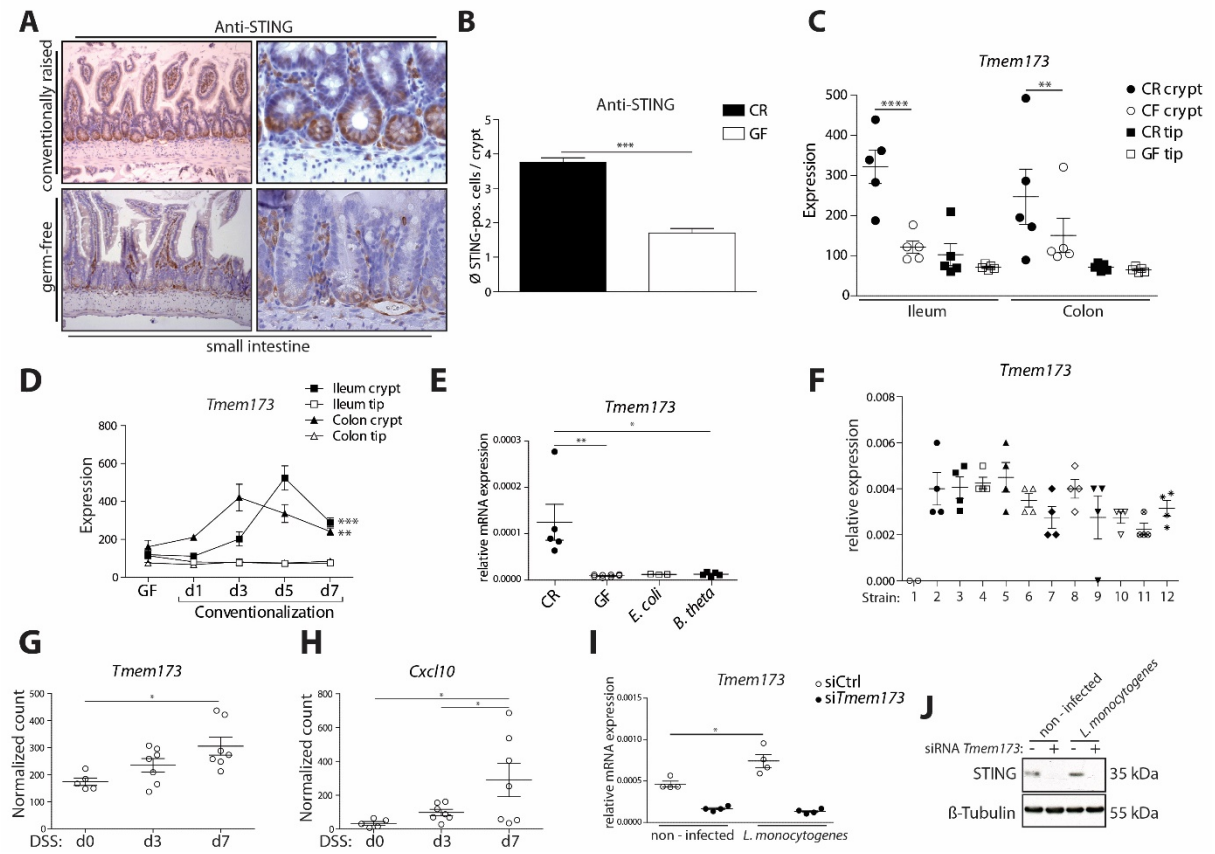

Figure 4-2: STING is regulated by the microbiota and induced upon bacterial infection.

(A) Immunohistochemistry for STING of SI sections of CR (n=13) and GF mice (n=3).
(B) According quantification in average STING – positive cells per crypt.
(C) Microarray analysis of *Tmem173* expression of laser capture microdissection - harvested ileal and colonic tip and crypt epithelial fractions of GF and CR mice
(D) and from mice during the time course of colonization. Data of a previously published study (Sommer et al, 2015[65]).
(E) *Tmem173* expression in whole tissue colon samples of CR, GF and *E. coli and Bacteroides theta* monocolonized mice. Experiment kindly performed by Dr. Felix Sommer and Jacob Hamm in cooperation with Fredrik Bäckhed, University of Gothenburg.
(F) Small intestinal epithelial cells (MODE-K) were exposed to metabolites of specific bacterial strains of the oligo-mouse-microbiota (OMM, also see chapter 3.5.3) to test for *Tmem173* inducing bacterial strains. Strains were: 1 - Acutalibacter muris, 2 - Akkermansia municiphila, 3 - Bacterioides ceacimuris, 4 - Bifidobacterium animalis, 5- Blautia coccoides, 6 - Clostridium clostridioforme, 7 - Enterococcus faecalis, 8 - Flavonifractor plautii, 9 - Lactobacillus reuteri, 10 - Muribaculum intestinale, 11 - Clostridium innocuum, 12 – Ctrl.
(G) Mice were treated with 1,5 % DSS over a time course of three, respectively seven days and IEC fraction isolated. Taqman assay of *Tmem173,*
(H) and *Cxcl10.* Experiment kindly performed by Jacob Hamm, data analysed by Dr. Neha Mishra.
(I) After siRNA knockdown of *Tmem173,* MODE-K cells were infected with *L. monocytogenes* for 24 h. Taqman assay of *Tmem173*.
(J) Western blot for STING of the same experiment.

CR: conventionally – raised; GF: germ – free; *E. coli*: *Escherichia coli*, *B. theta*: *Bacteroides theta*; DSS: dextransodiumsulfate; *L. monocytogenes*: *Listeria monocytogenes*

mice in both ileum and colon crypts with slightly more expression in the ileal crypts (Figure 4-2D). To test for specific bacterial strains, we analysed *Tmem173* expression in CR, GF or mice monocolonized with a single bacterial strain. Consistently, *Tmem173* expression was elevated in CR mice compared to GF mice, however both *E. coli* and *Bacteroides theta* monocolonized mice did not show any increase in *Tmem173* expression (Figure 4-2E). Exposure of small intestinal epithelial cells (MODE-K) to metabolites of single bacterial strains of the major bacterial phyla of the murine gut microbiota (namely: *Acutalibacter muris*, *Akkermansia municiphila*, *Bacterioides ceacimuris*, *Bifidobacterium animalis subsp. animalis*, *Blautia coccoides*, *Clostridium clostridioforme*, *Enterococcus faecalis*, *Flavonifractor plautii*, *Lactobacillus reuteri*, *Muribaculum intestinale*, *Clostridium innocuum*)[296] also failed to reveal any induction of *Tmem173* compared to the control mediated by a single bacterium, pointing towards a more complex microbial environment regulating *Tmem173* expression. To check *Tmem173* expression in a different model of microbial infection we investigated time-dependent *Tmem173* expression in dextran sodium sulfate (DSS) treated wildtype mice. DSS treatment induces a breakdown of the intestinal barrier integrity and thereby promotes microbial invasion[298]. Indeed, *Tmem173* expression was induced by DSS treatment (Figure 4-2G), which coincided with induction of the interferon-stimulated-gene (ISG) Cxcl10[231,303], indicating STING activation and interferon activity following induction of experimental colitis (Figure 4-2H).

While DSS treatment allows for infection with a broad set of pathogens or opportunistic bacteria, we next sought to test *Tmem173* regulation by intracellular infection with a single bacterial strain. STING has been shown to be involved specifically in sensing gram - positive bacteria via cGAS-synthesized cGAMP or directly via bacteria-derived CDNs such as cyclic di-GMP or cyclic di-AMP[240,241,245]. Thus we chose to infect small intestinal epithelial cells (MODE-K[285]) with the gram-positive intracellular pathogen *Listeria monocytogenes*. *Tmem173* expression was induced upon infection as shown by gene and protein expression (Figure 4-2I, J).

4.3 STING expression is induced by ER-stress and correlates with disease activity in IBD patients

Paneth cells are known to be especially prone to accumulate unfolded proteins, i.e. ER-stress, and unresolved ER-stress in Paneth cells has been shown to result in intestinal inflammation, in turn enabling pathogen invasion[19,40,42,45]. Conversely, bacteria are able to induce ER-stress, for example by disrupting the secretory pathway in Paneth cells[37,39]. Based on our observation that i) STING was mainly expressed in the small intestinal crypt ground and induced upon microbiota exposure or bacterial intracellular infection, we thus hypothesized that ER-stress induced by infection might underly *Tmem173* induction in response to microbial stimuli and infection.

Indeed, during colonization of GF mice with a conventional microbiota, ER-stress was induced as seen by increase in *Grp78* and *Hsp90b1* expression during colonization mainly in crypts of ileum and colon, less in the tips (Figure 4-3A, B). Given that *Tmem173* regulation by the microbiota was also most pronounced in ileal crypts, we speculated that ER-stress and *Tmem173* induction might go hand in hand during colonization. Thus, we next analysed whether *Tmem173* correlates with ER-stress in ileal crypts during microbial colonization. Both *Hsp90b1* and *Grp78* showed significant correlation with

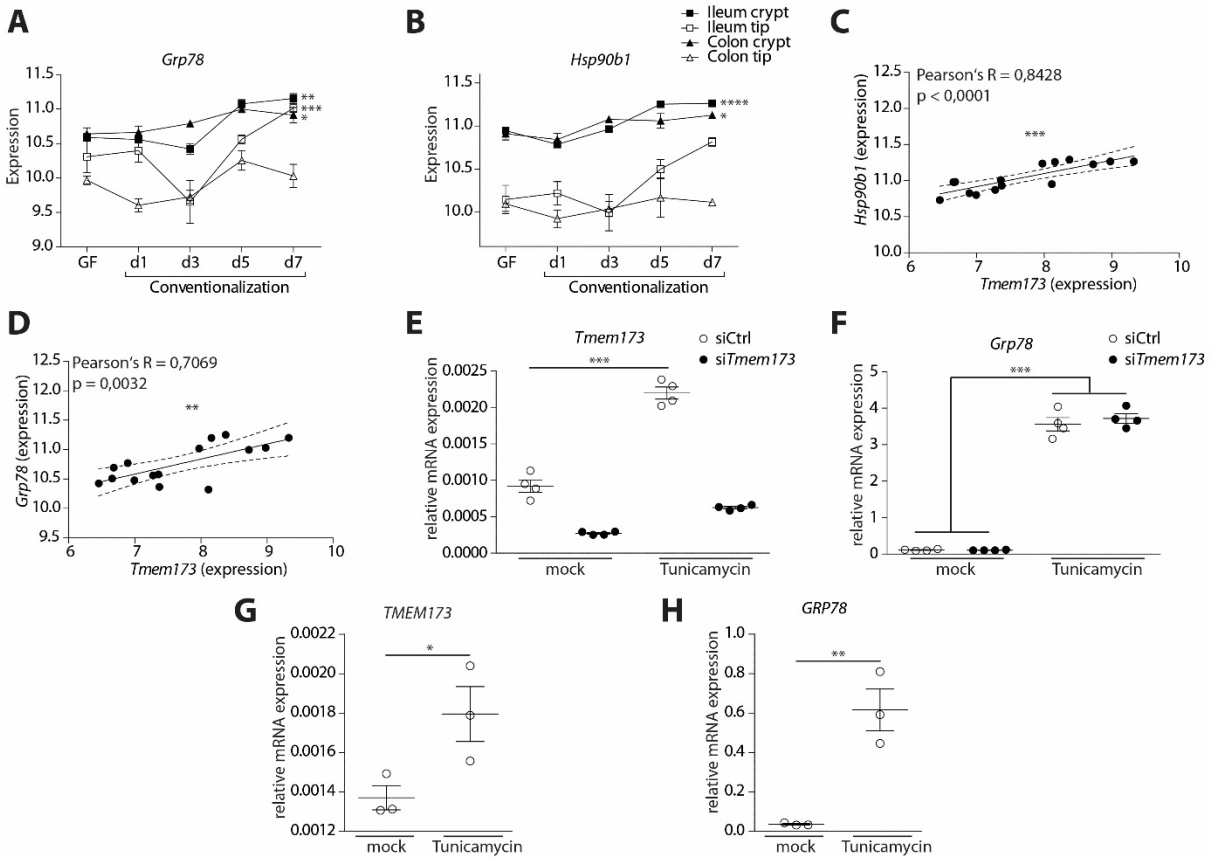

Figure 4-3: *Tmem173* is induced by ER – stress.

(A) Laser capture microdissection - harvested ileal and colonic tip and crypt epithelial fractions of GF mice colonized with a conventional microbiota (data from Sommer et al., 2015[65]), *Grp78* expression
(B) and *Hsp90b1* expression.
(C) Correlation analysis of *Tmem173* and *Hsp90b1* expression of the same dataset in ileal crypts only.
(D) Correlation analysis of *Tmem173* and *Grp78* expression of the same dataset in ileal crypts only.
(E) MODE-K cells were stimulated with 1 µg/ml Tunicamycin for 24 h to induce ER – stress after previous knockdown of *Tmem173*. Taqman assay of *Tmem173*
(F) and *Grp78*.
(G) Human organoids of healthy donors were stimulated with 1 µg/ml Tunicamycin for 24 h to induce ER – stress. Taqman assay of *TMEM173*
(H) and *GRP78*. Experiment kindly performed by Dr. Go Ito.

siCtrl: small interfering control RNA; si*Tmem173*: small interfering *Tmem173* RNA

Tmem173 expression (Figure 4-3C, D). While it has been shown that STING activation can result in ER - stress[37], we suspected that ER-stress precedes and thereby mediates *Tmem173* induction upon microbial colonization (Figure 4-2D).

To test whether ER-stress is a direct inducer of *Tmem173*, MODE-K cells were stimulated with Tunicamycin, blocking N-glycosylation, thereby inducing ER-stress[304]. This resulted in robust induction of both *Tmem173* (Figure 4-3E) and *Grp78* (Figure 4-3F). Specificity was confirmed using an siRNA-based knockdown of *Tmem173*. Consistently, human organoids derived from healthy donors also displayed increased *TMEM173* and *GRP78* expression when treated with Tunicamycin (Figure 4-3G, H), altogether suggesting that ER-stress is a direct inducer of human and murine *Tmem173*.

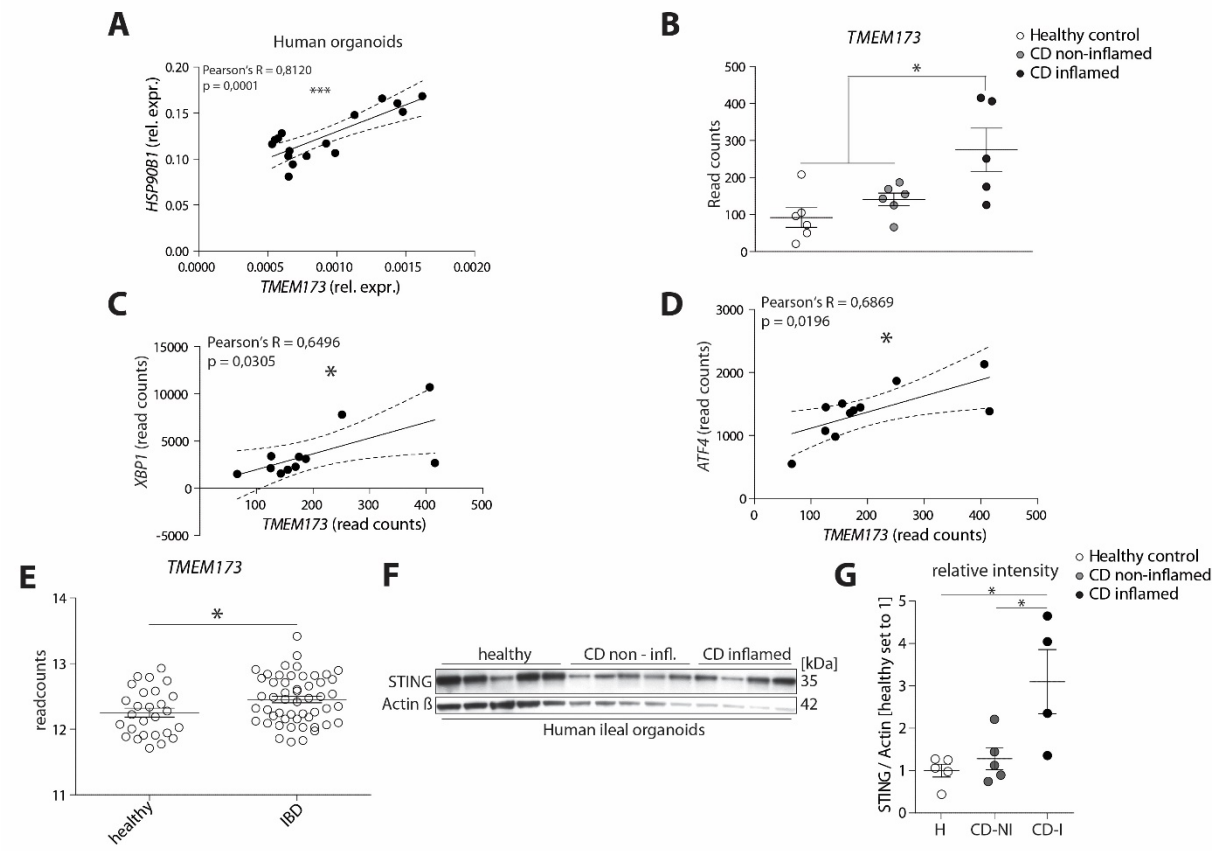

Figure 4-4: Human *TMEM173* is associated with ER-stress and inflammatory bowel disease activity.

(A) Human organoids from two healthy donor, one CD – inflamed and one CD – noninflamed donor. Correlation analysis of Taqman assay data for *HSP90B1* and *TMEM173*.
(B) *Tmem173* expression in small intestine biopsies of CD patients and healthy controls (data from a previously published study by Häsler et al., 2017[280]).
(C) Correlation analysis of *TMEM173* and *XBP1* expression of the same dataset.
(D) Correlation analysis of *TMEM173* and *ATF4* expression of the same dataset.
(E) *TMEM173* expression in a dataset of pediatric IBD patients by Howell et al., 2018[285]. Data kindly analysed by Dr. Joana Pimenta Bernardes with a wilcoxon rank sum test with Bonferroni correction for multiple comparison. Healthy vs. IBD: W=489 P=0.02806.
(F) Western blot of human ileal organoids of either healthy (H), non-inflamed (CD-NI) or inflamed CD (CD-I) patients. Analysis kindly performed by Dr. Stephanie Stengel.
(G) Relative intensity analysis of the Western blot in (F), kindly analysed by Dr. Stephanie Stengel.

H: healthy; CD-NI: Crohn's disease non-inflamed; CD-I: Crohn's disease inflamed.

Since ER-stress in the intestinal epithelium has been shown to be a common feature in IBD patients[19,41,46,49], and we have found *Tmem173* expression to strongly correlate with ER-stress, we further characterized *Tmem173* expression IBD patient samples and organoids, suspecting a tight

interplay between ER-stress induction and *TMEM173* expression (Figure 4-4). We observed a positive correlation between *HSP90B1* expression, indicative of ER-stress, and *TMEM173* expression in human organoids from two healthy donors and two IBD patients (Figure 4-4A). Analysis of dataset from a previously published study of our group[305] showed an increase in *TMEM173* expression in ileal biopsies of inflamed Crohn's disease (CD) patients compared to non-inflamed CD patients and healthy donors (Figure 4-4B). In line with the induction of *Tmem173* by ER-stress, *TMEM173* expression in those biopsies significantly correlated with ER-stress marker genes such as *XBP1* or *ATF4* (Figure 4-4C, D).

Howell et al.[281] used a dataset of pediatric IBD patients in a paper published in 2018 to show that *TMEM173* is hypomethylated in these patients, indicating that STING might be upregulated and overexpressed in these patients. Thus, we analysed differential expression of *TMEM173* in the transcriptome dataset of the paper published by Howell et al.[281]. This showed that *TMEM173* was indeed not only hypomethylated, but also actually upregulated on a transcriptome level (Figure 4-4E). We next aimed to gather evidence on STING proteinlevels in IBD patients to investigate whether higher mRNA levels also translate to increased protein expression. We therefore aquired protein samples of human organoids from either healthy, inflamed or non-inflamed CD patients (Figure 4-4F). STING to β-actin ratio was significantly increased in inlamed CD patient organoids compared to either non-inflamed or healthy donors (Figure 4-4F, G).

4.4 Acute ER-stress elicits a cGAS/STING-dependent type I interferon response in intestinal epithelial cells

Previous studies have shown that immune responses to bacterial signals can be significantly enhanced by parts of the unfolded protein response (UPR) or that vice versa pattern recognition receptors engage ER-stress responses to boost pathogen defense[37,255,256,306], indicating a close reciprocal relationship between ER-stress responses and innate immune pathways. Our results illustrate that in the intestinal epithelium, *Tmem173* is critically regulated by both microbial signals and ER-stress. Given that ER-stress can occur as a consequence of intracellular infection[37,39], we hypothesized that both ER-stress and microbial signals synergistically shape STING responses to infection. While it is well known that microbial signals engage STING[240,307], we aimed to investigate whether ER-stress induction directly affects STING-dependent type I IFN induction.

As a first approach, MODE-K cells were stimulated with Tunicamycin (1 µg/ml) for 24 h hours. Following Tunicamycin stimulation, STING was nearly completely degraded within 24 h, accompanied by robust STING-dependent TBK1 phosphorylation (Figure 4-5A), indicative of STING activation and downstream signalling. Indeed, Tunicamycin also induced STING-dependent induction of the ISG *Cxcl10* in parallel with *Grp78* (Fig. 4B), indicating an ER-stress driven and STING-dependent type I IFN induction. This was

confirmed using another ER-stress inducer, MG132, which blocks the proteasome, indirectly resulting in ER - stress[200]. MG132 treatment lead to both robust STING[225,227] and TBK1 phosphorylation and subsequent STING degradation (Figure 4-5C), indicative of the activation of the STING pathway.

Given the fact that STING can be activated by either bacteria-derived CDNs or cGAMP synthesized by the double-stranded DNA (dsDNA) sensor cGAS, we next wanted to check whether ER-stress mediated type I IFN induction requires cGAS, TBK1 and IRF3, i.e. the canonical STING-signalling cascade. As expected and demonstrated by siRNA knockdown of the respective genes, *Cxcl10* induction by ER-stress necessitates all above mentioned components of the STING pathway (Figure 4-5D). The

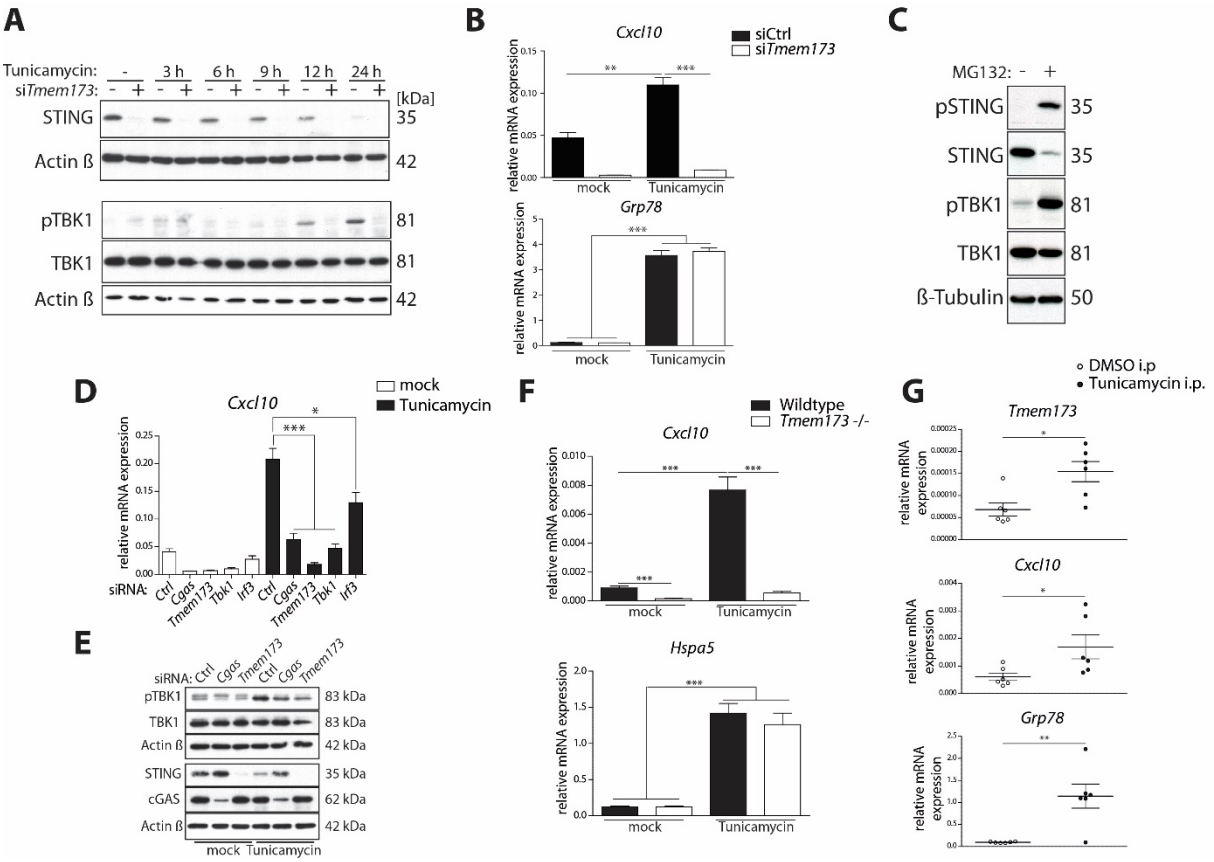

Figure 4-5: ER - stress elicits a cGAS/STING - dependent type I IFN response

(A) Western blot of MODE-K cells stimulated with 1 µg/ml Tunicamycin for 3 h, 6 h, 9 h, 12 h and 24 h.
(B) Taqman assay of MODE-K cells stimulated with 1 µg/ml Tunicamycin for 24 h after siRNA knockdown of *Tmem173*.
(C) Western blot of MODE-K cells stimulated with 3 µM MG132 for 24 h to induce ER – stress.
(D) Taqman assay for *Cxcl10* after knockdown of the STING signalling cascade (*Cgas*, *Tmem173*, *Tbk1*, *Irf3*) and 1 µg/ml Tunicamycin stimulation for 24 h.
(E) Western blot of MODE-K cells after *Cgas* and *Tmem173* knockdown using siRNA and 1 µg/ml Tunicamycin stimulation.
(F) Taqman assay or *Cxcl10* and *Hspa5* of wildtype and *Tmem173* -/- organoids stimulated with 5 ng/ml Tunicamycin for 24 h.
(G) Mice were injected with 1 µg/g bodyweight Tunicamycin to induce ER – stress and sacrificed 24 h later. SI crypts were isolated and taqman assays performed for *Tmem173*, *Cxcl10* and *Grp78*.

i.p.: intraperitoneally

requirement of cGAS was further confirmed using western blot, in which Tunicamycin dependent TBK1 phosphorylation was dependent on both cGAS and STING (Figure 4-5E).

To further corrobate our finding that ER-stress directly activates STING, we verified our findings using murine small intestinal organoids. Consistent with results from MODE-K experiments, Tunicamycin treatment induced robust ISG induction along with ER-stress in SI organoids (Figure 4-5F). Importantly, ISG induction was completely dependent on STING as it was abrogated in *Tmem173* -/- organoids (Figure 4-5F). Finally, we administered Tunicamycin intraperitoneally to mice for 24 h. As expected, we could detect both *Tmem173* induction by ER-stress as well as STING activation in SI crypts (Figure 4-5G).

4.4.1 STING is dispensable for ER-stress mediated cell death

A study of our own group has previously demonstrated that epithelial STING signalling in response to the cytokine IL22 can induce proinflammatory cell death, i.e. necroptosis, in the intestinal epithelium[164], consistent with other studies reporting a role for STING in cell death induction[247,250,251]. We therefore investigated whether ER-stress dependent cell death was mediated via STING activation. Propidiumiodide-staining and FACS quantification however revealed that while Tunicamycin treatment indeed results in robust cell death induction (Figure 4-6A, B, E, F), STING is dispensable for ER-stress

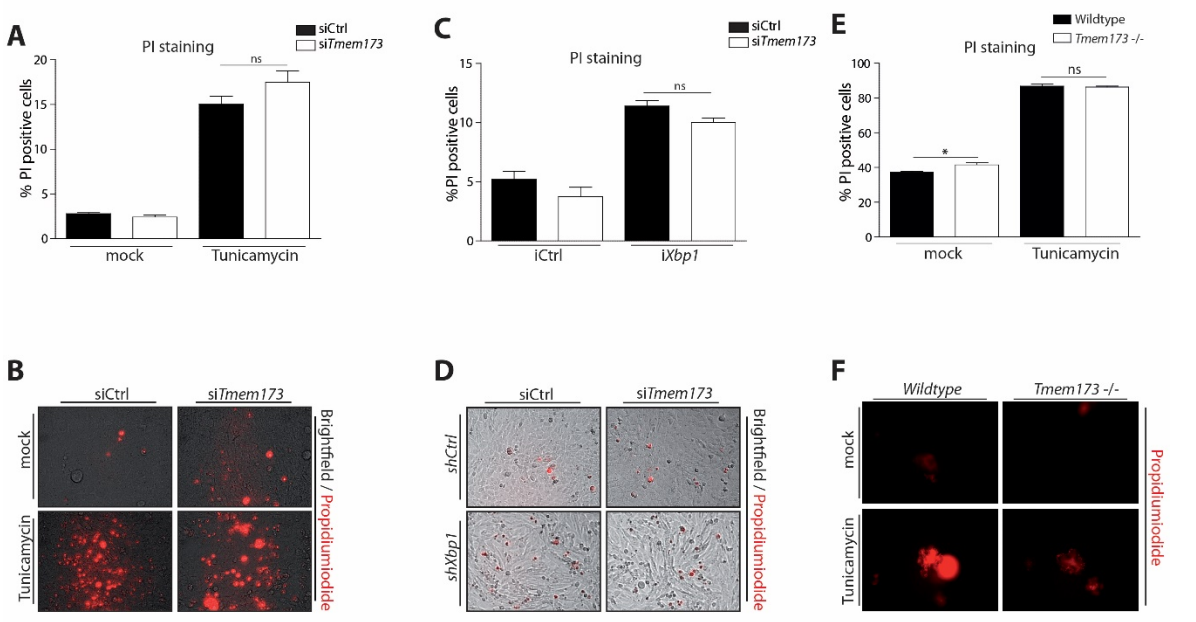

Figure 4-6: STING is dispensable for ER - stress induced cell death

(A) MODE-K cells were stimulated with 1 µg/ml Tunicamycin after knockdown of STING using siRNA. After 24 h, cells were stained with Propidiumiodide and measured by FACS to quantify dead cells.
(B) Representative images.
(C) MODE-K cells harbouring an shRNA knockdown of *Xbp1* or control shRNA were additionally subjected to siRNA knockdown of STING and dead cells were quantified using Propidiumiodide staining and FACS.
(D) Representative images.
(E) Wildtype or *Tmem173* -/- SI organoids were stimulated with 5 ng/ml Tunicamycin and dead cells were quantified with Propidiumiodide staining and FACS measurement.
(F) Representative images.

PI: Propidiumiodide; ns: not significant

induced cell death in MODE-K cells and organoids treated with Tunicamycin (Figure 4-6A, B, E, F). Also, cell death due to *Xbp1* - deficiency induced ER-stress[19,40] did not depend on STING as shown by siRNA knockdown of STING (Figure 4-6C, D) in *Xbp1*-deficient cells, suggesting that at least for IECs, STING is dispensable for cell death induction in response to ER - stress.

4.5 Chronic ER-stress suppresses STING-signalling in intestinal epithelial cells

Having shown that microbial stimuli and ER-stress induce *Tmem173* expression and STING-dependent type I IFNs expression, we aimed to understand to which extent chronic ER-stress affects epithelial cGAS/STING function. We specifically hypothesized that low-grade, chronic ER-stress obstructs STING

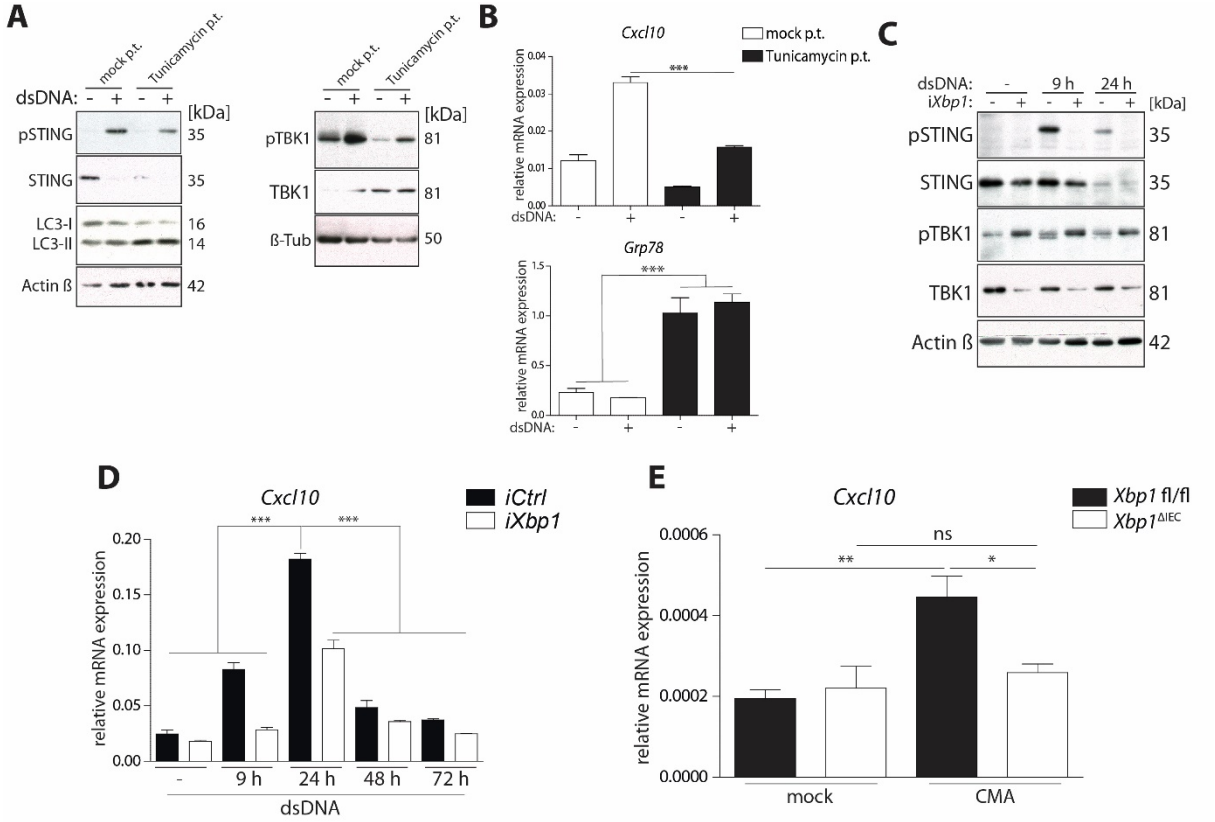

Figure 4-7: Chronic ER - stress suppresses STING signalling

(A) Western blot of MODE-K cells pretreated (p.t.) with either 0,1 µg/ml Tunicamycin or DMSO (mock) for 24 h, followed by 1 µg/ml dsDNA or mock transfection for 24 h.
(B) According Taqman assays.
(C) Western blot of MODE-K cells harbouring an shRNA knockdown of *Xbp1* or control shRNA stimulated with 1 µg/ml dsDNA for the indicated time course.
(D) Taqman assay of MODE-K cells harbouring the respective shRNA, transfected with 1 µg/ml dsDNA for the indicated time course.
(E) Taqman assay of SI organoids of the indicated genotypes stimulated with 500 µg/ml CMA for 24 h.

p.t: pretreated

signalling in response to microbial signals by degrading STING and thereby impairing STING-dependent type I IFN induction in response to PAMPs such as *E. coli* dsDNA.

Therefore, we subjected MODE-K cells to low-dose Tunicamycin pre-treatment, inducing mild, prolonged ER-stress, before transfecting *E. coli* dsDNA to induce a cGAS/STING-dependent type I IFN response. Tunicamycin pre-treatment resulted in lower phosphorylation levels of both STING and TBK1 compared to mock pre-treatment when additionally stimulated with dsDNA, presumably due to lower STING protein levels before dsDNA administration (Figure 4-7A) as a consequence of ER-stress induced degradation. Consistently, *Cxcl10* expression in response to dsDNA was strongly impaired, while *Grp78* expression indicated ER-stress induction in the pre-treated cells (Figure 4-7B). Of note, Tunicamycin pre-treatment also resulted in a shift from LC3-I towards LC3-II, pointing towards an increase in

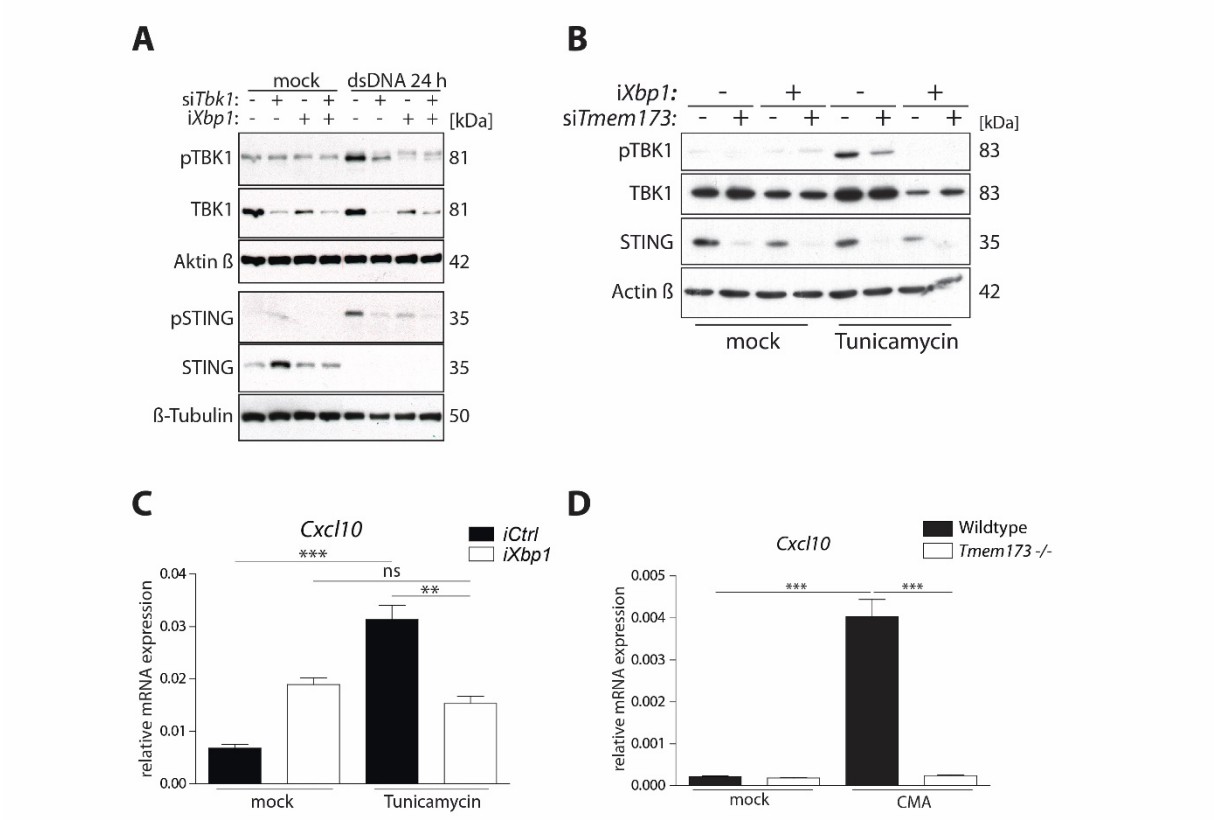

Figure 4-8: Chronic ER - stress suppresses STING signalling and CMA is a direct STING agonist

(A) Western blot of MODE-K cells harbouring the indicated shRNA and additional siRNA knockdown of *Tbk1*, transfected with 1 µg/ml dsDNA for 24 h or mock transfected.
(B) Western blot of i*Xbp1* and iCtrl MODE-K with additional knockdown of STING using siRNA stimulated with 1 µg/ml Tunicamycin for 24 h.
(C) According Taqman assay.
(D) Taqman assay of wildtype and *Tmem173* -/- SI organoids stimulated with 500 µg/ml CMA for 24 h.

autophagic flux[154] (Figure 4-7A), possibly responsible for lowered STING levels and a diminished type I IFN response.

To test our hypothesis in a model of genetically caused chronic ER-stress, we repeated the dsDNA stimulation experiment in context of *Xbp1*-deficiency, which has been shown to result in ER-stress[37,39]. MODE-K cells harbouring an shRNA knockdown of *Xbp1* (i*Xbp1*) or control shRNA (iCtrl) were stimulated with dsDNA. In line with the Tunicamycin pre-treatment (Figure 4-7), chronically stressed i*Xbp1* cells failed to activate STING as shown by a lack of (TBK1-dependent) STING or TBK1 phosphorylation (Figure 4-7C, Figure 4-8A), while displaying similarly reduced STING protein levels prior to stimulation (Figure 4-7C, Figure 4-8B). Accordingly, while *Cxcl10* induction following dsDNA administration peaked at 24 h in the iCtrl cells, it was nearly absent in context of *Xbp1*-deficiency (Figure 4-7D). Additionally, *Xbp1*-deficient cells also failed to activate STING when stimulated with a higher dose of Tunicamycin (Figure 4-8B, C), which induces robust activation in the iCtrl cells. Finally, treatment of SI organoids derived from *Xbp1*$^{\Delta IEC}$ mice with the direct STING agonist CMA[308] (Figure 4-8D) revealed mild *Cxcl10* induction in the control organoids, while *Xbp1*$^{\Delta IEC}$ organoids failed to induce *Cxcl10* (Figure 4-7E).

4.5.1 Chronic genetic ER-stress suppresses STING signalling *in vivo*

To validate our *in vitro* findings, we next sought to study STING expression and signalling *in vivo* under chronic ER-stress conditions. As models of chronic ER-stress *in vivo*, we chose to employ two genetic alterations (*Xbp1* deletion, *Atf6* overexpression) known to reliably result in ER-stress, specifically in the intestinal epithelium[19,196]. First, we analysed STING expression and function in context of *Xbp1*-deficiency.

Analysis of SI sections of *Xbp1*$^{\Delta IEC}$ mice by immunohistochemistry revealed severely altered STING expression compared to *Xbp1*$^{fl/fl}$ mice (Figure 4-9A, B). We further validated this analysing STING protein expression in SI crypts. Again, *Xbp1*$^{\Delta IEC}$ crypts showed a complete lack of STING compared to the *Xbp1*$^{fl/fl}$ crypts (Figure 4-9C). Importantly, the absence of STING in the *Xbp1*$^{\Delta IEC}$ mice was not due to a plain downregulation of *Tmem173* (Figure 4-9D), as one might have hypothesized according to the function of spliced Xbp1 as a transcription factor. Consistent with a lack of STING expression, *Xbp1*$^{\Delta IEC}$ mice also displayed reduced basal type I IFNs, as shown by small intestinal crypt gene expression (Figure 4-9D).

As a second model for chronic ER-stress *in vivo*, we investigated STING expression in context of a Tamoxifen - inducible overexpression of active *Atf6* (n*Atf6*^{IEC} tg/tg) in the intestinal epithelium, which results in disturbed epithelial mucine production, indicative of ER-stress, and impaired epithelial barrier function resulting in bacterial invasion[196]. Mice were treated with Tamoxifen for four days to allow for robust *Atf6* overexpression, and subsequently sacrificed[196]. In analogy to our finding of reduced STING protein levels in the *Xbp1*-deficient epithelium, we found STING to be less expressed in

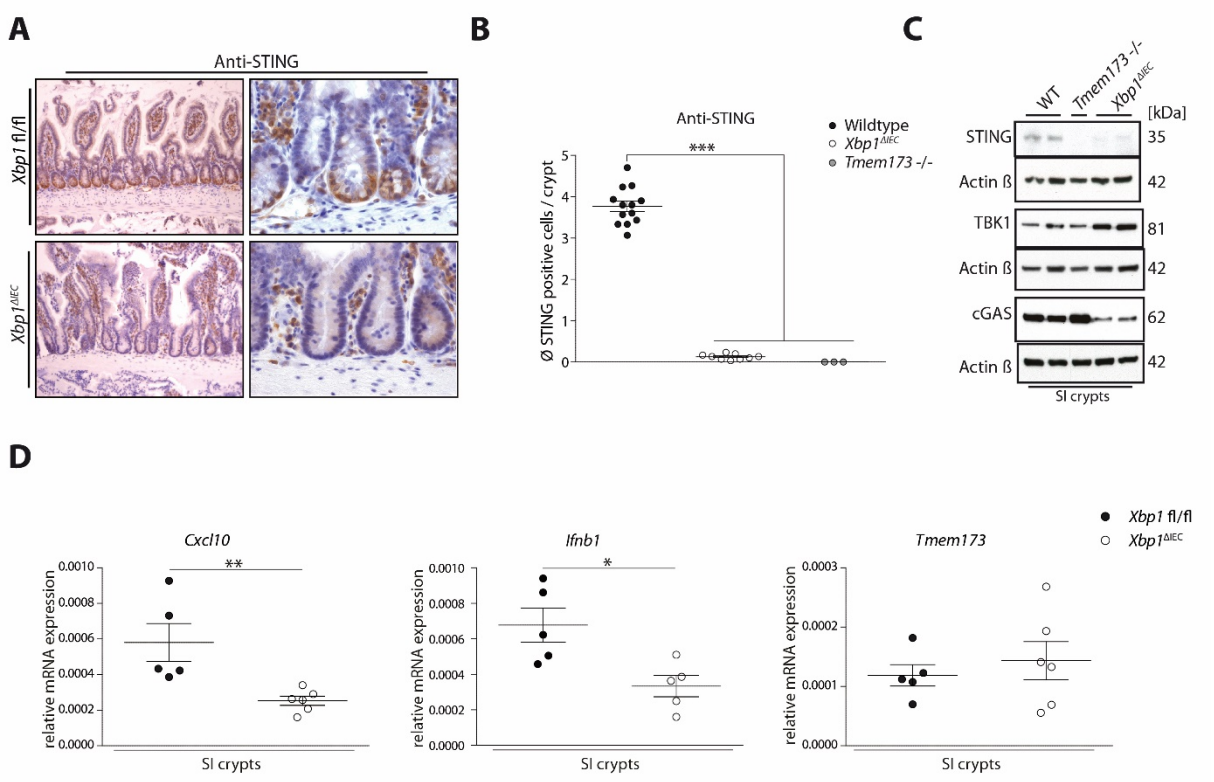

Figure 4-9: Chronic genetic ER – stress due to *Xbp1* deficiency suppresses STING signalling *in vivo*

(A) Representative pictures of immunohistochemistry stainings for STING of SI sections of *Xbp1*$^{\Delta IEC}$ (n=13), *Xbp1*$^{fl/fl}$ mice (n=9) and *Tmem173* -/- mice as negative control (n=3).
(B) According quantification as average positive cells per crypt.
(C) Western blot of SI crypts of the indicated genotypes.
(D) Taqman assays of SI crypts of the indicated genotypes

SI: small intestine; WT: wildtype

the n*Atf6*^{IEC} tg/tg mice (Figure 4-10A, B). The effect was however less pronounced than in the *Xbp1*-deficient situation (see Figure 4-9A, B for comparison). To further quantify STING protein levels in the n*Atf6*^{IEC} tg/tg mice, but also heterozygous n*Atf6*^{IEC} tg/fl mice, we analysed protein levels in lysates of the isolated epithelial fraction and expected to encounter gradually lowered protein levels of STING in the heterozygous, and even lower levels in the homozygous mice. Indeed, STING levels were slightly reduced in the homozygous n*Atf6*^{IEC} tg/tg mice compared to the fl/fl controls (Figure 4-10C), however again the difference was less pronounced than in the *Xbp1*-deficiency model, but matched our finding in the immunohistochemistry of the n*Atf6*^{IEC} tg/tg mice (Figure 4-10A, B). Of note, also TBK1 phosphorylation was reduced (Figure 4-10C). We next sought to validate the *in vivo* finding *in vitro* and employed SI organoids derived from either n*Atf6*^{IEC} tg/tg or n*Atf6*^{IEC} fl/fl control mice to check for consequences of impaired STING protein levels on type I IFN levels. Organoid treatment with Tamoxifen for up to 72 h surprisingly revealed type I IFN induction over time, with *Tmem173*

expression however declining in parallel (Figure 4-10D). ER-stress was robustly induced as observed by *Hspa5* induction, already after 24 h of Tamoxifen treatment (Figure 4-10D).

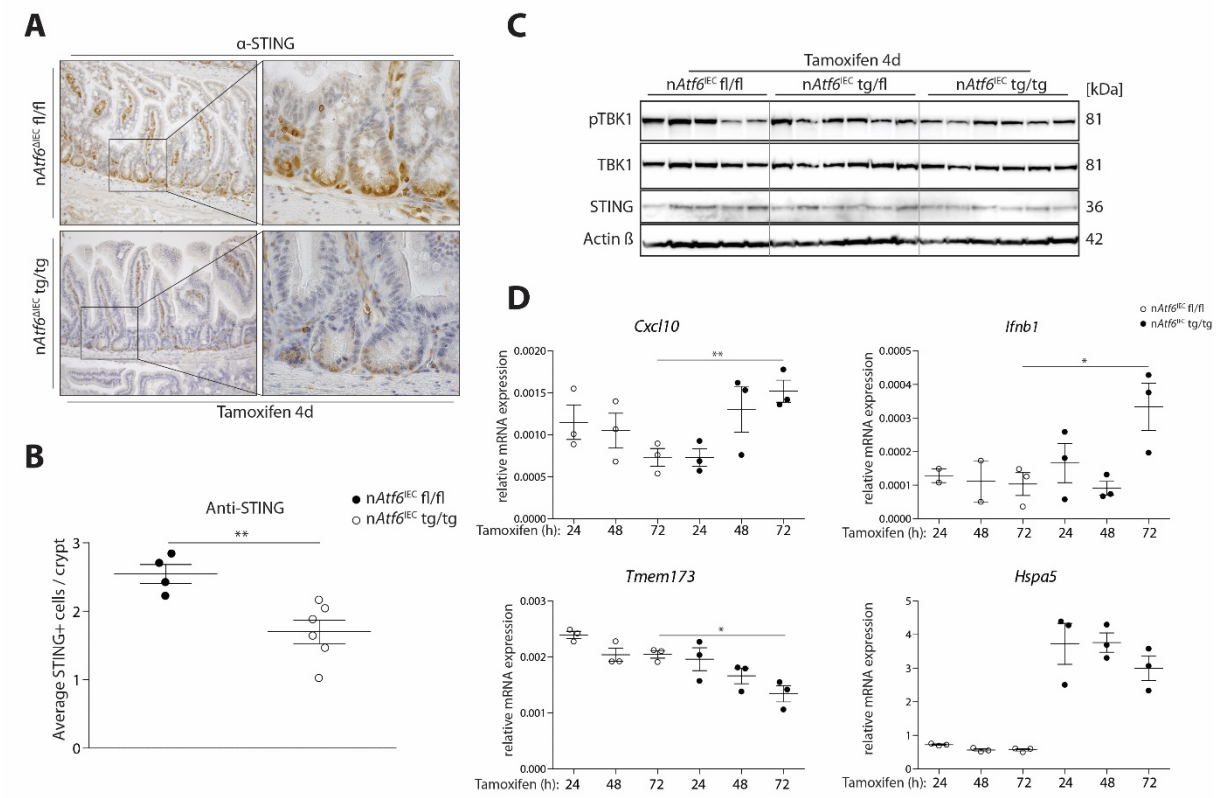

Figure 4-10: *Atf6* overexpression phenocopies lower STING levels in context of chronic ER-stress due to *Xbp1* deficiency.

(A) n*Atf6*^{IEC} tg/tg (n=6) and fl/fl (n=4) control mice were treated with Tamoxifen to induce overexpression of active Atf6 as a model of chronic ER-stress, as described previously by Coleman et al.[196]. Representative pictures of STING immunohistochemistry staining of SI sections. SI sections were kindly provided by Olivia Coleman and Dirk Haller, TU München.

(B) Respective quantification as average positive cells per crypt.

(C) IECs were isolated of n*Atf6*^{IEC} tg/tg (n=6), n*Atf6*^{IEC} tg/fl (n=6) and n*Atf6*^{IEC} fl/fl (n=5) mice treated with Tamoxifen to induce active Atf6 overexpression for four days as described previously by Coleman et al.[196]. Western blot of indicated proteins. IEC isolates were kindly provided by Olivia Coleman and Dirk Haller, TU München.

(D) SI organoids derived from n*Atf6*^{IEC} tg/tg and n*Atf6*^{IEC} fl/fl mice were treated with Tamoxifen at 0,5 µM over the indicated time course and quantitative gene expression analysed.

4.5.2 Chronic ER-stress impairs STING signalling in intestinal epithelial cells independently of the microbiota

We have observed that i) *Tmem173* expression critically depends on microbial signals (Figure 4-2) and ii) chronic ER-stress disturbs epithelial *Tmem173* expression (Figure 4-7, Figure 4-9 and Figure 4-10).

We therefore hypothesized that STING activation by the altered microbiota and subsequent degradation of STING could account for impaired STING expression in *Xbp1*$^{\Delta IEC}$ mice.

This would be in line with previous studies showing that microbial DNA and fecal contents can activate STING[283]. If so, STING expression should be restored in GF *Xbp1*$^{\Delta IEC}$ mice due to a lack of STING-stimulatory microbial signals. Immunohistochemistry of GF *Xbp1*$^{\Delta IEC}$ mice compared to CR *Xbp1*$^{\Delta IEC}$ mice however showed that STING expression is equally affected in the GF *Xbp1*$^{\Delta IEC}$ mice (Figure 4-11A, B).

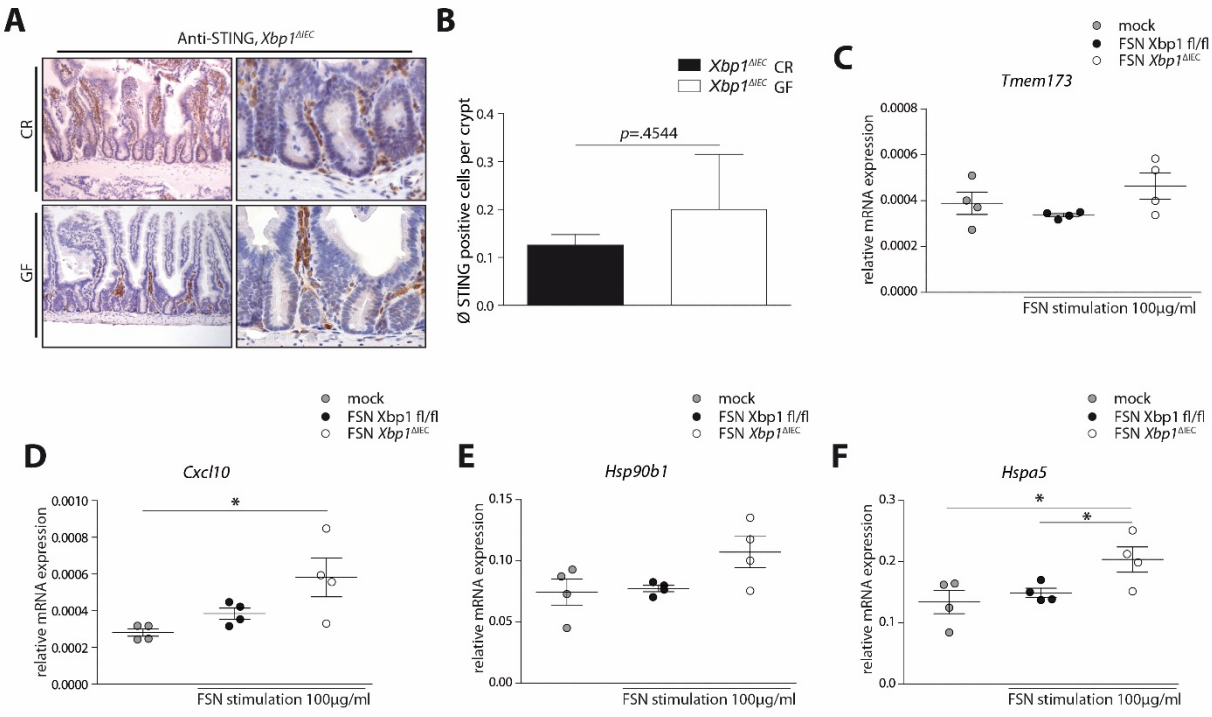

Figure 4-11: Chronic ER - stress impairs STING signalling independent of the microbiota

(A) Representative pictures of immunohistochemistry stainings for STING of SI sections of either GF (n=6) or CR *Xbp1*$^{\Delta IEC}$ mice (n=9).
(B) According quantification as average STING positive cells per crypt.
(C) – (F): Taqman assays of wildtype SI organoids stimulated with faecal supernatants of either *Xbp1*$^{\Delta IEC}$ or *Xbp1*$^{fl/fl}$ mice.
CR: conventionally – raised; GF: germ – free; FSN: faecal supernatant

Accordingly, organoid stimulation with fecal supernatants from either *Xbp1*$^{fl/fl}$ or *Xbp1*$^{\Delta IEC}$ mice did not differentially regulate *Tmem173* expression (Figure 4-11C).

However, fecal supernatants of *Xbp1*$^{\Delta IEC}$ mice did induce mild ER-stress and likewise mild type I IFNs compared to control fecal supernatants (Figure 4-11D-F), indicating at least modest effects of an altered microbial composition in context of *Xbp1* - deficiency on ER-stress and thereby on STING signalling in IECs.

4.5.3 Chronic ER-stress suppresses STING-signalling in intestinal epithelial cells in response to bacterial and viral infection

We have shown that ER-stress shapes STING signalling in response to canonical microbial stimuli such as dsDNA. Accordingly, we expected to observe a similar impact of ER-stress on STING signalling in response to live pathogens. Thus, we next investigated STING signalling exposed to live bacteria and

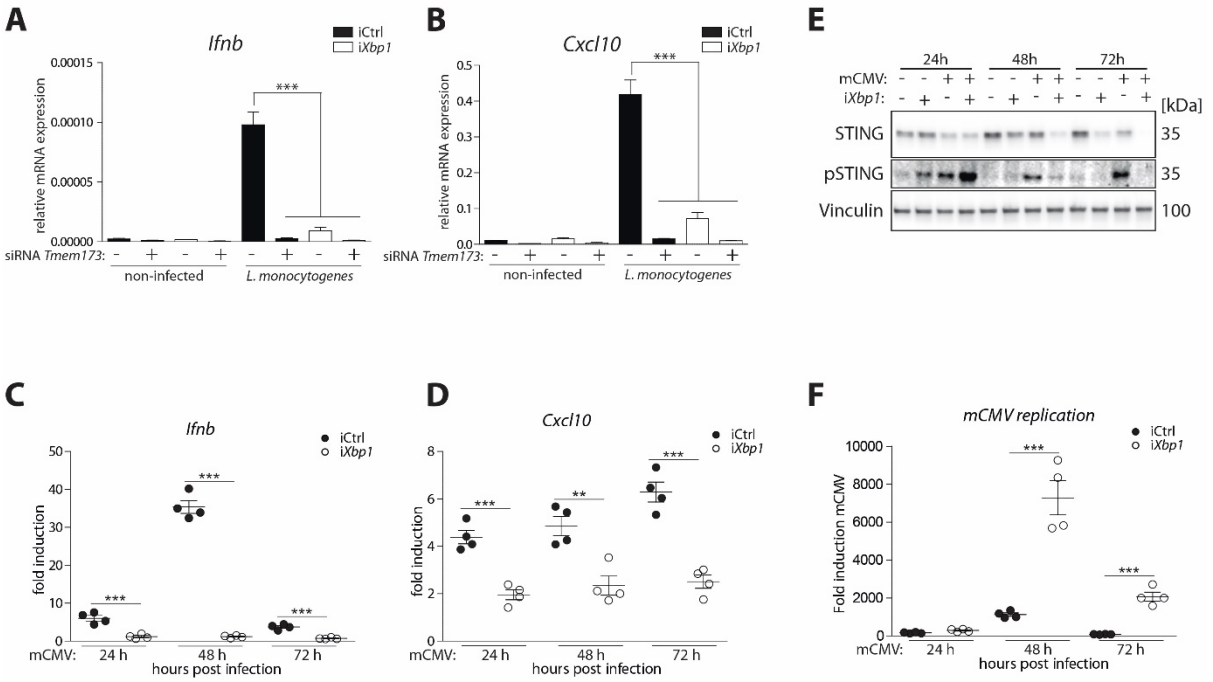

Figure 4-12: Chronic ER - stress suppresses STING signalling in response to bacterial and viral infection

(A) Taqman assay of MODE-K cells harbouring *Xbp1* or control shRNA and additional siRNA knockdown of STING, infected with *L. monocytogenes* for 24 h (also see 3.5.1).
(B) Taqman assay of the same experiment.
(C) Taqman assay of MODE-K cells harbouring *Xbp1* or control shRNA and infected with murine CMV at a multiplicity of infection (MOI) of 10 for the indicated time course. Data generated in collaboration with Samuel Windross & Søren Riis Paludan, Aarhus University.
(D) Taqman assay of the same experiment.
(E) Western blot of the same experiment.
(F) Viral replication as assessed by fold induction of the same experiment.

viruses in context of chronic ER-stress. In order to do so, we subjected the chronically stressed i*Xbp1* MODE-K cells to infection with either *L. monocytogenes* or murine cytomegalovirus (mCMV), which both frequently cause gastrointestinal infection, especially in immunocompromised patients[94,309]. Infection with *L. monocytogenes* is well known to involve STING signalling in the host's immune response[241,244,245]. Infection with CMV (a dsDNA virus, also see 1.1.4.1 on CMV infection in IBD) is interesting from a clinical perspective because CMV infection in IBD is associated with steroid-

refractory disease and generally impaired prognosis, representing a feared complication during IBD therapy[99–102].

L. monocytogenes infection resulted in strong type I IFN induction in the iCtrl cells, which was nearly completely absent in the i*Xbp1* cells (Figure 4-12A, B), in line with previous dsDNA stimulation experiments. Likewise, iCtrl cells responded to mCMV infection with type I IFN induction, while i*Xbp1* cells failed to induce any type I IFNs (Figure 4-12C, D). Additionally, STING phosphorylation was strongly impaired in i*Xbp1* cells following mCMV infection (Figure 4-12E). Consequently, mCMV could replicate much more in the i*Xbp1* cells (Figure 4-12F), suggesting that impaired STING signalling by chronic ER-stress also translates to infection susceptibility via suppressing proper antiviral IFN induction.

4.6 Chronic ER-stress engages ATG16L1-dependent autophagy to remove STING

Induction of autophagy is well established as a compensatory mechanism for ER-stress, most especially in Paneth cells[37,39,40,54,135], as well as STING has been shown to be targeted by autophagy for degradation[146,227,228]. Based on our findings of diminished STING expression as a consequence of chronic ER-stress (see Figure 4-7, Figure 4-9 and Figure 4-10), we suspected that autophagy might be engaged by ER-stress to remove STING.

We observed quick colocalization of STING with the autophagy proteins ATG16L1, LC3 and p62 following short Tunicamycin stimulation (Figure 4-13A). Consistently, after siRNA-based knockdown of *Atg16l1*, STING degradation in response to Tunicamycin treatment was diminished, while LC3-II to LC3-I ratio indicated activation of autophagy, which was impaired by the *Atg16l1* knockdown (Figure 4-13B). This also resulted in a moderately more pronounced TBK1 phosphorylation (Figure 4-13B). When stimulated with Tunicamycin, *Atg16l1*$^{\Delta IEC}$ organoids accordingly showed higher levels of *Cxcl10* induction compared to *Atg16l1*$^{fl/fl}$ organoids (Figure 4-13C). Most importantly, additional knock-out of *Atg16l1* in *Xbp1*$^{\Delta IEC}$ mice (*Atg16l1*/*Xbp1*$^{\Delta IEC}$) partially restored STING expression in the intestinal epithelium compared to *Xbp1*$^{\Delta IEC}$ mice (Figure 4-13D, E).

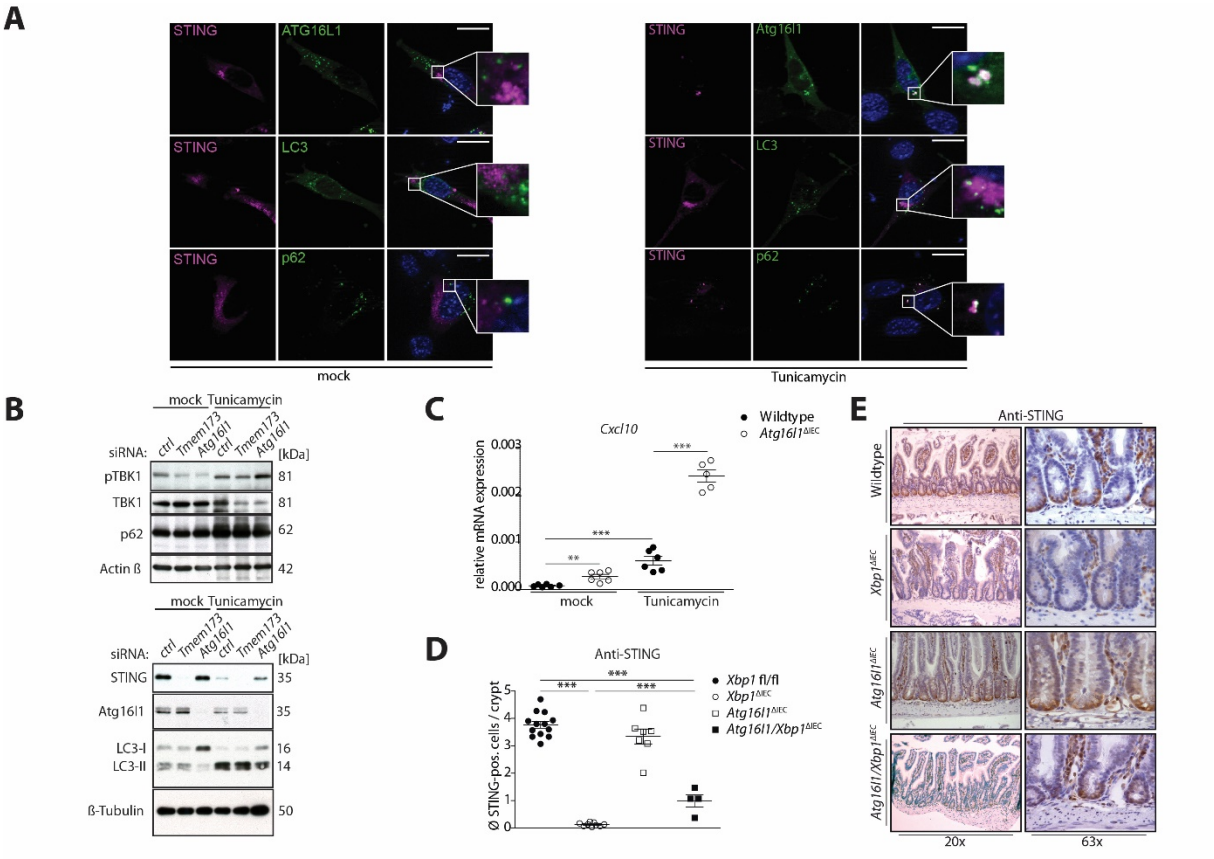

Figure 4-13: ER-stress engages Atg16l1-dependent autophagy to remove STING

(A) Immunofluorescence staining for p62, LC3, Atg16l1 and HA-tag of MODE-K cells transfected with an HA-mSTING plasmid and stimulated with 1 µg/ml Tunicamycin for 5 h. Experiment kindly performed by Dr. Stephanie Stengel.
(B) Western blot of MODE-K cells stimulated with 1 µg/ml Tunicamycin following siRNA knockdown of *Tmem173* or *Atg16l1*.
(C) Taqman assay of SI organoids of the indicated genotypes stimulated with 0,1 µg/ml Tunicamycin for 24 h.
(D) Quantification as average STING – positive cells per crypt of E.
(E) Immunohistochemistry staining for STING of control (n=13), *Xbp1*$^{\Delta IEC}$ (n=9), *Atg16l1*$^{\Delta IEC}$ (n=7) and *Atg16l1/Xbp1*$^{\Delta IEC}$ (n=4), representative pictures.

4.6.1 Removal of STING by autophagy is not altered by Bafilomycin A1 or Brefeldin A treatment

According to the quick colocalization of STING with autophagy proteins such as Atg16l1, p62 or LC3 and partially restored STING expression in *Atg16l1/Xbp1*$^{\Delta IEC}$ mice (Figure 4-13A, D, E), we assume that ER-stress recruits the autophagy machinery to mediate degradation of STING. Consequently, STING degradation should be less pronounced if either trafficking of STING from ER to Golgi or acidification of autolysosomes is blocked.

Thus, we treated MODE-K cells with either Bafilomycin A1 (blocking acidification of autolysosomes and thereby preventing final degradation) or Brefeldin A (blocking ER to Golgi transport) in addition to Tunicamycin. In line with our previous experiment, knockdown of *Atg16l1* altered ER-stress mediated

STING degradation (Figure 4-14A), although knockdown efficacy was only moderate. As expected, Bafilomycin A1 treatment resulted in an increase in LC3-II and p62 (Figure 4-14A). Surprisingly, neither Bafilomycin A1 nor Brefeldin A treatment could successfully block STING degradation (Figure 4-14A). Moreover, Bafilomycin A1 treatment per se was sufficient to induce phosphorylation of TBK1, while Brefeldin A treatment seemed to have no effect at all (Figure 4-14A).

In context of chronic ER-stress due to *Xbp1*-deficiency, we tried to block STING degradation by Bafilomycin A1 treatment. Again, Bafilomycin A1 was not able to restore STING protein levels (Figure 4-14B). Additionally, Bafilomycin A1 surprisingly also failed to block STING degradation following dsDNA transfection (Figure 4-14B). We suspect that if autophagic degradation of STING is blocked, other compensatory degradation mechanisms that have been described for STING might be upregulated such as for example proteasomal degradation[310,311].

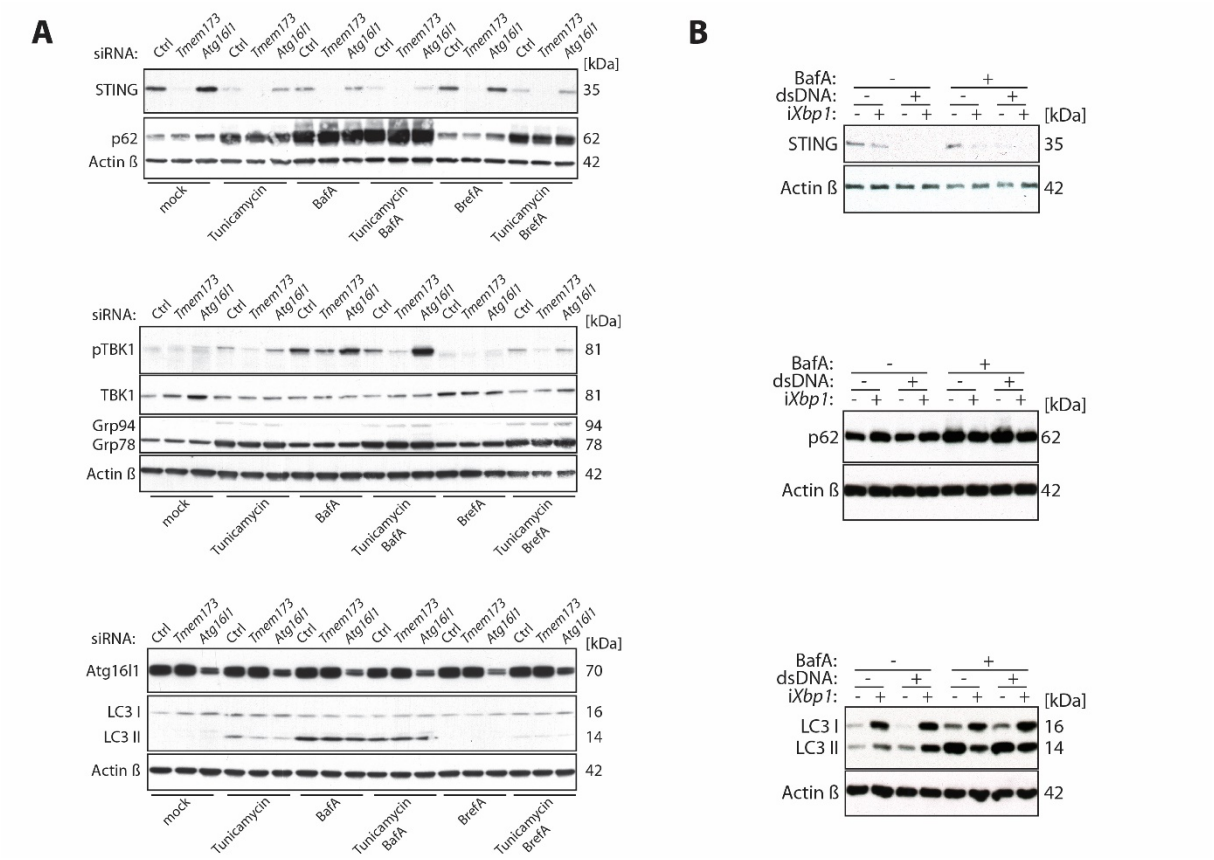

Figure 4-14: Removal of STING by autophagy is not altered by Bafilomycin A1 or Brefeldin A treatment

(A) Western blot of MODE-K cells treated with 1 µg/ml Tunicamycin, 0,1 µM Bafilomycin A1, 1 µg/ml Brefeldin A or Tunicamycin and Bafilomycin A1 or Brefeldin A for 24 h after siRNA knockdown of either *Tmem173* or *Atg16l1*.

(B) Western blot of MODE-K cells harbouring *Xbp1* or control shRNA stimulated with 1 µg/ml dsDNA, Bafilomycin A1 or both for 24 h.

BafA: Bafilomycin A1; BrefA: Brefeldin A

5 Discussion

5.1 *Tmem173* in the epithelial crypt: cell-type specific function?

Understanding of the cGAS-STING-type I IFN signalling pathway has started with the discovery of STING in 2008[215]. Since then, a plethora of diverse functions have been described for both cGAS and STING, ranging from classic pathogen sensing to more diverse, uncanonical functions such as autophagy or cell death induction[37,164,216,258]. Most research has however focussed on STING signalling in the innate, but also adaptive immune system. It was neglected to explore possible functions of this diverse pathway in other immunologically highly active tissues, such as the intestinal epithelium. Recent results of our own group clearly reveal a role for STING in cell death induction in intestinal epithelial cells[164]. Systematic knowledge regarding the role of STING in the intestinal epithelium is however still lacking. Bearing this in mind, we set out to investigate STING regulation and function specifically in the intestinal epithelium.

Employing a murine *Tmem173* knockout model, we show that in the small intestine, STING is expressed in the intestinal epithelium (Figure 4-1). With regard to the colonic mucosa, we could not observe STING to be expressed in the epithelium (data not shown). Thus, we concentrated our further experiments on the small intestinal mucosa. We demonstrate STING expression on protein level, applying immunohistochemistry and Western blot analysis of isolated intestinal crypts, but also on RNA level, as shown by q-RT-PCR of small intestinal organoids, isolated from wildtype and *Tmem173* -/- mice. We also rule out mistaking epithelium and lamina propria expression due to unpure isolation by analysing epithelial organoids, in which only the epithelium is purified. While Western blot and q-RT-PCR reveal little about the localization of STING within the intestinal epithelium, immunohistochemistry shows an unexpected expression pattern with STING found mainly in the crypt base (Figure 4-1A). Given the organization of the intestinal epithelium with cellular specialization in various subtypes (see 1.2.1), a cell-type specific expression of STING is not surprising however. Yet, the exclusive localization of STING to the crypt base was unexpected. We would have speculated STING to be 1) not exclusively expressed in one, or maybe two cell types, but more gradiently distributed over the cellular subtypes and 2) much more expressed in cell types residing in the villi or upper crypt (mainly enterocytes and Goblet cells) based on STING's well described role as a highly immunoactive PRR[215,216]. In addition, the epithelial mucus system is set up to maintain a crypt milieu poor in pathogens[312]. Therefore, localization of pathogen-sensing proteins in enterocytes or Goblet cells would make sense, as these are much more exposed to pathogens. Nevertheless, our results illustrate very clearly an exclusive distribution of epithelial STING, limited to cells residing in the crypt base of the small intestine (Figure 4-1A).

Taking advantage of our intestinal organoid model, we proceeded to explore the cellular subtype that predominantly expresses STING. Enrichment of intestinal organoids for specific cell types[289] showed increased expression of *Tmem173*, respectively STING, in Paneth-cell enriched organoids (Figure 4-1E). This would be in line with the current understanding of STING function as a PRR, proposing a model of epithelial STING function in Paneth cells. Hypothetically, during microbial penetration of the crypt base mucus layer, STING would subsequently serve its innate immune function and initiate a downstream type I IFN response or mediate initiation of a lamina propria immune cell based immune response. Additionally, exclusive expression of STING in Paneth cells is in line with STING being found in the small intestine, but not the colon, as the colonic epithelium does not harbour Paneth cells.

However, this data only provides a hint on the exact cell type responsible for epithelial STING expression, so that we are limited on speculating on the precise function of STING in the intestinal epithelium. Also, it can not be ruled out that in fact both Paneth cells and intestinal stem cells express STING. Unfortunately, methodological limitations prevented us from analysing STING's location in detail, as e.g. fluorescence STING-lysozyme-costainings could not be performed due to unavailability of STING antibodies working for immunofluorescence staining. Single cell sequencing analysis of the intestinal epithelium for example could serve to reveal cell type specific *Tmem173* expression in the intestinal epithelium.

5.2 STING safeguarding the intestinal crypt: an indicator of general danger?

The function of STING in crypt base cells, presumably Paneth cells, is virtually unknown. Although we speculated that STING in Paneth cells would carry out mainly immune response related functions (i.e. type I IFN induction), other functions are to be considered and discussed. Recent literature has shaped an understanding of cGAS/STING-dependent immunosurveillance of genomic damage and subsequent cGAS/STING-mediated senescence induction[169,170]. Immunosenescence is a mechanism similar to pathogen defence, but instead of PAMPs triggered by self-DNA e.g. released from the nucleus during DNA-damage, and cytokines preventing cells from proliferating, instead of trapping and eliminating pathogens. Ultimately, senescence results in immune recognition of cytosolic DNA and proliferative arrest of faulty cells carrying a defective genome, preventing carcinogenesis.

Intestinal cancerogenesis originates from the intestinal stem cell, which resides at the crypt base, and is kept vital by surrounding cells constituting the intestinal stem cell niche[206,313]. In a murine model of DNA-damage acquired due to defective nucleotide excision repair, we have previously demonstrated that such stem cells can accumulate DNA damage and are subsequently directed to cellular senescence in a p53-dependent manner[171,314]. Interestingly, other studies have found that DNA-damage induced senescence also requires the cGAS/STING pathway, establishing a role for STING in self-DNA sensing

and senescence and proliferation control[169,170]. Moreover, antiproliferative functions of type I IFNs are well described[277,279,315]. Accordingly, our results might indicate a role for STING in constituting the stem cell niche and governing stem cell proliferation and senescence. It could be interesting to study whether STING acts as a second switch governing proliferative capabilities of damaged stem cells besides p53[314]. We speculate that STING, residing deep down in the crypt base, fulfils a dual role centered around pathogen defence and stemness control. In the context of pathogen infiltration, STING could transmit signals of microbial presence towards Lamina propria based immune cells. During DNA-damage on the other hand, STING could engage in proliferation and senescence control.

Ultimately, our data illustrates that STING is expressed in the intestinal epithelium. At the same time, our data also gives rise to the next question, which we could only partly address within this thesis. Organoid enrichment data reasonably points towards a cell-type specific function of epithelial STING. In light of a recent, new understanding of cGAS/STING-signalling managing proliferation and cell death modalities (also see 1.3.4), it is conceivable that STING carries out a cell-type-specific function. The precise function and mechanism however remain to be uncovered using a proper model to investigate *specifically epithelial* STING function (i.e. *Tmem173*$^{\Delta IEC}$ mice).

5.3 Hallmarks of IBD pathophysiology regulate *Tmem173* expression

We established that STING is expressed in crypts of the small intestinal epithelium, possibly Paneth cells. Next, we aimed to approach regulatory mechanisms of *Tmem173* expression. The epithelium is located at the interface between Lamina propria-resident immune cells and the luminal commensal microbial flora. Accordingly, a microbial regulation of *Tmem173* expression seemed highly likely. Additionally, STING can be activated by fecal components and microbial DNA, and *Tmem173* -/- mice show signs of an altered microbial composition (also see 1.3.8)[283]. Therefore, we felt expected a microbiota-dependent expression of epithelial *Tmem173*.

Using small intestinal sections of germ-free and conventionally-raised mice, we show that without a conventional microbiota, a physiological *Tmem173* expression cannot be established (Figure 4-2A-D). Conventionalization of germ-free mice with a conventional microbiota reliably induces *Tmem173* expression, confirming the conventional microbiota as a strong inducer of *Tmem173* expression (Figure 4-2D). Importantly, even germ-free mice showed a similar pattern of epithelial STING distribution with much weaker STING expression though (Figure 4-2A). Thus, a small proportion of STING expression does not necessitate microbial stimuli (Figure 4-2A). We previously speculated that epithelial crypt-localized STING might possess functions in stemness, senescence and proliferation control (see 5.2). If so, this could explain the small fraction of STING expression maintained even in germ-free mice.

Canesso et al. reported that STING can be activated by fecal components, in line with a role for STING as a PRR[283]. It is reasonable to hypothesize that during sudden colonization of germ-free mice with a microbial community, the sudden amount of microbes causes tremendous immunological stress in the mucosa. Also, it seems unlikely that during recolonization, the intestinal crypt remains poor in microbes simply protected by the mucus layer. Infection could occur due to breaching of the epithelial layer by commensal or pathogenic microbes. Epithelial sensing of specific bacterial small molecules, (possibly by STING itself) and subsequent induction of *Tmem173* expression could be another possible mechanism to explain *Tmem173* induction. We approached these mechanisms by testing specific bacterial strains or specific bacteria-derived metabolites for their capability to induce *Tmem173* expression, and by infection experiments.

Unlike colonization of germ-free mice with a complete conventional microbiota, colonization with single bacterial strains such as *E. coli* or *B. theta* failed to lift *Tmem173* expression (Figure 4-2E). Also, exposure of small intestinal epithelial cells to a broad spectrum of bacterial metabolites did not reveal any specific bacteria strain possibly responsible for the microbial regulation of *Tmem173* (Figure 4-2E, F). The possibility that there is a specific, but still unidentified bacterial strain responsible for *Tmem173* expression in conventionally-raised mice accordingly seems less likely. Proper *Tmem173* expression in the epithelial crypt apparently requires a more complex set of microbial stimuli. It would be interesting to further investigate the underlying mechanism responsible for microbial induction of *Tmem173* expression. We speculated that either, the epithelium actively transmits microbial signals, e.g. by sensing of bacterial metabolites in the lumen, such as STING does[283], or microbial presence is sensed during infection. Importantly, also more complex models of *Tmem173* induction (respectively, host-microbe-crosstalk) are to be considered. Involvement of cytokines derived from immune cells or paracrine signalling from epithelial cells residing in the tips, where possibly enterocytes could sense microbial metabolites or be constantly exposed to “microinfections” are reasonable options. With regard to *Tmem173* induction in context of microbial infection however, we demonstrate that *Tmem173* is upregulated during intestinal barrier disruption (i.e. DSS-colitis) and subsequent microbial invasion (Figure 4-2G, H), and during *in vitro* infection of small intestinal cells with the intracellular pathogen *Listeria monocytogenes*, known to be sensed by STING (Figure 4-2I, J)[245].

In conclusion, we show that *full* epithelial STING expression strictly requires a conventional microbial community. The microbial regulation of epithelial STING also nicely fits our finding of predominant STING expression in Paneth cells. Both findings together support a model in which epithelial STING function is centred around pathogen defence. For this phenomenon we propose different mechanisms, of which we consider sensing or metabolites of a single, specific strain to be rather unlikely. Instead, *Tmem173* induction during DSS-colitis and direct pathogen infection demonstrate

that at least, delivery of microbial signals by intracellular infection is one possible mechanism for reduced *Tmem173* expression in germ-free mice. Considering the complexity of host-microbe-crosstalk, further mechanisms however are highly likely.

A disturbed microbial ecology, referred to as dysbiosis, is commonly acknowledged as a main contributor of inflammation during IBD, as well as the presence of risk-mediating gene variants associated to IBD. Ultimately, the interplay of dysbiosis, environmental stress and risk-variants results in ER-stress and defective autophagy (also see 1.1.3, 1.2.5). Importantly, cells with high secretory activity, such as Paneth cells, are highly susceptible to ER-stress, and intestinal inflammation can arise from ER-stress or defective autophagy in Paneth cells alone[39,40,45,51]. On top of that, dysbiosis and microbial infection are potent triggers of ER-stress[37,39].

We now know that STING is expressed predominantly in Paneth cells and strongly regulated by microbial signals. Accordingly, we hypothesized that STING expression in Paneth cells might be due to ER-stress. ER-stress on the other hand could be a consequence of the microbial burden during recolonization or infection. Along this line, we further suspected that if ER-stress occurs during recolonization, and *Tmem173* induction might be attributed to ER-stress, we should be able to confirm this analysing biopsies of IBD patients, where presumably both dysbiosis and ER-stress are present.

In Figure 4-3, we provide evidence that besides the microbiota, ER-stress indeed is a strong inducer of both murine and human *TMEM173*. Recolonization data shows that ER-stress goes hand in hand with microbial recolonization, as expected, and correlates with *Tmem173* expression (Figure 4-3A-D). The reconventionalization experiment however is limited to demonstrating an association between ER-stress, microbial colonization and *Tmem173*. In opposite, stimulation of both murine and human organoids with Tunicamycin (an ER-stress inducing chemical agent) proves ER-stress is a regulatory element upstream of *Tmem173* expression, even without microbial stimuli (Figure 4-3E-H).

We established that *Tmem173* expression is subjected to regulatory effects of *both* the microbiota and ER-stress. IBD patients presumably harbour either a dysbiotic microbiota or a (ER-) stressed epithelium. Therefore, a distinct signature of *Tmem173* expression in IBD patients was to be expected. In order to ensure a strictly epithelial result, we employed the human organoid model. Analysis of *Tmem173* expression in human organoids revealed that in IBD patients, *Tmem173* expression goes hand in hand with ER-stress (Figure 4-4A). Likewise, in a study by Häsler et al.[305], *Tmem173* expression in CD small intestinal biopsies was highest in biopsies of inflamed CD patients and showed the same correlation as in our human organoid dataset (Figure 4-4B-D).

Although *TMEM173* has not directly been linked to IBD (i.e. to date no risk-mediating SNP has been identified), a few studies provide direct evidence that *TMEM173* is dysregulated in IBD[316]. In a recent

study by Howell et al. analysing a cohort of pediatric IBD patients, *TMEM173* was hypomethylated in IBD patients[281]. Importantly, transcriptome data of this study showed that hypomethylation of *TMEM173* results in significant upregulation of *TMEM173* (Figure 4-4E), in line with data from the study by Häsler et al. [305] (Figure 4-4B-D). Taking advantage of the human organoid model, we were able to confirm that in IBD, *TMEM173* is upregulated, which translates to increased STING protein expression (Figure 4-4F, G).

In conclusion, this data establishes that 1) *Tmem173* expression reliably correlates with ER-stress triggered by microbial colonization, 2) that *Tmem173* (or *TMEM173*, respectively*)* expression can be directly targeted by induction of ER-stress and 3) that TMEM173 is overexpressed in the inflamed epithelium of IBD patients. In context of inflammation, ER-stress and dysbiosis in IBD, *TMEM173* overexpression could simply reflect another feature *associated* with inflammation, without being causally involved in IBD pathophysiology. However, hypomethylation of *TMEM173*, increased expression of *TMEM173* and increased STING protein levels in human IBD organoids prompted us to speculate to which extent STING might participate in IBD pathophysiology. STING in fact is an ER-resident protein. An impact of ER-stress on STING function therefore seems conceivable. Moreover, Moretti et al.[37] show that STING activation in turn provokes ER-stress, suggesting a dense STING-ER-stress crosstalk beyond plain gene regulation (see 1.3.5). Our results stress the fact that hallmarks of IBD pathophysiology (ER-stress and dysbiosis) profoundly regulate epithelial *Tmem173*. Thus, the question arises to which extent STING causally contributes to the pathophysiology of inflammation in IBD.

5.4 STING sensing ER-stress: function beyond pathogen sensing?

STING has first been described as a primarily antibacterial and antiviral pathway[215,216]. Nonetheless, our data implicates that STING function goes beyond pathogen sensing. For STING in Paneth cells, we propose a function centred around both pathogen defence and stem cell control. On the other hand, our results investigating the regulation of *Tmem173* by ER-stress (Figure 4-3) and in IBD (Figure 4-4) implicate a new aspect of STING-signalling. Thus, we continued taking advantage of the model of chemically induced ER-stress (i.e. using Tunicamycin to induce ER-stress). We demonstrate that ER-stress results in STING-mediated type I IFN induction (Figure 4-5A, B). Additionally, we exclude any non-ER-stress-related activity of Tunicamycin (which might potentially be responsible for activation of STING) by validating this experiment using MG132. MG132 is a chemical stimulant blocking the proteasome, thereby preventing degradation of misfolded proteins and inducing ER-stress[317]. Accordingly, stimulation of cells with MG132 phenocopied the Tunicamycin experiment. This demonstrates that ER-stress alone reliably induces a STING-dependent type I IFN response (Figure

4-5C). Likewise, *ex vivo* treatment of small intestinal organoids (Figure 4-5F) and *in vivo* treatment of mice (Figure 4-5G) with Tunicamycin provides evidence that ER-stress evokes a STING-dependent type I IFN response.

Canonically, STING is degraded by autophagy following activation and signalling. Degradation occurs presumably in order to terminate signalling activity and prevent excessive type I IFN induction[227,228]. Importantly, we noted complete degradation of STING following Tunicamycin stimulation. This suggests that Tunicamycin, ER-stress respectively, somehow triggers activation of canonical STING-signalling (Figure 4-5A). ER-stress mediated degradation of STING might have a profound impact on a setting in which ER-stress persists chronically (e.g. in IBD), possibly resulting in lower STING levels. However, we were first prompted to investigate whether ER-stress indeed elicits a *canonical* STING-mediated type I IFN response that involves all compounds of the canonical cGAS/STING-signalling (that is: cGAS, STING, TBK1, IRF3). To date, an activation of STING has mostly been described by cyclic dinucleotides, derived from bacteria or synthesized by cGAS. Therefore, we were curious to see whether ER-stress mediated STING activation also relies on CDNs, or if ER-stress somehow could recruit a STING-signalling process independent of CDN release and sensing. Additionally, downstream effects of STING-signalling are known to be mediated by TBK1, IRF3 and finally type I IFNs (mainly IFNβ, also see 1.3.1)[217]. On the other hand, alternative downstream effects of STING-signalling (apart from type I IFN induction) have recently been identified, most prominently engagement of autophagy, ER-phagy and activation of the NFκB pathway[37,234,258]. Thus, given the uncanonical activator (ER-stress), we hypothesized that also the downstream cascade might differ from canonical STING-signalling. However, we could show by knockdown of the respective parts of the STING-signalling cascade, both upstream (cGAS) and downstream (TBK1, IRF3), that ER-stress engages a pathway involving classic STING-signalling (Figure 4-5D, E). Additionally, this data also clearly reveals that ER-stress-mediated STING activation requires the presence of CDNs, as cGAS-knockdown abrogated STING activation (Figure 4-5D, E).

In sum, our data offers a new, so far unknown perspective on STING function and signalling. We demonstrate in cell culture, small intestinal organoid and mouse model that ER-stress also launches a cGAS/STING-dependent type I IFN response, establishing a role for cGAS/STING beyond pathogen sensing. Engagement of STING by ER-stress suggests that STING in fact might participate in inflammatory disease involving ER-stress, most prominently IBD[19], but also other diseases involving inflammation are worth considering, e.g. cancer[318], cardiovascular disease and atherosclerosis[319], rheumatoid arthritis[320] or diabetes[321]. In light of our previous findings on distinct regulation of *Tmem173* expression by the microbiota, ER-stress and in IBD patients (see 4.2 and 4.3), it is reasonable to speculate on an involvement of STING in IBD pathophysiology. Recent literature further supports

this idea[164,281]. To this end, our data showing ER-stress-mediated STING activation point towards STING *actively* being involved in induction and maintenance of inflammation in IBD, rather than simply correlating with dysbiosis for example. Accordingly, the question arises to which extent recruitment of STING by ER-stress translates to a clinical phenotype in intestinal inflammation.

Based on our data, we speculate that exacerbation of IBD that goes along acute ER-stress transmits proinflammatory signals via cGAS/STING-mediated type I IFNs. Another reasonable idea would be that chronic ER-stress in "steady-state" low-grade inflammation continuously activates and degrades STING and thereby gives rise to enhanced infection susceptibility due to lowered STING levels (Figure 5-1).

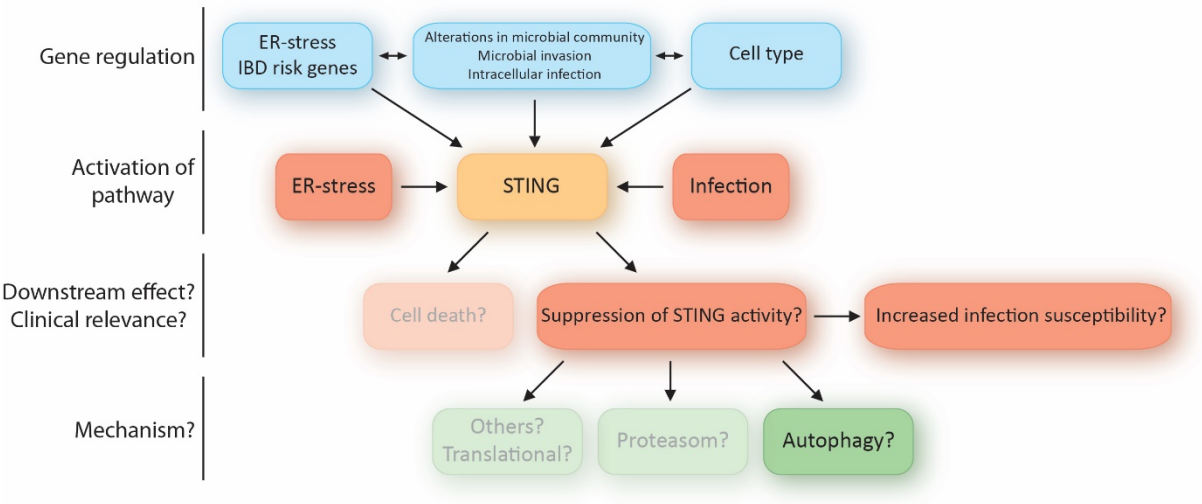

Figure 5-1: Study rationale based on new findings on STING regulation and function

As discussed above (5.1 and 5.2), we obtained data on intestinal *Tmem173* expression and localization, from which we generated further hypotheses resulting in discovery of a new function of STING, namely the execution of ER-stress triggered type I IFN production. Based on previous findings and features of ER-stress mediated STING activity (including STING degradation), we proposed two main downstream outcomes implying clinical significance. Both were tested accordingly and a brief investigation of possible mechanisms conducted afterwards.

In the second setting, dysfunctional STING-signalling would presumably rather deteriorate the phenotype by increased infection susceptibility, instead of being beneficial. In the first setting however, another trigger of ER-stress resulting in STING activation is conceivable, e.g. ER-stress occurring as a consequence of virus infection and replication. In this situation, possibly beneficial impacts of acute ER-stress-mediated STING activation could include well-known antiviral functions of STING-signalling, e.g. cytokine or cell death induction.

We first investigated likely consequences of STING activation during acute ER-stress, and then proceeded to gain an understanding of the phenotypic impact of diminished STING in context of chronically present ER-stress, as it is characteristic for IBD.

5.5 Cell death: an alternate route of ER-stress related STING activity?

During virus infection, ER-stress might occur as a consequence of a high rate of virus protein biosynthesis. Therefore, ER-stress could be associated with uncontrolled virus infection. This would implicate a situation, in which the cell and the surrounding tissue would face overwhelming virus replication and infection. Accordingly, ER-stress in this context might serve as an indicator to recruit antiviral immune response pathways, such as the STING pathway. In this context, an activation of STING would match the physiological function of STING as an antiviral type I IFN inducer. This would provide a possible explanation to why ER-stress directly activates STING.

Additionally, various forms of cell death have been described as another outcome of STING activation besides interferon induction (see 1.3.4)[164,247,248,250,251,257]. Possibly, if the viral replication load is exceeding immune response capacities, ER-stress-mediated STING activation might start a cell death pathway in order to limit viral replication. This would prevent major viral replication in the tissue in total, although the individual cell perishes. Thus, we speculated that unresolved ER-stress activates STING to accomplish cell death induction by STING activation, possibly as a physiological last resort barrier designed for overwhelming viral replication. Additionally, in light of recent findings of our own group[164], STING-dependent cell death appeared to be highly likely as a downstream effect, especially in the intestinal epithelium.

Applying three different models (Tunicamycin-induced acute ER-stress, genetically determined ER-stress, i.e. *Xbp1* deficiency[19], and small intestinal organoids defective for *Tmem173*), we show that acute ER-stress does induce severe cell death. In contrast to our expectation however, absence or presence STING does not affect cell death induction by ER-stress (Figure 4-6).

Accordingly, it can be concluded that ER-stress, while inducing type I IFN release via cGAS/STING, on the other hand relies on pathways apart from cGAS/STING to mediate cell death. This came as a surprise, as in a study of our own group (Aden et al., 2018[164]), in context of defective autophagy, STING was found to mediate susceptibility to necroptosis in response to the (usually) protective cytokine IL22. Since this study also focussed on the intestinal epithelium, we had expected STING to inherit the same role during our intestinal epithelial ER-stress models. Based on previous literature, we can say for certain, STING is able to induce various kinds of cell death (see 1.3.4). STING is however not responsible for cell death in our models. To further understand STING-induced cell death, it could be rewarding to investigate pathways interfering with cell death inducing capabilities of STING-signalling and identify a molecular switch determining effects of STING on proliferation or cell death modalities. One idea could be to investigate autophagic removal of STING following activation, as regulation of STING by autophagy is extensively studied and documented. In the intestinal epithelium, STING predominantly

mediated necroptosis in context of defective autophagy[164]. Accordingly, it is reasonable to speculate that STING-signalling only results in proinflammatory cell death induction, if both a trigger (e.g. ER-stress) and defective signalling-resolution mechanisms (e.g. dysfunctional autophagy) are present. Both could synergize to result in excessive STING-signalling and thus cell death. Nonetheless, we propose that mechanisms modifying the cell death favouring properties of STING-signalling also highly depend on the specific trigger. Since ER-stress is known to trigger numerous potent cell death-inducing pathways (also see 1.2.4), ER-stress might simply not require STING-signalling to accomplish cell death at all.

5.6 Pathological, unresolved STING-recruitment during chronic ER-stress?

We have established ER-stress as an upstream trigger of STING activation and excluded cell death as a potential downstream outcome of ER-stress induced STING activity. Thus, we continued to further disentangle downstream effects with the aim to provide a clinically relevant mechanistic understanding of STING in context of ER-stress. Our data illustrates that STING activation can not only occur as a consequence of infection, but also due to ER-stress without the presence of invading bacteria or viruses. We assumed that to achieve clinically insightful data, adapting our experimental model to the "real world" complexity of IBD would improve chances. As described in the introduction, IBD is most likely triggered by maximized stress as a result of multiple stressors *and* defective resolution mechanisms, e.g. ER-stress *and* simultaneous microbial infection or dysbiosis. Thus, we next analysed STING function in response to microbial stimuli in context of pre-existing, low to moderate ER-stress, applying different *in vitro* and *in vivo* models.

Exposure of MODE-K cells to low-dose Tunicamycin prior to *E. coli* dsDNA transfection, a canonical activator of the cGAS/STING pathway, revealed three important features of STING function in response to microbial stimuli during simultaneous ER-stress (Figure 4-7A). This was consistent with our results analysing ER-stress dependent STING activation. First, ER-stress lowers STING protein levels drastically. Second, this goes along with a reduced STING activity when additionally challenged with dsDNA, as shown by reduced phosphorylation levels of both STING itself and TBK1 (Figure 4-8A). Third, reduced STING protein levels and activity translates to reduced type I IFN induction (Figure 4-7B). Importantly, TBK1 protein levels were not altered, excluding transcriptional or translational effects of ER-stress on TBK1.

While we know for certain that ER-stress activates STING and results in type I IFN release (see 5.4), from this data we draw the conclusion that prolonged ER-stress impedes STING activity in response to additional stimulation with canonical activators, such as *E. coli* dsDNA. Degradation of STING following activation to restrain STING activity is a well-known aspect of the STING pathway[227,228,262]. Accordingly,

lowered STING protein levels following just mild, but prolonged ER-stress most likely result from activation and subsequent degradation of STING. This would be in line with our repeated observation of LC3-I to LC3-II shifting after ER-stress. Autophagy therefore appears to be a likely candidate responsible for ER-stress induced STING degradation. We picture that in this experimental setting, ER-stress activates STING, which is then removed (lower protein levels) and thus unavailable for repeated activation by dsDNA (lower phosphorylation status, lower type I IFN induction).

Mechanistically, although we propose degradation by autophagy as the main factor, we do not exclude further deterioration of STING activity by other mechanisms. However, we are limited to speculate on additional features involved. As shown in Figure 4-3, ER-stress critically regulates *Tmem173* expression. On the other hand, it is also known that during ER-stress, the main arms of the UPR (see 1.2.4) synergize to lower ER protein load, among other mechanisms by inhibiting transcriptional and translational activity[175,176]. We can exclude suppression of STING protein levels by lowered *Tmem173* transcription based on our data (as demonstrate the opposite way in Figure 4-3), but regulation of STING translation during prolonged ER-stress could be another mechanism possibly resulting in both lowered STING protein levels and impaired STING activity as shown by our data (Figure 4-7A). Due to the complex properties of ER-stress, i.e. multiple pathways being activated during ER-stress, we cannot disentangle lowered translational activity and increased (autophagic) degradation from this data alone. However, previous data involving research on STING degradation and ER-stress induced autophagy is highly suggestive of degradation at least as a very likely mechanism to impair STING activity in response to dsDNA in context of pre-existent ER-stress. Additional mechanisms are however worth considering and could be of interest for further research (see Figure 4-14).

In sum, we show *in vitro* that prolonged ER-stress impairs STING activity in response to canonical stimuli, opposite to direct STING activation by ER-stress observed previously. This is facilitated in a way involving lowered STING protein levels, presumably resulting in lowered STING and TBK1 activity.

In order to extend our set of experimental models for a combined stressor setting, we challenged STING activity with either dsDNA or the direct chemical STING agonist CMA in context of *Xbp1* deficiency. *XBP1* gene variants have been associated with both UC and CD[19]. Mechanistically, defective versions of *XBP1* predispose for development of inflammation by decreasing the ER's ability to cope with ER-stress, thus increasing general likelihood of ER-stress. *XBP1* deficiency can also directly result in CD-reminiscent inflammation in case of additional autophagy defects, respectively[40]. For our purpose, *Xbp1* deficiency also resembles a good *in vitro* and *in vivo* model, as the phenotype of *XBP1* deficiency has been extensively studied in murine *in vivo* and *in vitro* models and can be easily combined with additional STING activating compounds, at least *in vitro*. In Figure 4-7 and Figure 4-8 we show that *in vitro*, *Xbp1* deficiency phenocopies low-dose Tunicamycin treatment in most aspects,

which further strengthens our conclusion from the Tunicamycin model. STING activity in context of *Xbp1* deficiency is lower in response to dsDNA (Figure 4-7C, D), CMA (Figure 4-7E) and also in response to high-dose Tunicamycin (Figure 4-8B, C), which we considered another STING agonist based on our previous results (Figure 4-5). Importantly, *Xbp1*-deficient small intestinal organoids display a similar phenotype consistent with the MODE-K models, but also increase comparability to the *in vivo* situation (Figure 4-7E, Figure 4-8C).

Comparing the results from these two approaches (using either low-dose Tunicamycin or *Xbp1* deficiency as a model for chronic ER-stress), we note that both models slightly differ, while sharing the main feature of the phenotype: a reduced STING activity in response to canonical STING activation in context of 'chronic' ER-stress. Lowered STING protein levels were a crucial finding of the Tunicamycin approach, suggestive of autophagy as the underlying mechanism. In contrasst, in the *Xbp1*-deficient model, STING levels were only moderately decreased. On the one hand, this could support the idea of another mechanism apart of autophagic degradation, on the other hand this could also be well explained by fundamental differences between chemical stimulation and gene deficiency as a model (Tunicamycin vs. *Xbp1* deficiency). That being said, one also has to take into account the primary function of XBP1 as a transcription factor. XBP1 has been found to influence IFNβ transcriptional activity directly by binding to an upstream promotor site[255]. Yet, we did not observe any suppression of *Tmem173* in context of *Xbp1* deficiency (data for this specific experiment not shown, but provided for another experiment in Figure 4-9). Therefore, we assumed transcriptional regulation to be a less likely cause for decreased STING activity in this context. Instead, we speculate that differences in ER-stress kinetics (genetic deficiency vs. comparably short, chemical stimulation) and cellular adaptation, respectively compensatory mechanisms, are responsible for subtle phenotype differences between both models. Shared features in both models however suggest an underlying common mechanism.

5.7 *XBP1* deficiency: prototype for clinical impact of ER-stress effects on STING activity?

Further support for this hypothesis lies within our *in vivo* data. Figure 4-9 illustrates how *Xbp1* is required to maintain STING and type I IFN expression in the intestinal epithelium. Notably, this data is derived from mice without any further experimental procedures such as infection or DSS-colitis. In light of this, we were surprised by the spectacular phenotype of virtually no STING present in the intestinal crypts. Based on our *in vitro* data we did not expect such a drastic difference. Likewise, the difference in type I IFNs on a basal level came as a surprise.

From this data, a few questions arise. First, our initial goal was to provide a clinically relevant insight into the role of STING during IBD. Considering the drastic phenotype of virtually eliminated STING in

context of *Xbp1* deficiency *in vivo*, we assume that patients carrying the *XBP1* risk variant would likewise lack STING nearly completely in the intestinal epithelium. This could imply potentially severe consequences. To this end, we are unfortunately (again) limited to speculate on the exact clinical outcome, because the role of epithelial STING is essentially unknown. Likewise, the consequence of absence of STING can only be anticipated.

Nevertheless, the *in vivo* data provides some critical insights, apart from verifying and extending the previous phenotype. On a transcriptional level, *Tmem173* is neither suppressed nor elevated, in context of *Xbp1* deficiency. Contrary to this, there is no protein expressed, again pointing towards degradation as a reasonable mechanism. Next, type I IFN expression is lowered as illustrated by reduced *Ifnb1* and *Cxcl10* expression (Figure 4-9D). Reduced *Ifnb1* implies that the *Xbp1* deficient epithelium in the steady state produces less type I IFNs. Reduced *Cxcl10* would certainly be consistent with this, while it could also be because of reduced type I IFN exposure of the epithelium, with the source of type I IFNs possibly outside the epithelium (i.e. within the lamina propria or submucosa). Notably, type I IFN expression is not decreased as much as STING expression in the epithelium. Despite STING's well established crucial role in type I IFN induction, other PRRs in the epithelium could take part in generating a basal amount of type I IFN. This could be of interest for further research focussing on the main source of type I IFNs in the intestine. Coming back to the clinical scenario, this would imply that the phenotype of IBD patients carrying the *XBP1* risk variant could possibly be compensated to a certain extent by other type I IFN inducing PRRs. On the other hand, compensation by other PRRs is only reasonable assuming that type I IFN induction indeed is the main function of epithelial STING. This remains subject to speculation for now.

In our very first experiments, we analysed STING expression and distribution in the intestinal epithelium using immunohistochemistry (Figure 4-1). Additionally, we applied advanced organoid models to gain insights on the distribution of STING expression among the specific epithelial subset of cell types. Taken together, this data suggested that STING is predominantly expressed in Paneth cells. Interestingly, absence of STING in the *Xbp1* deficient epithelium indicates a correlation of STING expression with Paneth cell presence in this scenario. *Xbp1* deficiency is well acknowledged for interfering with epithelial physiology so far, that Paneth cells are not detectable anymore[19]. This can be seen having a closer look on the images of Figure 4-9A, where by eye no granules characteristic for Paneth cells can be seen. Accordingly, one could argue that with the Paneth cells gone, also epithelial STING vanishes. We consider this possibility to be rather unlikely to explain the *full* phenotype, based on a number of findings: first, absence of Paneth cells can not sufficiently explain drastically decreased STING activity in our *in vitro* models (especially in the *Xbp1* deficient MODE-K cells, where STING levels were only moderately decreased). Additionally, "absence of Paneth cells" primarily refers to the fact

that lysozyme, a canonical Paneth cell marker, cannot be detected. Accordingly, this could in fact simply resemble inability to produce sufficient amounts of lysozyme (due to ER-stress), while the original differentiation into a "Paneth cell" is not affected. Recalling the high susceptibility to ER-stress of cells with high secretory demand (such as Paneth or Goblet cells)[42,45–48], it is comprehensible that defects in the UPR (i.e. *Xbp1* deficiency) impair protein biosynthesis so severely that maintenance of an adequate amount of lysozyme is no longer feasible. Additionally, lysozyme (unlike STING in basal state), is continuously produced and secreted. Thus, defects in the protein biosynthesis machinery would impair lysozyme production first. On the other hand, STING should still be present, if not previously activated and degraded. Also, we explicitly demonstrate that at least *Tmem173* expression is essentially not affected by the genotype. If STING was indeed entirely coupled to presence of lysozyme, one would have expected to observe altered *Tmem173* transcription in context of *Xbp1* deficiency. Taking this into account, there is no clue pointing towards lysozyme expression (respectively absence of "Paneth cells") as an explanatory mechanism for abolished STING expression in context of *Xbp1* deficiency.

Yet, our data from Figure 4-1 suggests that predominantly Paneth cells express STING: the organoid differentiation experiment in Figure 4-1 demonstrates that Paneth cell enrichment goes along with increased *Tmem173* expression. At first glance, this appears to be contradictory to the idea explained here that absence of lysozyme-positive cells ("Paneth cells") in *Xbp1* deficient mice does *not* resemble the mechanism underlying abolished STING expression. However, we know that *Xbp1* deficient (Paneth?) cells are not able to produce detectable amounts of lysozyme anymore (referred to as "no Paneth cells"). From our understanding, this alone does not equal absence of Paneth cells, because presumably the differentiation into "Paneth cells" is unaffected. Instead, it is known that the secretory function *of* Paneth cells is severely affected due to ER-stress[42,45–48].

5.8 Shared features of ATF6 and STING signalling extending clinical implication of suppressed STING activity during chronic ER-stress?

In Figure 4-10 we further evaluate how ER-stress suppresses the STING pathway applying another *in vivo* model. ATF6 is a transmembrane protein and part of the third branch of the UPR apart from the XBP1/IRE1α and PERK/ATF4 pathway (also see 1.2.4 and Figure 1-5). Opposite to *Xbp1* deficiency, *Atf6* overexpression, not suppression, has been found to profoundly disturb ER homeostasis. Overexpression results in altered mucine production, troubled epithelial barrier function and inflammation induction via NFκB recruitment, altogether indicative of ER-stress[196,197]. Using a model of Tamoxifen-inducible overexpression of *Atf6* specifically in the intestinal epithelium, we validate our conclusion from the *Xbp1* model. As illustrated in Figure 4-10, *Atf6* overexpression results in reduced

STING levels in the intestinal epithelium, phenocopying *Xbp1* deficiency. Unlike in *Xbp1* deficiency, the difference is not as striking, but still substantial. Importantly, during *Atf6* overexpression, Paneth cells are presumably present (given that these mice were comparable to a wildtype four days before sacrifice), yet the phenotype is similar. Accordingly, simple association of STING expression to presence of lysozyme (Paneth cells, respectively) is even more unlikely. In addition to a generally weaker effect, differences in the expression pattern of type I IFNs and *Tmem173* itself are noteworthy. In opposite to lowered type I IFN expression in the *Xbp1* deficient situation, during induction of *Atf6* overexpression, type I IFNs are induced, while on the other hand *Tmem173* is decreased (Figure 4-10D). This could be explained by a much faster kinetic of four days of overexpression, in contrast to a conditional knock-out of *Xbp1*. Additionally, ATF6 and XBP1, while sharing a similar downstream effect, have a very different mechanism of action. Contrary to XBP1, ATF6 travels from the endoplasmic reticulum across the Golgi apparatus, where it is cleaved, before finally acting as a transcription factor in form of the ATF6 p50 fragment (also see Figure 1-5). XBP1 on the other hand is only translated in response to ER-stress as a consequence of alternative splicing and does not perform any trans-organelle travelling. Thus, for XBP1 it was prompting to think of transcriptional alteration as a mechanism to impact STING expression. In case of ATF6 on the other hand, it has to be acknowledged that ATF6 and STING both share a similar trafficking mechanism. This involves COPII-mediated translocation from the ER to the Golgi during the activation process[322,323]. Although we did not observe transcriptional alteration of *Tmem173* in case of *Xbp1* deficiency, ATF6 overexpression (not absence!) seems to result in suppression of *Tmem173* expression (Figure 4-10D). Taking both into account, we consider possible effects of ATF6 directly on *Tmem173* transcription. More importantly however, we speculate that during trafficking of ATF6 from the ER to the Golgi, STING activation (respectively trafficking) could be a side effect of processes required for ATF6 delivery to the Golgi apparatus. This idea would in part explain slight differences between the *Xbp1* deficiency and *Atf6* overexpression model. Moreover, it could be rewarding to study shared trafficking mechanisms between both STING and ATF6, given that both are activated by ER-stress, both complete a similar translocation following activation, but also that the precise circumstances of how STING travels from ER to Golgi and is finally degraded remain elusive.

With regard to clinical relevance, the effect of *Atf6* overexpression on STING could be of interest for both inflammation and cancerogenesis pathology. First, this data validates critical findings obtained from the *Xbp1* deficiency model (Figure 4-9). It supports the idea of STING suppression as a general feature of ER-stress. It also excludes some pitfalls from the *Xbp1* model and strengthens our conclusion that ER-stress is not only able to activate STING, but also involved in suppressing STING and type I

interferon induction if chronically present. Mechanistically, degradation of STING in context of chronic activation appears to be more likely than plain downregulation on a transcriptional level.

We project a second clinically relevant insight from the *Atf6* overexpression model in the role of STING during tumorigenesis in the intestine. Coleman et al. have shown that ATF6 overexpression reliably results in intestinal tumorigenesis[196]. This was dependent on alterations in the microbial community, microbial invasion and subsequent MyD88/TRIF-dependent signal transduction[196]. We have previously speculated on a role for STING apart of pathogen defence in the intestinal epithelium, based on our findings of a distinct expression pattern within the epithelium (see 5.1). Another ongoing study of our own group focusses on STING function during DNA damage accumulation and adds further evidence to this idea (data not shown). Apart from pathogen defence, it is well known that cGAS/STING form a critical safety step to prevent proliferation of cells accumulating DNA damage by inducing cell cycle arrest, respectively senescence[169,170,208]. In addition to the mechanism described by Coleman et al. [196], one could therefore speculate that during ATF6 overexpression, cancerogenesis can only occur due to suppression of STING. Thus, cGAS/STING would be impaired in their function in genome integrity surveillance and cell cycle arrest induction. Again, a shared mechanism of activation between STING and ATF6 is suggestive of possible interactions resulting in clinically relevant phenotypes.

Finally, another study of our own group focussing on regulation and implication of ATF6 signalling in IBD and intestinal inflammation has recently been published[197]. In this study, we identify ATF6 as a critical executor of inflammation. During ER-stress in context of e.g. *Atg16l1* or *Xbp1* deficiency, ATF6 mediated proinflammatory signals via NFκB activation. This ultimately resulted in elevated levels of proinflammatory signals such as TNFα. From this perspective, multiple scenarios seem possible with regard to our finding of reduced STING activity in chronic ER-stress. In context of *Xbp1* deficiency, one could speculate that ATF6 is activated as an execution mechanism of ER-stress-mediated inflammation. This could result in even further suppression of STING activity due to a synergizing effect of both *Xbp1* deficiency and ATF6 activation. If *Xbp1* deficiency is upstream of ATF6 activation, but both suppress STING levels, this could also in part explain why we observed only moderately lowered STING levels in context of only ATF6 overexpression. Accordingly, the *Xbp1* deficiency phenotype would be reversed by *Atf6* knockout instead of overexpression. If ATF6 is indeed downstream of *Xbp1* deficiency related ER-stress, suppression of STING could resemble an essential step not only during tumorigenesis (see above), but also during development of severe inflammation since we have shown that ATF6 activation is able to direct both inflammation induction and STING suppression. Unfortunately, we are again limited to speculate on the effects of this specifically in the intestinal epithelium. It could however be very rewarding to investigate whether ATF6 overexpression in the intestinal epithelium requires suppression of STING to mediate either inflammation or cancerogenesis.

5.9 But what about the microbiome?

Initially, our goal was to increase the comparability of our experimental model to the "real life" situation by combining both ER-stress and presence of microbial stimuli. Thus, taking potentially strong effects mediated by the microbiota into account is mandatory. Dysbiosis is a key feature of IBD, and the potential of the microbiota in modifying phenotypes is well acknowledged. Additionally, we have specifically shown that *Tmem173* expression is critically dependent on microbial presence (Figure 4-2). *Xbp1* deficiency on the other hand is known to cause alterations of the microbiota[135]. Thus, we were prompted to test whether *Xbp1* deficiency requires the microbiota to suppress STING.

Although the effect of *Xbp1* deficiency did not include any effect on *Tmem173* transcription (Figure 4-7D), we sought to investigate whether ER-stress in context of *Xbp1* deficiency is aggravated or even exclusively present in context of microbial presence. If so, removing the stressor (i.e. microbiota) would accordingly rescue the phenotype. This would reflect the pathophysiologal model of environmental stressors triggering inflammation in case of predisposing risk variants.

Analysing germ-free and conventionally-raised *Xbp1* deficient mice, we can exclude any of the above mentioned effects. There was no difference between GF and CR *Xbp1* deficient mice regarding STING levels in the intestinal epithelium (Figure 4-11A, B). This alone excludes any effect of the microbial environment on this specific phenotype. However, we further excluded the idea that the *Xbp1*-associated altered microbiome has a distinct effect on *Tmem173* expression by stimulation experiments with fecal supernatants of either $Xbp1^{\Delta IEC}$ or *Xbp1* fl/fl mice (Figure 4-11C - F). Interestingly, we observed small effects of knock-out derived fecal supernatants on ER-stress and likewise type I IFNs. Importantly, there was no effect on *Tmem173* expression, matching the phenotype of GF and CR *Xbp1* deficient mice.

Taken together, an altered microbial composition seems to be irrelevant for the interaction of chronic ER-stress and STING activity. This must be acknowledged carefully, as from a clinical perspective, a role of the altered microbial composition is still very likely. Specifically, we propose that chronic ER-stress, whether it may be due to environmental stressors, genetic predisposition or mediated by ATF6 activation, drastically suppresses STING activity in the intestinal epithelium. If STING is predominantly present in Paneth cells and fulfils an antimicrobial function, an impaired STING function during infection might be the consequence. While dysbiosis according to our data is not an option as the cause of altered STING levels, it could well be involved as a trigger in a clinical setting for which we postulate a relevance of these findings.

5.10 A clinical setting: faulty STING-signalling boosts pathogen replication during chronic ER-stress?

There are multiple clinical scenarios in which STING suppression could resemble an essential step licensing disease progression (e.g. cancerogenesis, ATF6-mediated inflammation). Here, we aimed to reveal how STING suppression might translate to a clinically relevant phenotype in IBD. We mainly followed the hypothesis that STING resides in Paneth cells and carries out a function centred around pathogen defence. Thus, we chose to investigate consequences of STING suppression in an experimental model of pathogen infection.

Infection with pathogenic bacteria or opportunistic viruses is an important feature of IBD, mainly UC, and is associated with poor clinical outcomes and aggravated disease courses (see 1.1.3.4 and 1.1.4.1). Most prominently, cytomegalovirus reactivation and subsequent CMV colitis can be frequently observed and present with problems in disease management and therapy[99,102]. STING and type I IFNs are vital for proper immune defence and clearance of CMV[324,325]. Accordingly, we suggest that in IBD, the high prevalence of simultaneous CMV reactivation is not only due to immunosuppressive drug regimens (see 1.1.4), but also a direct effect of chronic ER-stress. According to our data, ER-stress would render the epithelium unresponsive to CMV replication and colitis by suppressing antiviral STING activity.

To gather a first insight into STING function during infection and to validate our previous data, we took advantage of an easily available experimental setup and chose to infect *Xbp1* deficient MODE-K cells with the intracellular pathogen *Listeria monocytogenes*. *L. monocytogenes* is also frequently involved in gastrointestinal infection[245,246]. Although during *L. monocytogenes* infection, type I IFN production has a rather detrimental effect[307], we could validate the previously documented defect in STING activity during *Xbp1* deficiency (Figure 4-12A, B). This is however not a clinical model in which a lack of STING activity would result in poorer prognosis. Yet, it is noteworthy to mention that unlike stimulation with dsDNA (or other agonists such as CMA), during *Listeria* infection, the whole intracellular pathogen sensing machinery is recruited and the downstream outcome (i.e. type I IFN induction) a sum of the whole process. Therefore, it was worth considering that the type I IFN response was intact due to other PRR pathways, even despite defective STING. Accordingly, *Listeria* infection indicates, that in intestinal epithelial cells, STING inherits a dominant role governing type I IFN production. Even during exposure to the full set of PAMPs released during intracellular infection with *Listeria*, type I IFN induction is essentially dependent on intact STING signalling. This data therefore rules out other mechanisms compensating for reduced STING activity, which could have made our previously observed phenotype irrelevant in the “real world” situation.

After validation of the phenotype in a bacterial infection model, next we took into account CMV infection as the clinically more interesting scenario. Again, MODE-K cells were chosen as a feasible model for intracellular infection experiments. We obtained data on STING function analysing gene expression and protein, but importantly also murine CMV replication. Type I IFN induction post CMV infection was notably slower than induction by e.g. dsDNA. In line with our previous results, STING activity was virtually eliminated in context of chronic ER-stress (Figure 4-12C, D, E). Strikingly, reduced type I IFN induction went along with drastically increased mCMV replication in the *Xbp1* deficient cells.

While this data shares the limitations of cell culture models in general, it is very consistent with our previous findings. Importantly, it is also consistent with our *in vivo* findings, and can therefore be seen as a critical insight into consequences of defective STING function and the underlying pathology (chronic ER-stress). Ideally, this data can be used to evolve the hypothesis of a more detailed study focussing on the role of STING during CMV reactivation or infection in IBD patients. We postulate that suppression of STING in chronically stressed IBD patients is a critical process giving rise to immunosuppression and eventually CMV reactivation and colitis. Although here we only went as far as investigating cell culture models (unfortunately, due to methodological limitations in our laboratory), taken together our data provide a new perspective on epithelial STING function. This provides an image of STING as a potentially very interesting target for further investigations. Future studies could focus on involvement of STING activation or suppression during gastrointestinal disease (inflammation, cancerogenesis). At the same time, STING also resembles a possibly rewarding therapeutical target since chemical STING agonists and antagonists enable feasible pharmacological modulation of STING. This has so far mainly been investigated in context of cancerogenesis. While DMXAA, a synthetic STING agonist, has been successfully evaluated in clinical phase I and II trials, it failed in phase III trials. This was most likely due to structural differences between murine and human STING[326–328]. Currently (2021), there is however another promising STING agonist under clinical evaluation (for possible use in cancer)[326]. Evaluation of such a well-studied, safely applicable STING agonist for treatment of opportunistic infections in IBD could remarkably extend the therapeutic spectrum in IBD.

We project that after further investigation and validation of our data in appropriate models (*in vivo* experiments, clinical studies), targeted therapy for CMV reactivation by modulating STING instead of using conventional antiviral drug regimens is a realistic outcome with the potential of significantly improving patient care.

5.11 Unresolved ER-stress: autophagy executing STING-suppression?

We have now developed a realistic idea of how to facilitate clinical translation of our data (see 5.10 and Figure 5-1). Yet, the precise mechanism by which chronic ER-stress results in altered STING function still remains elusive. We have frequently mentioned and suspected an involvement of autophagy before, while keeping other mechanisms in mind. Nevertheless, investigation of autophagy was prompting as it is a very well acknowledged pathway involved in both ER-stress[37,40,135] and STING signalling[37,146,227,228,262].

Based on these thoughts and previous critical findings (i.e. *Xbp1* deficiency resulting in ER-stress and autophagy induction[19,40]), we accordingly propose the idea that the shared phenotype in the chemical and genetical ER-stress model is also based on a shared mechanism. Slight phenotype differences might however be based on subtle differences in e.g. different kinetics of the model. Recapitulating what we know based on literature and our data, we feel confident to summarize that:

- STING is activated by ER-stress,
- ER-stress rather increases than decreases *Tmem173* expression,
- STING is usually removed by autophagy following activation,
- ER-stress activates autophagy,
- and in context of chronic ER-stress, STING levels and activity are drastically reduced.

Altogether, these facts make autophagy as the main responsible mechanism sound very likely. Thus, we tested key findings of our previous data (e.g. abolished STING levels in *Xbp1*$^{\Delta IEC}$ mice) in context of additionally impaired autophagy. Additionally we extended our spectrum of readouts in order to gain an insight into the interaction of STING and autophagy pathways during ER-stress.

In Figure 4-13 and Figure 4-14 we provide compelling data supporting the idea that ER-stress results in autophagic removal of STING. This ultimately predisposes for reduced STING signalling in response to additional stimuli, as described previously. Applying immunofluorescence staining, we demonstrate that following Tunicamycin stimulation, STING colocalizes with different proteins involved in canonical autophagy processes (Atg16l1, LC3 and p62, also see 1.2.3.1). This indicates translocation of STING to a shared location with these proteins. In light of the transorganelle-trafficking described for the process of STING activation itself[146,224], one could also reasonably argue that Tunicamycin-mediated activation of STING alone could be responsible for such colocalization. However, diminished STING levels following ER-stress both *in vivo* and *in vitro* suggest that STING degradation takes place after Tunicamycin stimulation in an autophagy process involving these proteins. On the other hand, autophagy is proposed for both activation and deactivation of STING signalling. Thus, we acknowledge that the whole process of STING activation, translocation and degradation is most likely rather a fluent

transition with a tightly monitored balance towards either degradation and signalling termination or signalling initiation.

Another lesson from this data can be obtained having a closer look on the subcellular localization and distribution of STING in both settings. In the mock-stimulated cells, STING seems to be broadly spread over the entire cytoplasma (Figure 4-13A). In the Tunicamycin-stimulated cells however, STING is apparently densely clustered (Figure 4-13A). This further supports the hypothesis of autophagic removal, as the clustering of STING likely resembles the completion of STING trafficking from larger parts of the cell's ER towards autophagic vacuoles.

ATG16L1 is an autophagy protein critically involved in formation of the autophagosome. In addition, variants in *ATG16L1* were among the first gene variants identified mediating risk for CD[16] (also see 1.1.3.1 and 1.2.3). Therefore, it was prompting to check for involvement of Atg16l1, given that immunofluorescence has shown considerable colocalization with STING after ER-stress. We show in Figure 4-13C-E that Atg16l1 takes part in removal of STING. Additionally, we speculate that absence of Atg16l1 can be compensated in our models by engagement of other degradation pathways. This would explain why absence of Atg16l1 in *Atg16l1/Xbp1*$^{\Delta IEC}$ mice does not fully restore STING levels, as we would have hypothesized before (Figure 4-13E).

Chemical intervention with the attempt to block either acidification of autophagic vesicles (Bafilomycin A1) or STING translocation from the ER to the Golgi (Brefeldin A) further supports the idea of compensatory mechanisms involved. Here, we applied both Tunicamycin and *Xbp1* deficiency as a model for ER-stress to investigate ER-stress related STING removal. Slight differences in the amount of STING removal can be observed using (admittedly quite inefficient) siRNA targeting *Atg16l1*. However, neither Brefeldin A nor Bafilomycin A1 treatment is able to prevent Tunicamycin-induced STING degradation (Figure 4-14A). LC3 conversion suggests autophagy activation following Tunicamycin, consistent with our previous results. Data obtained from challenging *Xbp1* deficient cells with dsDNA and Bafilomycin is rather inconclusive, because Bafilomycin failed to block STING degradation due to either *Xbp1* deficiency or to dsDNA-mediated activation (Figure 4-14B). We suspect that in this case, our approach of chemical inhibition of STING degradation and translocation simply failed to effectively prevent STING activation and degradation due to other mechanisms involved. Matching this hypothesis, STING activation was not impaired by Brefeldin A treatment. We would have expected to block STING translocation with Brefelding A and therefore also activation as described previously[329].

The knockdown of *Atg16l1* in either cell, organoid or mouse model as a rescue mechanism for impaired STING function in context of *Xbp1* deficiency or chemical ER-stresss has to be acknowledged carefully. We picture a vision of STING in which defective STING due to chronic ER-stress results in infection

susceptibility and thereby poorer disease course. On the contrary, *Atg16l1/Xbp1*$^{\Delta IEC}$ mice are defective for two essential stress resolution mechanisms (UPR and autophagy). Therefore, they show signs of severe, spontaneous intestinal inflammation very similar to human Crohn's disease[40]. From a clinical perspective, it would accordingly seem odd if despite the aggravated inflammatory phenotype, additional *Atg16l1* deficiency would also mediate a beneficial effect by preventing removal of STING and thus maintaining type I IFN inducing capability.

While we cannot satisfyingly provide an answer for this issue, we understand this data as a hint pointing towards at least one mechanism involved in suppression of STING during ER-stress. We assume that *Atg16l1/Xbp1*$^{\Delta IEC}$ mice would surely prove themselves to be even more susceptible to any infectious threat than *Xbp1*$^{\Delta IEC}$ mice[19]. This is probably based on a strongly increased grade of epithelial barrier disruption and spontaneous inflammation. At the same time, it is unknown to what extent epithelial STING is involved in antiviral or antibacterial immunity in the intestine, since an investigation of e.g. *Tmem173* $^{\Delta IEC}$ mice has not been performed so far. Thus, our model serves as a test for the impact of Atg16l1-dependent autophagy. However, it should be well considered that strong proinflammatory signals in *Atg16l1/Xbp1*$^{\Delta IEC}$ mice by far outweigh a potential benefit of partially restored STING activity.

A recent study of our own group has demonstrated that defective autophagy (*Atg16l1*$^{\Delta IEC}$ mice) is able to reverse the outcome of STING signalling from beneficial to detrimental effects in response to IL22[164]. Bearing this in mind, restored STING levels in the double-deficient setting could also imply a shift towards proinflammatory signalling, despite a seemingly "rescue" of the phenotype of *Xbp1* deficiency.

5.12 Clinical application: another step on the road to "precision medicine"?

Precision medicine refers to a strategy of treating each patient individually by acknowledging that each patient also presents with unique features giving rise to either resilience or disease susceptibility. The National Health Service (NHS) England defines "precision medicine" as "*a move away from a 'one size fits all' approach to the treatment and care of patients with a particular condition, to one which uses new approaches to better manage patients' health and target therapies to achieve the best outcomes in the management of a patient's disease or predisposition to disease.*"[330]. For IBD, the urgency for new treatment strategies including ideas of "personalized medicine" or "precision medicine" is huge. Patient risk stratification, therapy response prediction and monitoring are key features that need improvement in order to enable reliable clinical application and ultimately better patient care[331].

For integrating our data into an applicable strategy for clinical translation, our data on autophagy suppressing STING activity is of little interest. More importantly, we project that recognizing decreased

STING ability during chronic ER-stress and subsequent immunosuppression in IBD patients will enable targeted modification of STING. Applying drugs already investigated for anticancer abilites[326], immunocompetence could potentially be restored. In addition, our results also present a potential benefit in disease monitoring, therapy adaptation and thus patient stratification. After clinical validation of our results, multiple settings seem realistic: first and most simply, patients with high chances of severe disease course could be tested for presence of the *XBP1* risk mediating variant. This could serve to identify IBD patients at high risk for development of CMV colitis later on. This would accordingly enable early recognition and countermeasures in order to better manage CMV colitis. Additionally, our data also implies that not only *Xbp1* deficiency, but ER-stress in general exerts a profound effect on STING function. Therefore, evaluation of ER-stress levels could also resemble a valuable tool for risk stratification. Further research could focus on development of a reliable and feasible biomarker easy to obtain to quickly gain an insight into susceptibility and presence of ER-stress in each patient. Finally, application of STING agonists might show potential for clinical use during immunosuppression or infection in IBD, if the respective patient has previously been identified to display reduced STING activity. That being said, STING agonists have to be approached with caution. Again, a detailed patient phenotyping regarding risk factors might be necessary to predict whether STING agonists could be useful. Aden et al. have shown in detail how defective autophagy is able to reverse beneficial effects of IL22 by recruiting STING to mediate necroptosis in the intestinal epithelium[164]. Thus, we project that the basis to success of STING as a potential therapeutic target lies within patient stratification and identifications of patients at risk.

6 Summary

We aimed to gain a basal understanding of intestinal epithelial STING function and its implication for IBD pathophysiology with the goal of providing data suitable for clinical translation.

Crohn's disease and Ulcerative colitis are the two main entities of inflammatory bowel disease. Both share a complex, multifactorial pathophysiology involving microbial dysbiosis, environmental aspects and genetically determined susceptibility resulting in dysregulation of stress resolution and homeostasis pathways such as the unfolded protein response or autophagy. The intestinal epithelium is of paramount importance in this context: it can both protect from and mediate severe inflammation.

The cGAS/STING pathway is an innate immunity pathway responsible for sensing of dsDNA and bacterial metabolites. STING signalling has many downstream effects which range from type I IFN induction mediating antiviral properties to cell death or senescence induction. STING signalling is therefore tightly regulated by a multitude of factors. Features of IBD pathophysiology are profoundly involved in controlling this pathway, most prominently autophagy. If and how STING plays a role in intestinal epithelial cell biology and in IBD is not known.

We have applied multiple *in vitro*, *ex vivo* and *in vivo* models to gain an insight in intestinal epithelial STING. STING is expressed in the intestinal epithelium in a distinct pattern with highest expression in the crypt base, likely in Paneth cells. We demonstrate that epithelial *Tmem173*, encoding STING, is regulated by the microbiota and ER-stress. This translates to a distinct regulation of *TMEM173* in IBD patients, where dysbiosis and ER-stress are present. We discovered a new aspect of STING signalling by identifying ER-stress as a direct trigger of STING activation and type I IFN production. This could imply that STING could carry out proinflammatory signals during ER-stress in IBD. On the other hand, we also show that prolonged, unresolved ER-stress is able to severely suppress STING responsiveness to canonical stimuli such as dsDNA or infection. This is due to decreasing STING levels drastically in a way involving autophagic degradation of STING. Importantly, this translates to markedly increased mCMV replication in case of chronic ER-stress.

As a clinical translation and explanatory approach to the frequent reactivation of CMV in IBD patients, we propose that chronic ER-stress contributes to immunosuppression by decreasing STING activity in the intestinal epithelium. This ultimately results in susceptibility to CMV colitis, giving rise to an aggravated disease course. One strategy to apply this knowledge could be to compensate for decreased STING levels in such patients administering STING agonists. STING agonists are already developed for cancer therapy and could help to restore immunocompetence and prevent or improve CMV infection.

7 Zusammenfassung

Ziel dieser Studie war es, ein grundlegendes Verständnis für die Funktion von STING im intestinalen Epithel zu entwickeln, dieses Wissen anschließend in unser Verständnis der Pathophysiologie von chronisch entzündlichen Darmerkrankungen (CED) zu integrieren und letztlich klinisch-relevante Erkenntnisse zu gewinnen. Morbus Crohn und Colitis ulcerosa sind die beiden Hauptentitäten von CED. Beide haben eine komplexe, multifaktorielle Pathophysiologie gemein. Sie beinhaltet mikrobielle Dysbiosis, Umweltfaktoren und genetisch bedingte Suszeptibilität mit Dysregulation in Stressresolutionssignalwegen, wie z.B. der *Unfolded protein response* oder Autophagie. Insbesondere das intestinale Epithel ist von herausragender Bedeutung in diesem Kontext, da es sowohl Schutz vor als auch Ursache von Entzündung sein kann.

Der cGAS/STING Signalweg ist ein Signalweg des angeborenen Immunsystems, der als Rezeptor für dsDNA und bakterielle Metabolite fungiert. Daraufhin vermittelt STING eine große Bandbreite an Effekten von Typ I Interferonen und antiviraler Immunität bis hin zu Zelltod oder Seneszenz. Der STING Signalweg wird daher von einer Vielzahl an Faktoren strikt kontrolliert und reguliert. Einige davon zeigen eine große Überschneidung mit Aspekten der CED Pathophysiologie, insbesondere Autophagie. Ob und inwiefern STING eine Rolle im Darmepithel und in CED spielt ist nicht bekannt.

In dieser Studie haben wir verschiedene *in vitro*, *ex vivo* und *in vivo* Modelle angewandt um ein grundlegendes Verständnis von epithelialem STING zu erhalten. STING ist im intestinalen Epithel in einer charakteristischen Verteilung exprimiert, wobei der Hauptteil in den Krypten und wahrscheinlich Paneth Zellen lokalisiert ist. Epitheliales *Tmem173*, kodierend für STING, wird sowohl von der Mikrobiota als auch von ER-Stress reguliert. Dies bedingt eine ausgeprägte Dysregulation von *TMEM173* in CED Patienten, wo sowohl Dysbiose als auch ER-Stress vorliegen. Wir haben mit ER-Stress als direktem Auslöser für STING Aktivierung und Typ I IFN Induktion außerdem einen neuen Aspekt des STING Signalwegs entdeckt. Dies könnte bedeuten, dass STING im Kontext von ER-Stress in CED eine proinflammatorische Rolle einnimmt. Andererseits supprimiert persistierender, chronischer ER-Stress die Responsivität von STING auf dsDNA oder Infektion durch Autophagie-vermittelte Degradation von STING gravierend. Darauf basiert eine deutlich erhöhte mCMV Anfälligkeit in Kontext von chronischem ER-Stress.

Immunsuppression durch ER-Stress bedingte, supprimierte STING Aktivität kommt als Erklärungsansatz für gehäuft auftretende CMV-Infektionen und -Kolitiden bei CED-Patienten infrage. Ein möglicher Ansatz zur klinischen Translation wäre erniedrigte STING Level in solchen Patienten mithilfe von STING Agonisten zu kompensieren und damit Immunkompetenz wiederherzustellen und CMV Infektionen zu verhindern oder Krankheitsverläufe abzumildern.

8 Supplements

8.1 Acknowledgements

This work was enabled by many people, who continuously supported my scientific work throughout this project which I greatly appreciate.

First of all, I would like to thank my supervisors Prof. Dr. Philip Rosenstiel and PD Dr. Konrad Aden for offering me an opportunity to work on this thesis in such a privileged laboratory environment and for scientific advice. I am very grateful to my scientific mentor and supervisor PD Dr. med. Konrad Aden for introducing me to this project, scientific thinking and working, and for continuous support. Thank you for your input in this project, for discussing ideas and your creativity and for enabling and organizing fruitful cooperations.

I owe many thanks to Nassim Kakavand for introducing me to lab work, for supporting my thesis most especially in the beginning and for always helping out wherever problems occurred.

I would like to express my gratitude also to Dr. Go Ito and Dr. Stephanie Stengel. Thank you for your input and guidance, your contribution to this work and for a very enjoyable and rewarding time working in this lab. Thank you Go for your expertise on organoids and your inspiring attitude and outstanding politeness. I appreciate very much the graphical illustrations by Dora Bordoni.

I greatly appreciate the work of everybody else who contributed to this project by providing or analysing data: thanks to Neha Mishra and Joana Pimenta Bernardes for statistical and bioinformative help; to Jacob Hamm, Lina Welz, Simon Imm and Gabriela Rios Martini for helping out with datasets or samples. I would also like to thank Dr. Felix Sommer and Prof. Fredrik Bäckhed, University of Gothenburg, for providing datasets and samples of germ-free and monocolonized mice.

Working in the lab would not have been the same without many students, doctoral researchers and especially technicians. Thanks especially to the laboratory assistance staff of our lab, Stefanie Baumgarten, Karina Greve, Tanja Klostermeier, Melanie Nebendahl, Dorina Ölsner, Sabine Kock, Maren Reffelmann and Myriam Rohm for always patiently supervising all of us and for forgiving us our numerous mistakes in the lab. I am very grateful for your help and advice in the lab.

I am very thankful to Samuel Windross and Prof. Dr. Søren Paludan from Aarhus University, Department of Biomedicine, for their interest in our work and their kind support with virus infection experiments, which we could not have performed on our own. Thanks also to Dr. Olivia Coleman and Prof. Dr. Dirk Haller from Technische Universität München for your interest in our work and your

participation in this project, which helped us to understand the interplay of ER-stress and STING signalling.

I am very grateful for financial support contributing to this thesis by the Collaborative Research Centre 877 *Proteolysis as a Regulatory Event in Pathophysiology* and the Research Training Group 1743 *Genes, Environment and Inflammation*.

8.2 Publications & scientific presentations

8.2.1 Publications

1. **Wottawa, F.**; Bordoni, D.; Baran, N.; Rosenstiel, P.; Aden, K. The Role of CGAS/STING in Intestinal Immunity. *European Journal of Immunology* **2021**, 51 (4), 785–797. https://doi.org/10.1002/eji.202048777.
2. Stengel, S. T.; Fazio, A.; Lipinski, S.; Jahn, M. T.; Aden, K.; Ito, G.; **Wottawa, F.**; Kuiper, J. W. P.; Coleman, O. I.; Tran, F.; Bordoni, D.; Bernardes, J. P.; Jentzsch, M.; Luzius, A.; Bierwirth, S.; Messner, B.; Henning, A.; Welz, L.; Kakavand, N.; Falk-Paulsen, M.; Imm, S.; Hinrichsen, F.; Zilbauer, M.; Schreiber, S.; Kaser, A.; Blumberg, R.; Haller, D.; Rosenstiel, P. Activating Transcription Factor 6 Mediates Inflammatory Signals in Intestinal Epithelial Cells Upon Endoplasmic Reticulum Stress. *Gastroenterology* **2020**, S0016508520349246. https://doi.org/10.1053/j.gastro.2020.06.088.
3. Aden, K.; Bartsch, K.; Dahl, J.; Reijns, M. A. M.; Esser, D.; Sheibani-Tezerji, R.; Sinha, A.; **Wottawa, F**.; Ito, G.; Mishra, N.; Knittler, K.; Burkholder, A.; Welz, L.; van Es, J.; Tran, F.; Lipinski, S.; Kakavand, N.; Boeger, C.; Lucius, R.; von Schoenfels, W.; Schafmayer, C.; Lenk, L.; Chalaris, A.; Clevers, H.; Röcken, C.; Kaleta, C.; Rose-John, S.; Schreiber, S.; Kunkel, T.; Rabe, B.; Rosenstiel, P. Epithelial RNase H2 Maintains Genome Integrity and Prevents Intestinal Tumorigenesis in Mice. *Gastroenterology* **2019**, *156* (1), 145-159.e19. https://doi.org/10.1053/j.gastro.2018.09.047.

8.2.2 Scientific presentations

1. Wottawa F.; Stengel S.; Kakavand N.; Ito G.; Windross S.; Paludan S.; Blumberg R.S.; Schreiber S.; Aden K.; Rosenstiel P. OP261 XBP1 governs endoplasmic reticulum stress driven STING signalling in the intestinal epithelium *United European Gastroenterol. j.* **2019**, *7* (S8), 139. https://doi.org/10.1177/2050640619854670.

   Best abstract presentation prize

8.3 Eidesstattliche Erklärung

Hiermit versichere ich, Felix Wottawa, an Eides statt, dass

- meine Dissertation, abgesehen von Ratschlägen meines Doktorvaters und meiner sonstigen akademischen Lehrer, in Form und Inhalt meine eigene Arbeit ist, dass ich außer den in der Arbeit aufgeführten keine weiteren Hilfsmittel benutzt habe, und dass meine Arbeit bisher, weder ganz noch in Teilen, keiner anderen akademischen Stelle als Dissertation vorliegt.
- dass wann immer Daten, die ich nicht eigenständig erhoben habe, in meine Arbeit eingeflossen sind, ich dies so gekennzeichnet habe.
- Veröffentlichungen nach den Richtlinien über Benotung von Dissertationen erfolgt sind.
- die zuständigen Behörden Forschungsvorhaben an Tieren oder mit Patientenproben und -daten zugestimmt haben.
- ich bis zum heutigen Tage 14 Semester an der Christian-Albrechts-Universität studiert habe.
- die Leiter des Instituts für klinische Molekularbiologie einverstanden sind, dass die Dissertation an deren Einrichtung geschrieben wurde.
- für die Nutzung von Arbeitsmöglichkeiten der wissenschaftlichen Einrichtung durch mich das Einverständnis der Leitung der Einrichtung vorliegt.

Ich erkläre, dass die Arbeit unter Einhaltung der Regeln guter wissenschaftlicher Praxis der Deutschen Forschungsgemeinschaft entstanden ist.

Kiel, August 2021

Felix Wottawa

9 Appendix

9.1 Buffers, solutions & media

The following buffers and solutions were used in this study:

Table 13: Buffers & Solutions

buffer or solution	composition or company
10x TBS	200 mM Tris (pH 7.6), 1.37 M sodium chloride
10x TGS buffer	25 mM Tris (pH 8.3), 192 mM glycine, 0.1 % (w/v) SDS
5x SDS loading dye	250 mM Tris (pH 6.8), 10 % (w/v) SDS, 50 % (v/v) glycerol, 500 mM DTT
Anode buffer 1	30 mM Tris, 20 % (v/v) methanol
Anode buffer 2	300 mM Tris, 20 % (v/v) methanol
Blocking solution	5 % (w/v) non-fat dry milk in TTBS
Cathode buffer	25 mM Tris, 20 % (v/v) methanol, 40 mM 6-amino-ncaproic acid
CO-IP binding and washing buffer	PBS, 0.02 % (v/v) Tween20
CO-IP elution buffer	50 mM Glycin (pH 2.8)
DNA loading dye	50 % (v/v) glycerol, 0.1 % (w/v) bromophenol blue, 0.1 % (w/v) xylene cyanol
ECL substrate	GE Healthcare, Freiburg, Germany, cat. nr. RPN2109
FCS	PAA Laboratories/ GE Healthcare, Freiburg, Germany, cat. nr. PAA A15-151
Ketanest S 25mg/ml, 10ml	Pfizer, New York, USA
Loading gel	0.5 M Tris (pH 6.8), 0.4 % (w/v) SDS
MOPS SDS Running Buffer (20X)	Novex/Life Technologies, Darmstadt, Germany, cat. nr. NP001
OPTI-MEM	Gibco/Life Technologies, Darmstadt, Germany, cat. nr. 31985-047
PBS	8 g/l sodium chloride, 0.2 g/l potassium chloride, 1.56 g/l disodium phosphate, 0.24 g/l monopotassium phosphate, pH 7.4
RIPA	150 mM sodium chloride, 1 % (v/v) NP40, 0.5 % (w/v) deoxycholic acid, 0.1 % (w/v) SDS, 50 mM Tris (pH 8.0)
Separation buffer	1.5 M Tris (pH 8.8), 0.4 % (w/v) SDS
SmartLadder	Eurogentec, Cologne, Germany, cat. nr. MW-1700-10
Stacking buffer	0.5 M Tris (pH 8.8), 0.4 % (w/v) SDS
Stripping buffer	62.5 mM Tris (pH 6.8), 2 % (w/v) SDS
SYBR Safe DNA gel stain	Life Technologies, Darmstadt, Germany cat. nr. S33102
TTBS	1x TBS, 0,1 % (v/v) Tween20

If no special media were used (listed in the methods section, see 3.2, p. 32), the following media were used in this study:

Table 14: Media

Media	Company
Advanced DMEM/F12 medium	Gibco (Darmstadt, Germany)
CryoStor™ CS10	StemCell Technologies (Cologne, Germany)
DMEM cell culture medium	Gibco (Darmstadt, Germany)
Hank´s Balanced Salt Solution (HBSS)	Gibco (Darmstadt, Germany)
IntestiCult™ Organoid Growth Medium (Mouse)	StemCell Technologies (Cologne, Germany)
MEM cell culture medium	Gibco (Darmstadt, Germany)
Matrigel™	BD Bioscience (Heidelberg, Germany)

9.2 Reagents & chemicals

Table 15: Reagents & chemicals

Chemical	Company
2-Mercaptoethanol	Sigma-Aldrich, Munich, Germany
6-amino-n-caproic acid	Sigma-Aldrich, Munich, Germany
Acrylamide Bis Sol. 30%	Bio-Rad, Munich, Germany
Ammonium persulfate (APS)	Sigma-Aldrich, Munich, Germany
Amphotericin	PAA Laboratories/ GE Healthcare, Freiburg, Germany
Ampicillin	Sigma-Aldrich, Munich, Germany
Bovine serum albumin (BSA)	Carl Roth, Karlsruhe, Germany
Bromophenol blue	Sigma-Aldrich, Munich, Germany
Deoxycholic acid	Sigma-Aldrich, Munich, Germany
Dimethylsulfoxid (DMSO)	Sigma-Aldrich, Munich, Germany
Dithiothreitol (DTT)	Th. Geyer, Renningen, Germany
DSS reagent grade, molecular weight 36000-50000	MP Biomedicals, Illkirch Cedex, France
Dynabeads Protein G	Life Technologies, Darmstadt, Germany
EDTA	Sigma-Aldrich, Munich, Germany
Ethanol	Merck, Darmstadt, Germany
Glycerol	Carl Roth, Karlsruhe, Germany
Glycine	Carl Roth, Karlsruhe, Germany
HEPES	Sigma-Aldrich, Munich, Germany
Isopropanol	Merck, Darmstadt, Germany
Kanamycin	Merck, Darmstadt, Germany
LE Agarose	Biozyme, Hessisch Oldendorf, Germany
Magnesium chloride	Merck, Darmstadt, Germany
Methanol	Merck, Darmstadt, Germany
N-Acetylcystein	Sigma-Aldrich, St. Louis, USA
Monopotassium phosphate	Sigma-Aldrich, Munich, Germany
Non-fat dry milk (NFDM)	Bio-Rad, Munich, Germany
Nonidet p 40 substitute	Sigma-Aldrich, Munich, Germany

Penicillin/Streptomycin	Life Technologies, Darmstadt, Germany
Potassium chloride	Sigma-Aldrich, Munich, Germany
Potassium dihydrogen phosphate	Merck, Darmstadt, Germany
Propidium iodide (PI)	Sigma Aldrich, Munich, Germany
RNase-free water	Qiagen, Hilden, Germany
Sodium chloride	Merck, Darmstadt, Germany
Sodium dodecyl sulfate (SDS)	Carl Roth, Karlsruhe, Germany
Sodium fluoride	Sigma-Aldrich, Munich, Germany
Sodium phosphate dibasic	Sigma-Aldrich, Munich, Germany
SYBR safe	Life Technologies
Tetramethylethylenediamine (TEMED)	Sigma-Aldrich, Munich, Germany
TRIS	Merck, Darmstadt, Germany
Triton-X	Sigma-Aldrich, Munich, Germany
Tween20	Carl Roth, Karlsruhe, Germany
Xylene cyanol	Sigma-Aldrich, Munich, Germany

The following enzymes were used:

Table 16: Enzymes

Enzyme	Company
Endonuclease H	New England Biolabs
GoTaq™ polymerase	Promega, Mannheim, Germany
Proteinase K	Thermo Scientific, Bremen, Germany
RNase-free DNase Set	Qiagen, Hilden, Germany
TrypLE Express	ThermoFischer Scientific, Darmstadt, Germany
Trypsin/EDTA	Life Technologies

The following small molecules and inhibitors were used:

Table 17: Small molecules & inhibitors

Small molecule / inhibitor	Company / derived from
Bafilomycin A1	Enzo Life Sciences GmbH, Lörrach, Germany
Brefeldin A	
CHIR99021	Stemgent, Cambridge, USA
DAPT	Stemgent, Cambridge, USA
EGF	Thermo Scientific, Bremen, Germany
Halt™ combined protease and phosphatase inhibitor	Thermo Scientific, Bremen, Germany
IWP-2	Stemgent, Cambridge, USA
Z-Leu-Leu-Leu-CHO (MG132)	Biomol, Hamburg, Germany
Noggin	Noggin-producing cell line, kindly gifted by Artur Kaser, University of Cambridge
R-Spondin 1	R-Spondin 1-producing cell line, kindly gifted by Artur Kaser, University of Cambridge

Tunicamycin	Calbiochem, Darmstadt, Germany
Valproic acid	Sigma-Aldrich, St. Louis, USA

9.3 Kits

Table 18: Kits

Kit	Company
DC™ Protein Assay	Bio-Rad (Munich, Germany)
GeneJET Plasmid Miniprep Kit	Thermo Scientific, Bremen, Germany
Maxima H Minus First Strand cDNA Synthesis Kit	Thermo Scientific, Bremen, Germany
PureLink® HiPure Plasmid Filter Midiprep Kit	Life Technologies, Darmstadt, Germany
QIAshredder	Qiagen, Hilden, Germany
Rapid DNA Ligation Kit	Roche, Mannheim, Germany
RNeasy Mini Kit	Qiagen, Hilden, Germany
Roti Histokit	Carl Roth, Karlsruhe, Germany
SYBR® Select Master Mix	Life Technologies, Darmstadt, Germany

9.4 Plasmids & siRNA

Table 19: Plasmids

Plasmid	Company / generated by
pcDNA3-HA	gifted by Søren Paludan, Department of Biomedicine, Aarhus University
pcDNA3-mSTING-HA	gifted by Søren Paludan, Department of Biomedicine, Aarhus University

Table 20: siRNA

siRNA target gene	Company	Catalog - No.
Atg5	Qiagen	GS11793
Atg9a	Qiagen	GS245860
Atg16l1	Qiagen	GS77040
Ifnar1	Qiagen	GS15975
Irf3	Qiagen	GS54131
Map1lc3b	Qiagen	GS67443
Mb21d1	Qiagen	GS214763
Sqstm1	Qiagen	GS18412
Tbk1	Qiagen	GS56480
Tmem173	Qiagen	GS72512
Xbp1	Qiagen	GS22433

9.5 Antibodies

Table 21: Primary antibodies

Target	Dilution	Company	Catalogue-Nr.
Actin β	1:1000	Sigma-Aldrich, Munich, Germany	A-5441
ATG16L1	1:1000	MBL International, Woburn, USA	M150-3
β - Tubulin	1:5000	Cell Signaling Technology, Leiden, The Netherlands	2128
cGAS	1:1000	Cell Signaling Technology, Leiden, The Netherlands	31659
GRP78	1:2000	Abcam, Cambridge, United Kingdom	ab21685
GRP94	1:1000	Cell Signaling Technology, Leiden, The Netherlands	20292
HA	1:1000	Roche, Mannheim, Germany	11 867 423 001
LC3	1:1000	Cell Signaling Technology, Leiden, The Netherlands	3868
Lysozyme	1:1000	Abcam, Cambridge, United Kingdom	ab108508
p62	1:1000	Cell Signaling Technology, Leiden, The Netherlands	8025
phospho - STING	1:1000	Cell Signaling Technology, Leiden, The Netherlands	72971
phospho - STING	1:400	Cell Signaling Technology, Leiden, The Netherlands	62912
phospho - TBK1	1:1000	Cell Signaling Technology, Leiden, The Netherlands	5483
STING	1:1000*	Cell Signaling Technology, Leiden, The Netherlands	13647
TBK1	1:1000	Cell Signaling Technology, Leiden, The Netherlands	38066
Vinculin	1:1000	Cell Signaling Technology, Leiden, The Netherlands	13901

*For immunohistochemistry, this antibody was used at a dilution of 1:50 according to the manufacturer's recommendation.

Table 22: Secondary antibodies

Antibody	Dilution	company	Catalog-Nr.
mouse HRP	1:2000	Amersham Biosciences, Glattbrugg, Switzerland	NA931V
rabbit HRP	1:2000	Amersham Biosciences, Glattbrugg, Switzerland	NA934V
goat HRP	1:2000	Sigma-Aldrich, Munich, Germany	A5420
Alexa Fluor 488 goat α-mouse	1:400	Thermo Scientific, Bremen, Germany	A11029
Alexa Fluor 488-goat α-rabbit	1:400	Thermo Scientific, Bremen, Germany	A11070
Alexa Fluor 555-goat α-mouse	1:400	Thermo Scientific, Bremen, Germany	A21424
Alexa Fluor 555-goat α-rabbit	1:400	Thermo Scientific, Bremen, Germany	A21430

9.6 TaqMan probes

Table 23: Taqman probes

Target	Species	Company	Catalog number
Atf4	murine	Life Technologies, Darmstadt, Germany	00515325
Atf6	murine	Life Technologies, Darmstadt, Germany	01295317
ATF6	human	Life Technologies, Darmstadt, Germany	00232586
Cxcl10	murine	Life Technologies, Darmstadt, Germany	04331182
CXCL10	human	Life Technologies, Darmstadt, Germany	04331182
Dnajc3	murine	Life Technologies, Darmstadt, Germany	01226332
Gapdh	murine	Life Technologies, Darmstadt, Germany	99999915
Hspa5	murine	Life Technologies, Darmstadt, Germany	00517690
HSPA5	human	Life Technologies, Darmstadt, Germany	04331182
Hsp90b1	murine	Life Technologies, Darmstadt, Germany	00441926
HSP90B1	human	Life Technologies, Darmstadt, Germany	04331182
Ifnb1	murine	Life Technologies, Darmstadt, Germany	04331182
Lyz1	murine	Life Technologies, Darmstadt, Germany	00657323
Tmem173	murine	Life Technologies, Darmstadt, Germany	04331182
TMEM173	human	Life Technologies, Darmstadt, Germany	04331182
Tnfα	murine	Life Technologies, Darmstadt, Germany	00443258
Xbp1	murine	Life Technologies, Darmstadt, Germany	03464496

9.7 Devices & consumables

Table 24: Devices

Devices	Company
7900 HT Fast Real-Time PCR System	Applied Biosystems/Life Technologies, Darmstadt, Germany
96-well thermocycler	Applied Biosystems/Life Technologies, Darmstadt, Germany
ABI PRISM® 3700 sequencer	Applied Biosystems/Life Technologies, Darmstadt, Germany
Analytic balance 870-15	Kern, Balingen, Germany
Assistent Mini-Centrifuge SPROUT	Heathrow Scientific, Nottingham, United Kingdom
Automated developer machine	Agfa, Mortsel, Belgium
Axio Imager.Z1	Zeiss, Jena, Germany
Cellometer Auto T4 Plus	PeqLab Biotechnologie GmbH, Erlangen, Germany
Centrifuge for 15/50 ml tubes: Megafuge 16R	Thermo Scientific, Bremen, Germany
Centrifuge for Eppendorf tubes: Fresco 21	Thermo Scientific, Bremen, Germany
Certomat MV, vortex mixer	B. Braun Biotech Internat., Melsungen, Germany
ChemiDoc XRS Imaging System	Bio-Rad, Munich, Germany
Confocal microscope: TCS SP5	Leica Microsystems, Wetzlar, Germany
Electronic pipet filler	Eppendorf, Hamburg, Germany
Eppendorf Research®, adjustable volume pipette	Eppendorf, Hamburg, Germany

FACSCalibur flow cytometer	BD Biosciences, Heidelberg, Germany
GeneAmp PCR System 9700	Applied Biosystems/Life Technologies, Darmstadt, Germany
Gentle-MACS™ Dissociator	Miltenyi Biotec, Bergisch Gladbach, Germany
Incubator for cell lines	Binder, Tuttlingen, Germany
Incubator for *E. coli* in media: Orbital Incubator SI50	Stuart Equipment, Staffordshire, United Kingdom
Incubator for *E. coli* on agar plates: Incucell 111	MMM Group, Planegg, Germany
Laminar flow workbench HERASafe KS	Thermo Scientific, Bremen, Germany
Leica RM 2255 microtome	Leica Microsystems, Wetzlar, Germany
Magnetic stirrer C-MAG HS 7 IKAMAG	IKA, Staufen, Germany
Microwave R-239	SHARP, Hamburg, Germany
Mini-Sub Cell GT	Bio-Rad, Munich, Germany
Molecular Imager ChemiDoc XRS Imaging System	Bio-Rad, Munich, Germany
NanoDrop ND-1000 spectrophotometer	PeqLab Biotechnologie GmbH, Erlangen, Germany
Power Pac 300	Bio-Rad, Munich, Germany
SympHony Benchtop Meters	VWR, Darmstadt, Germany
Tecan Infinite F200 pro plate reader	Tecan, Männedorf, Switzerland
Thermomixer compact 5350	Eppendorf, Hamburg, Germany
Trans-Blot® Turbo™ Transfer System	Bio-Rad, Munich, Germany
Tube roller SRT6	Stuart Equipment, Staffordshire, United Kingdom
Vortex-Genie 2 Variable Speed	Sartorius, Göttingen, Germany
Water bath 1003	GFL, Burgwedel, Germany
Water purification system	TKA, Niederelbert, Germany
Wide Mini ReadySub-Cell GT	Bio-Rad, Munich, Germany
XCell *SureLock*® Mini-Cell	Life Technologies, Darmstadt, Germany

Table 25: Consumables

Consumable	**Company**
0.5 ml, 1.5 ml and 2 ml reaction tubes	Sarstedt, Nümbrecht, Germany
1 ml syringes	BD Biosciences, Heidelberg, Germany
100 ml culture flasks	Schott, Mainz, Germany
15 ml and 50 ml tubes	Sarstedt, Nümbrecht, Germany
26G needles	B. Braun, Melsungen, Germany
Blot paper	Bio-Rad, Munich, Germany
Chemiluminescence hyperfilm	Applied Biosystems/Life Technologies, Darmstadt, Germany
Glass beads	Carl Roth, Karlsruhe, Germany
HistoBond	Paul Marienfeld GmbH& Co. KG
MicroAmp Optical 384-Well Reaction Plates	Applied Biosystems
Microvette 500 (Potassium-EDTA)	Sarstedt, Nümbrecht, Germany

NuPAGE® Bis-Tris gel	Life Technologies, Darmstadt, Germany
Pipette tips and filter tips	Sarstedt, Nümbrecht, Germany
Pipette tips for electronic pipette	Biohit, Göttingen, Germany
Polyvinylidene difluoride (PVDF) membranes	Bio-Rad, Munich, Germany
Rotilabo 0.22 µm syringe filter	Carl Roth, Karlsruhe, Germany
Serological pipettes	Sarstedt, Nümbrecht, Germany
Surgical disposable scalpels	B. Braun, Melsungen, Germany
Tissue culture dishes 96-, 24- and 6well	Sarstedt, Nümbrecht, Germany

10 References

1. Baumgart DC, Sandborn WJ. Crohn's disease. *The Lancet*. 2012;380(9853):1590-1605. doi:10.1016/S0140-6736(12)60026-9
2. Ordás I, Eckmann L, Talamini M, Baumgart DC, Sandborn WJ. Ulcerative colitis. *The Lancet*. 2012;380(9853):1606-1619. doi:10.1016/S0140-6736(12)60150-0
3. Baumgart DC, Sandborn WJ. Inflammatory bowel disease: clinical aspects and established and evolving therapies. *The Lancet*. 2007;369(9573):1641-1657. doi:10.1016/S0140-6736(07)60751-X
4. Molodecky NA, Soon IS, Rabi DM, et al. Increasing Incidence and Prevalence of the Inflammatory Bowel Diseases With Time, Based on Systematic Review. *Gastroenterology*. 2012;142(1):46-54.e42. doi:10.1053/j.gastro.2011.10.001
5. Kaplan GG. The global burden of IBD: from 2015 to 2025. *Nat Rev Gastroenterol Hepatol*. 2015;12(12):720-727. doi:10.1038/nrgastro.2015.150
6. Jess T, Frisch M, Simonsen J. Trends in Overall and Cause-Specific Mortality Among Patients With Inflammatory Bowel Disease From 1982 to 2010. *Clin Gastroenterol Hepatol*. 2013;11(1):43-48. doi:10.1016/j.cgh.2012.09.026
7. Yu AP, Cabanilla LA, Wu EQ, Mulani PM, Chao J. The costs of Crohn's disease in the United States and other Western countries: a systematic review. *Curr Med Res Opin*. 2008;24(2):319-328. doi:10.1185/030079908X260790
8. Baumgart DC, Carding SR. Inflammatory bowel disease: cause and immunobiology. *The Lancet*. 2007;369(9573):1627-1640. doi:10.1016/S0140-6736(07)60750-8
9. Zhang Y-Z, Li Y-Y. Inflammatory bowel disease: Pathogenesis. *World J Gastroenterol*. 2014;20(1):91-99. doi:10.3748/wjg.v20.i1.91
10. Ananthakrishnan AN. Epidemiology and risk factors for IBD. *Nat Rev Gastroenterol Hepatol*. 2015;12(4):205-217. doi:10.1038/nrgastro.2015.34
11. Van Limbergen J, Russell RK, Drummond HE, et al. Definition of Phenotypic Characteristics of Childhood-Onset Inflammatory Bowel Disease. *Gastroenterology*. 2008;135(4):1114-1122. doi:10.1053/j.gastro.2008.06.081
12. Ogura Y, Bonen DK, Inohara N, et al. A frameshift mutation in NOD2 associated with susceptibility to Crohn's disease. *Nature*. 2001;411(6837):603-606. doi:10.1038/35079114
13. Sabbah A, Chang TH, Harnack R, et al. Activation of innate immune antiviral responses by Nod2. *Nat Immunol*. 2009;10(10):1073-1080. doi:10.1038/ni.1782
14. Jostins L, Ripke S, Weersma RK, et al. Host–microbe interactions have shaped the genetic architecture of inflammatory bowel disease. *Nature*. 2012;491(7422):119-124. doi:10.1038/nature11582
15. Adler J, Rangwalla S, Dwamena B, Higgins P. The Prognostic Power of the NOD2 Genotype for Complicated Crohn's Disease: A Meta-Analysis. *Am J Gastroenterol*. 2011;106(4):699-712. doi:10.1038/ajg.2011.19
16. Hampe J, Franke A, Rosenstiel P, et al. A genome-wide association scan of nonsynonymous SNPs identifies a susceptibility variant for Crohn disease in *ATG16L1*. *Nat Genet*. 2007;39(2):207-211. doi:10.1038/ng1954
17. Pugazhendhi S, Baskaran K, Santhanam S, Ramakrishna BS. Association of ATG16L1 gene haplotype with inflammatory bowel disease in Indians. *PLOS ONE*. 2017;12(5):e0178291. doi:10.1371/journal.pone.0178291
18. Rioux JD, Xavier RJ, Taylor KD, et al. Genome-wide association study identifies new susceptibility loci for Crohn disease and implicates autophagy in disease pathogenesis. *Nat Genet*. 2007;39(5):596-604. doi:10.1038/ng2032
19. Kaser A, Lee A-H, Franke A, et al. XBP1 Links ER Stress to Intestinal Inflammation and Confers Genetic Risk for Human Inflammatory Bowel Disease. *Cell*. 2008;134(5):743-756. doi:10.1016/j.cell.2008.07.021
20. Zheng W, Rosenstiel P, Huse K, et al. Evaluation of AGR2 and AGR3 as candidate genes for inflammatory bowel disease. *Genes Immun*. 2006;7(1):11-18. doi:10.1038/sj.gene.6364263
21. Barrett JC, Hansoul S, Nicolae DL, et al. Genome-wide association defines more than 30 distinct susceptibility loci for Crohn's disease. *Nat Genet*. 2008;40(8):955-962. doi:10.1038/ng.175
22. McGovern DPB, Gardet A, Törkvist L, et al. Genome-wide association identifies multiple ulcerative colitis susceptibility loci. *Nat Genet*. 2010;42(4):332-337. doi:10.1038/ng.549
23. Levine B, Mizushima N, Virgin HW. Autophagy in immunity and inflammation. *Nature*. 2011;469(7330):323-335. doi:10.1038/nature09782
24. Benjamin JL, Sumpter R, Levine B, Hooper LV. Intestinal Epithelial Autophagy Is Essential for Host Defense against Invasive Bacteria. *Cell Host Microbe*. 2013;13(6):723-734. doi:10.1016/j.chom.2013.05.004
25. Thurston TLM, Wandel MP, von Muhlinen N, Foeglein Á, Randow F. Galectin 8 targets damaged vesicles for autophagy to defend cells against bacterial invasion. *Nature*. 2012;482(7385):414-418. doi:10.1038/nature10744
26. Randall-Demllo S, Chieppa M, Eri RD. Intestinal Epithelium and Autophagy: Partners in Gut Homeostasis. *Front Immunol*. 2013;4. doi:10.3389/fimmu.2013.00301

27. Billmann-Born S, Lipinski S, Böck J, Till A, Rosenstiel P, Schreiber S. The complex interplay of NOD-like receptors and the autophagy machinery in the pathophysiology of Crohn disease. *Eur J Cell Biol*. 2011;90(6):593-602. doi:10.1016/j.ejcb.2010.10.015

28. Travassos LH, Carneiro LAM, Ramjeet M, et al. Nod1 and Nod2 direct autophagy by recruiting ATG16L1 to the plasma membrane at the site of bacterial entry. *Nat Immunol*. 2010;11(1):55-62. doi:10.1038/ni.1823

29. Haq S, Grondin J, Banskota S, Khan WI. Autophagy: roles in intestinal mucosal homeostasis and inflammation. *J Biomed Sci*. 2019;26(1):19. doi:10.1186/s12929-019-0512-2

30. Murthy A, Li Y, Peng I, et al. A Crohn's disease variant in *Atg16l1* enhances its degradation by caspase 3. *Nature*. 2014;506(7489):456-462. doi:10.1038/nature13044

31. Alsaadi RM, Losier TT, Tian W, et al. ULK1-mediated phosphorylation of ATG16L1 promotes xenophagy, but destabilizes the ATG16L1 Crohn's mutant. *EMBO Rep*. 2019;20(7):e46885. doi:10.15252/embr.201846885

32. Lassen KG, Kuballa P, Conway KL, et al. Atg16L1 T300A variant decreases selective autophagy resulting in altered cytokine signaling and decreased antibacterial defense. *Proc Natl Acad Sci*. 2014;111(21):7741-7746. doi:10.1073/pnas.1407001111

33. Saitoh T, Fujita N, Jang MH, et al. Loss of the autophagy protein Atg16L1 enhances endotoxin-induced IL-1beta production. *Nature*. 2008;456(7219):264-268. doi:10.1038/nature07383

34. Plantinga TS, Crisan TO, Oosting M, et al. Crohn's disease-associated ATG16L1 polymorphism modulates pro-inflammatory cytokine responses selectively upon activation of NOD2. *Gut*. 2011;60(9):1229-1235. doi:10.1136/gut.2010.228908

35. Lee H-M, Kim C-W, Hwang K-A, Choi D-W, Choi K-C. Three components of cigarette smoke altered the growth and apoptosis of metastatic colon cancer cells via inducing the synthesis of reactive oxygen species and endoplasmic reticulum stress. *Environ Toxicol Pharmacol*. 2016;45:80-89. doi:10.1016/j.etap.2016.05.016

36. He B. Viruses, endoplasmic reticulum stress, and interferon responses. *Cell Death Differ*. 2006;13(3):393-403. doi:10.1038/sj.cdd.4401833

37. Moretti J, Roy S, Bozec D, et al. STING Senses Microbial Viability to Orchestrate Stress-Mediated Autophagy of the Endoplasmic Reticulum. *Cell*. 2017;171(4):809-823.e13. doi:10.1016/j.cell.2017.09.034

38. Dohrman A, Miyata S, Gallup M, et al. Mucin gene (MUC 2 and MUC 5AC) upregulation by Gram-positive and Gram-negative bacteria. *Biochim Biophys Acta BBA - Mol Basis Dis*. 1998;1406(3):251-259. doi:10.1016/S0925-4439(98)00010-6

39. Bel S, Pendse M, Wang Y, et al. Paneth cells secrete lysozyme via secretory autophagy during bacterial infection of the intestine. *Science*. 2017;357(6355):1047-1052. doi:10.1126/science.aal4677

40. Adolph TE, Tomczak MF, Niederreiter L, et al. Paneth cells as a site of origin for intestinal inflammation. *Nature*. 2013;503(7475):272-276. doi:10.1038/nature12599

41. Deuring JJ, Fuhler GM, Konstantinov SR, et al. Genomic ATG16L1 risk allele-restricted Paneth cell ER stress in quiescent Crohn's disease. *Gut*. 2014;63(7):1081-1091. doi:10.1136/gutjnl-2012-303527

42. Stengel S, Messner B, Falk-Paulsen M, Sommer N, Rosenstiel P. Regulated proteolysis as an element of ER stress and autophagy: Implications for intestinal inflammation. *Biochim Biophys Acta BBA - Mol Cell Res*. 2017;1864(11):2183-2190. doi:10.1016/j.bbamcr.2017.07.008

43. McGuckin MA, Eri RD, Das I, Lourie R, Florin TH. Intestinal secretory cell ER stress and inflammation. *Biochem Soc Trans*. 2011;39(4):1081-1085. doi:10.1042/BST0391081

44. Ma X, Dai Z, Sun K, et al. Intestinal Epithelial Cell Endoplasmic Reticulum Stress and Inflammatory Bowel Disease Pathogenesis: An Update Review. *Front Immunol*. 2017;8. doi:10.3389/fimmu.2017.01271

45. Zhao F, Edwards R, Dizon D, et al. Disruption of Paneth and goblet cell homeostasis and increased endoplasmic reticulum stress in Agr2−/− mice. *Dev Biol*. 2010;338(2):270-279. doi:10.1016/j.ydbio.2009.12.008

46. Heazlewood CK, Cook MC, Eri R, et al. Aberrant Mucin Assembly in Mice Causes Endoplasmic Reticulum Stress and Spontaneous Inflammation Resembling Ulcerative Colitis. *PLOS Med*. 2008;5(3):e54. doi:10.1371/journal.pmed.0050054

47. Garg AD, Kaczmarek A, Krysko O, Vandenabeele P, Krysko DV, Agostinis P. ER stress-induced inflammation: does it aid or impede disease progression? *Trends Mol Med*. 2012;18(10):589-598. doi:10.1016/j.molmed.2012.06.010

48. Cao SS. Epithelial ER Stress in Crohn's Disease and Ulcerative Colitis. *Inflamm Bowel Dis*. 2016;22(4):984-993. doi:10.1097/MIB.0000000000000660

49. Tréton X, Pédruzzi E, Cazals–Hatem D, et al. Altered Endoplasmic Reticulum Stress Affects Translation in Inactive Colon Tissue From Patients With Ulcerative Colitis. *Gastroenterology*. 2011;141(3):1024-1035. doi:10.1053/j.gastro.2011.05.033

50. Thachil É, Hugot J, Arbeille B, et al. Abnormal Activation of Autophagy-Induced Crinophagy in Paneth Cells From Patients With Crohn's Disease. *Gastroenterology*. 2012;142(5):1097-1099.e4. doi:10.1053/j.gastro.2012.01.031

51. VanDussen KL, Liu T-C, Li D, et al. Genetic Variants Synthesize to Produce Paneth Cell Phenotypes That Define Subtypes of Crohn's Disease. *Gastroenterology*. 2014;146(1):200-209. doi:10.1053/j.gastro.2013.09.048
52. Wehkamp J, Salzman NH, Porter E, et al. Reduced Paneth cell α-defensins in ileal Crohn's disease. *Proc Natl Acad Sci*. 2005;102(50):18129-18134. doi:10.1073/pnas.0505256102
53. Cadwell K, Liu JY, Brown SL, et al. A key role for autophagy and the autophagy gene Atg16l1 in mouse and human intestinal Paneth cells. *Nature*. 2008;456(7219):259-263. doi:10.1038/nature07416
54. Ogata M, Hino S, Saito A, et al. Autophagy Is Activated for Cell Survival after Endoplasmic Reticulum Stress. *Mol Cell Biol*. 2006;26(24):9220-9231. doi:10.1128/MCB.01453-06
55. Kouroku Y, Fujita E, Tanida I, et al. ER stress (PERK/eIF2*α* phosphorylation) mediates the polyglutamine-induced LC3 conversion, an essential step for autophagy formation. *Cell Death Differ*. 2007;14(2):230-239. doi:10.1038/sj.cdd.4401984
56. Zuk O, Hechter E, Sunyaev SR, Lander ES. The mystery of missing heritability: Genetic interactions create phantom heritability. *Proc Natl Acad Sci*. 2012;109(4):1193-1198. doi:10.1073/pnas.1119675109
57. Hunt KA, Mistry V, Bockett NA, et al. Negligible impact of rare autoimmune-locus coding-region variants on missing heritability. *Nature*. 2013;498(7453):232-235. doi:10.1038/nature12170
58. Rivas MA, Beaudoin M, Gardet A, et al. Deep resequencing of GWAS loci identifies independent rare variants associated with inflammatory bowel disease. *Nat Genet*. 2011;43(11):1066-1073. doi:10.1038/ng.952
59. Eichler EE, Flint J, Gibson G, et al. Missing heritability and strategies for finding the underlying causes of complex disease. *Nat Rev Genet*. 2010;11(6):446-450. doi:10.1038/nrg2809
60. Kaplan GG, Ng SC. Understanding and Preventing the Global Increase of Inflammatory Bowel Disease. *Gastroenterology*. 2017;152(2):313-321.e2. doi:10.1053/j.gastro.2016.10.020
61. Ananthakrishnan AN, Bernstein CN, Iliopoulos D, et al. Environmental triggers in IBD: a review of progress and evidence. *Nat Rev Gastroenterol Hepatol*. 2018;15(1):39-49. doi:10.1038/nrgastro.2017.136
62. Zimmer J, Lange B, Frick J-S, et al. A vegan or vegetarian diet substantially alters the human colonic faecal microbiota. *Eur J Clin Nutr*. 2012;66(1):53-60. doi:10.1038/ejcn.2011.141
63. Turpin W, Espin-Garcia O, Xu W, et al. Association of host genome with intestinal microbial composition in a large healthy cohort. *Nat Genet*. 2016;48(11):1413-1417. doi:10.1038/ng.3693
64. Lynch SV, Pedersen O. The Human Intestinal Microbiome in Health and Disease. *N Engl J Med*. 2016;375(24):2369-2379. doi:10.1056/NEJMra1600266
65. Sommer F, Nookaew I, Sommer N, Fogelstrand P, Bäckhed F. Site-specific programming of the host epithelial transcriptome by the gut microbiota. *Genome Biol*. 2015;16(1):62. doi:10.1186/s13059-015-0614-4
66. Geuking MB, Köller Y, Rupp S, McCoy KD. The interplay between the gut microbiota and the immune system. *Gut Microbes*. 2014;5(3):411-418. doi:10.4161/gmic.29330
67. Kostic AD, Xavier RJ, Gevers D. The Microbiome in Inflammatory Bowel Disease: Current Status and the Future Ahead. *Gastroenterology*. 2014;146(6):1489-1499. doi:10.1053/j.gastro.2014.02.009
68. Liu T-C, Gurram B, Baldridge MT, et al. Paneth cell defects in Crohn's disease patients promote dysbiosis. *JCI Insight*. 2016;1(8). doi:10.1172/jci.insight.86907
69. Ohkusa T, Yoshida T, Sato N, Watanabe S, Tajiri H, Okayasu I. Commensal bacteria can enter colonic epithelial cells and induce proinflammatory cytokine secretion: a possible pathogenic mechanism of ulcerative colitis. *J Med Microbiol*. 2009;58(5):535-545. doi:10.1099/jmm.0.005801-0
70. Aden K, Rehman A, Waschina S, et al. Metabolic Functions of Gut Microbes Associate With Efficacy of Tumor Necrosis Factor Antagonists in Patients with Inflammatory Bowel Diseases. *Gastroenterology*. Published online July 18, 2019. doi:10.1053/j.gastro.2019.07.025
71. Moayyedi P, Surette MG, Kim PT, et al. Fecal Microbiota Transplantation Induces Remission in Patients With Active Ulcerative Colitis in a Randomized Controlled Trial. *Gastroenterology*. 2015;149(1):102-109.e6. doi:10.1053/j.gastro.2015.04.001
72. Smoking Cessation Induces Profound Changes in the Composition of the Intestinal Microbiota in Humans. Accessed September 3, 2019. https://journals.plos.org/plosone/article?id=10.1371/journal.pone.0059260
73. Rangan P, Choi I, Wei M, et al. Fasting-Mimicking Diet Modulates Microbiota and Promotes Intestinal Regeneration to Reduce Inflammatory Bowel Disease Pathology. *Cell Rep*. 2019;26(10):2704-2719.e6. doi:10.1016/j.celrep.2019.02.019
74. Cadwell K, Patel KK, Maloney NS, et al. Virus-Plus-Susceptibility Gene Interaction Determines Crohn's Disease Gene Atg16L1 Phenotypes in Intestine. *Cell*. 2010;141(7):1135-1145. doi:10.1016/j.cell.2010.05.009
75. Kuballa P, Huett A, Rioux JD, Daly MJ, Xavier RJ. Impaired Autophagy of an Intracellular Pathogen Induced by a Crohn's Disease Associated ATG16L1 Variant. *PLOS ONE*. 2008;3(10):e3391. doi:10.1371/journal.pone.0003391

76. Frank DN, Robertson CE, Hamm CM, et al. Disease phenotype and genotype are associated with shifts in intestinal-associated microbiota in inflammatory bowel diseases. *Inflamm Bowel Dis*. 2011;17(1):179-184. doi:10.1002/ibd.21339
77. Gutiérrez A, Scharl M, Sempere L, et al. Genetic susceptibility to increased bacterial translocation influences the response to biological therapy in patients with Crohn's disease. *Gut*. 2014;63(2):272-280. doi:10.1136/gutjnl-2012-303557
78. Miranda-Bautista J, Padilla-Suárez C, Bouza E, Muñoz P, Menchén L, Marín-Jiménez I. Listeria monocytogenes infection in inflammatory bowel disease patients: case series and review of the literature. *Eur J Gastroenterol Hepatol*. 2014;26(11):1247-1252. doi:10.1097/MEG.0000000000000188
79. Azimi T, Nasiri MJ, Chirani AS, Pouriran R, Dabiri H. The role of bacteria in the inflammatory bowel disease development: a narrative review. *APMIS*. 2018;126(4):275-283. doi:10.1111/apm.12814
80. Magin WS, Van Kruiningen HJ, Colombel J-F. Immunohistochemical search for viral and bacterial antigens in Crohn's disease. *J Crohns Colitis*. 2013;7(2):161-166. doi:10.1016/j.crohns.2012.03.021
81. Simpson KW, Dogan B, Rishniw M, et al. Adherent and Invasive Escherichia coli Is Associated with Granulomatous Colitis in Boxer Dogs. *Infect Immun*. 2006;74(8):4778-4792. doi:10.1128/IAI.00067-06
82. Meconi S, Vercellone A, Levillain F, et al. Adherent-invasive Escherichia coli isolated from Crohn's disease patients induce granulomas in vitro. *Cell Microbiol*. 2007;9(5):1252-1261. doi:10.1111/j.1462-5822.2006.00868.x
83. Carvalho FA, Barnich N, Sauvanet P, Darcha C, Gelot A, Darfeuille-Michaud A. Crohn's disease-associated Escherichia coli LF82 aggravates colitis in injured mouse colon via signaling by flagellin. *Inflamm Bowel Dis*. 2008;14(8):1051-1060. doi:10.1002/ibd.20423
84. Lapaquette P, Glasser A-L, Huett A, Xavier RJ, Darfeuille-Michaud A. Crohn's disease-associated adherent-invasive E. coli are selectively favoured by impaired autophagy to replicate intracellularly. *Cell Microbiol*. 2010;12(1):99-113. doi:10.1111/j.1462-5822.2009.01381.x
85. Sokol H, Pigneur B, Watterlot L, et al. Faecalibacterium prausnitzii is an anti-inflammatory commensal bacterium identified by gut microbiota analysis of Crohn disease patients. *Proc Natl Acad Sci U S A*. 2008;105(43):16731-16736. doi:10.1073/pnas.0804812105
86. Neurath MF. Current and emerging therapeutic targets for IBD. *Nat Rev Gastroenterol Hepatol*. 2017;14(5):269-278. doi:10.1038/nrgastro.2016.208
87. Schölmerich J. Systemic and topical steroids in inflammatory bowel disease. *Aliment Pharmacol Ther*. 2004;20(s4):66-74. doi:10.1111/j.1365-2036.2004.02059.x
88. Colombel JF, Sandborn WJ, Reinisch W, et al. Infliximab, Azathioprine, or Combination Therapy for Crohn's Disease. *N Engl J Med*. 2010;362(15):1383-1395. doi:10.1056/NEJMoa0904492
89. Panaccione R, Ghosh S, Middleton S, et al. Combination Therapy With Infliximab and Azathioprine Is Superior to Monotherapy With Either Agent in Ulcerative Colitis. *Gastroenterology*. 2014;146(2):392-400.e3. doi:10.1053/j.gastro.2013.10.052
90. Sandborn WJ, Feagan BG, Rutgeerts P, et al. Vedolizumab as Induction and Maintenance Therapy for Crohn's Disease. *N Engl J Med*. 2013;369(8):711-721. doi:10.1056/NEJMoa1215739
91. Fiocchi C. Towards a 'Cure' for IBD. *Dig Dis*. 2012;30(4):428-433. doi:10.1159/000338148
92. Powell RD, Warner NE, Levine RS, Kirsner JB. Cytomegalic inclusion disease and ulcerative colitis; report of a case in a young adult. *Am J Med*. 1961;30:334-340. doi:10.1016/0002-9343(61)90105-x
93. Sager K, Alam S, Bond A, Chinnappan L, Probert CS. Review article: cytomegalovirus and inflammatory bowel disease. *Aliment Pharmacol Ther*. 2015;41(8):725-733. doi:10.1111/apt.13124
94. Siegmund B. Cytomegalovirus infection associated with inflammatory bowel disease. *Lancet Gastroenterol Hepatol*. 2017;2(5):369-376. doi:10.1016/S2468-1253(16)30159-5
95. Domènech E, Vega R, Ojanguren I, et al. Cytomegalovirus infection in ulcerative colitis: a prospective, comparative study on prevalence and diagnostic strategy. *Inflamm Bowel Dis*. 2008;14(10):1373-1379. doi:10.1002/ibd.20498
96. D'Ovidio V, Vernia P, Gentile G, et al. Cytomegalovirus infection in inflammatory bowel disease patients undergoing anti-TNFalpha therapy. *J Clin Virol Off Publ Pan Am Soc Clin Virol*. 2008;43(2):180-183. doi:10.1016/j.jcv.2008.06.002
97. Kim CH, Bahng S, Kang KJ, et al. Cytomegalovirus colitis in patients without inflammatory bowel disease: a single center study. *Scand J Gastroenterol*. 2010;45(11):1295-1301. doi:10.3109/00365521.2010.499962
98. Cottone M, Pietrosi G, Martorana G, et al. Prevalence of cytomegalovirus infection in severe refractory ulcerative and Crohn's colitis. *Am J Gastroenterol*. 2001;96(3):773-775. doi:10.1111/j.1572-0241.2001.03620.x
99. Criscuoli V, Casà A, Orlando A, et al. Severe acute colitis associated with CMV: a prevalence study. *Dig Liver Dis Off J Ital Soc Gastroenterol Ital Assoc Study Liver*. 2004;36(12):818-820. doi:10.1016/j.dld.2004.05.013
100. Kishore J, Ghoshal U, Ghoshal UC, et al. Infection with cytomegalovirus in patients with inflammatory bowel disease: prevalence, clinical significance and outcome. *J Med Microbiol*. 2004;53(Pt 11):1155-1160. doi:10.1099/jmm.0.45629-0

101. Wada Y, Matsui T, Matake H, et al. Intractable ulcerative colitis caused by cytomegalovirus infection: a prospective study on prevalence, diagnosis, and treatment. *Dis Colon Rectum*. 2003;46(10 Suppl):S59-65. doi:10.1097/01.DCR.0000087486.21981.C6

102. Steroid-refractory inflammatory bowel disease is a risk factor for CMV infection. *Eur Rev*. Published online March 15, 2016. Accessed August 30, 2019. https://www.europeanreview.org/article/10429

103. Targan SR, Karp LC. Defects in mucosal immunity leading to ulcerative colitis. *Immunol Rev*. 2005;206:296-305. doi:10.1111/j.0105-2896.2005.00286.x

104. Ginsburg CH, Dambrauskas JT, Ault KA, Falchuk ZM. Impaired natural killer cell activity in patients with inflammatory bowel disease: evidence for a qualitative defect. *Gastroenterology*. 1983;85(4):846-851.

105. Kaufman HS, Kahn AC, Iacobuzio-Donahue C, Talamini MA, Lillemoe KD, Hamilton SR. Cytomegaloviral enterocolitis: clinical associations and outcome. *Dis Colon Rectum*. 1999;42(1):24-30. doi:10.1007/BF02235178

106. Garrido E, Carrera E, Manzano R, Lopez-Sanroman A. Clinical significance of cytomegalovirus infection in patients with inflammatory bowel disease. *World J Gastroenterol*. 2013;19(1):17-25. doi:10.3748/wjg.v19.i1.17

107. Wakefield AJ, Fox JD, Sawyerr AM, et al. Detection of herpesvirus DNA in the large intestine of patients with ulcerative colitis and Crohn's disease using the nested polymerase chain reaction. *J Med Virol*. 1992;38(3):183-190. doi:10.1002/jmv.1890380306

108. Lawlor G, Moss AC. Cytomegalovirus in inflammatory bowel disease: pathogen or innocent bystander? *Inflamm Bowel Dis*. 2010;16(9):1620-1627. doi:10.1002/ibd.21275

109. McCurdy JD, Enders FT, Khanna S, et al. Increased Rates of Clostridium difficile Infection and Poor Outcomes in Patients with IBD with Cytomegalovirus. *Inflamm Bowel Dis*. 2016;22(11):2688-2693. doi:10.1097/MIB.0000000000000939

110. Kou T, Nakase H, Tamaki H, Kudo T, Nishio A, Chiba T. Cytomegalovirus infection in patients with ulcerative colitis diagnosed by quantitative real-time PCR analysis. *Dig Dis Sci*. 2006;51(6):1052-1055. doi:10.1007/s10620-006-8006-y

111. Kambham N, Vij R, Cartwright CA, Longacre T. Cytomegalovirus infection in steroid-refractory ulcerative colitis: a case-control study. *Am J Surg Pathol*. 2004;28(3):365-373. doi:10.1097/00000478-200403000-00009

112. Maconi G, Colombo E, Zerbi P, et al. Prevalence, detection rate and outcome of cytomegalovirus infection in ulcerative colitis patients requiring colonic resection. *Dig Liver Dis Off J Ital Soc Gastroenterol Ital Assoc Study Liver*. 2005;37(6):418-423. doi:10.1016/j.dld.2005.01.011

113. Eyre-Brook IA, Dundas S. Incidence and clinical significance of colonic cytomegalovirus infection in idiopathic inflammatory bowel disease requiring colectomy. *Gut*. 1986;27(12):1419-1425. doi:10.1136/gut.27.12.1419

114. de Saussure P, Lavergne-Slove A, Mazeron M-C, Alain S, Matuchansky C, Bouhnik Y. A prospective assessment of cytomegalovirus infection in active inflammatory bowel disease. *Aliment Pharmacol Ther*. 2004;20(11-12):1323-1327. doi:10.1111/j.1365-2036.2004.02273.x

115. Zhang W-X, Ma C-Y, Zhang J-G, et al. Effects of cytomegalovirus infection on the prognosis of inflammatory bowel disease patients. *Exp Ther Med*. 2016;12(5):3287-3293. doi:10.3892/etm.2016.3763

116. Maher MM, Nassar MI. Acute Cytomegalovirus Infection Is a Risk Factor in Refractory and Complicated Inflammatory Bowel Disease. *Dig Dis Sci*. 2008;54(11):2456. doi:10.1007/s10620-008-0639-6

117. Zagórowicz E, Bugajski M, Wieszczy P, Pietrzak A, Magdziak A, Mróz A. Cytomegalovirus Infection in Ulcerative Colitis is Related to Severe Inflammation and a High Count of Cytomegalovirus-positive Cells in Biopsy Is a Risk Factor for Colectomy. *J Crohns Colitis*. 2016;10(10):1205-1211. doi:10.1093/ecco-jcc/jjw071

118. Papadakis K, Tung J, Binder S, et al. Outcome of Cytomegalovirus Infections in Patients With Inflammatory Bowel Disease. *Am J Gastroenterol*. 2001;96(7):2137-2142. doi:10.1111/j.1572-0241.2001.03949.x

119. Castaneda D, Melendez-Rosado J, Hasan B, Charles R. Increased Risk of Colectomy in Hospitalized Patients With Inflammatory Bowel Disease and Cytomegalovirus Infection: 714. *Am J Gastroenterol*. 2019;114:S420. doi:10.14309/01.ajg.0000592392.61499.80

120. Hahn G, Jores R, Mocarski ES. Cytomegalovirus remains latent in a common precursor of dendritic and myeloid cells. *Proc Natl Acad Sci U S A*. 1998;95(7):3937-3942. doi:10.1073/pnas.95.7.3937

121. Hommes DW, Sterringa G, van Deventer SJH, Tytgat GNJ, Weel J. The pathogenicity of cytomegalovirus in inflammatory bowel disease: a systematic review and evidence-based recommendations for future research. *Inflamm Bowel Dis*. 2004;10(3):245-250. doi:10.1097/00054725-200405000-00011

122. Söderberg-Nauclér C, Nelson JY. Human cytomegalovirus latency and reactivation - a delicate balance between the virus and its host's immune system. *Intervirology*. 1999;42(5-6):314-321. doi:10.1159/000053966

123. Söderberg-Nauclér C, Fish KN, Nelson JA. Interferon-gamma and tumor necrosis factor-alpha specifically induce formation of cytomegalovirus-permissive monocyte-derived macrophages that are refractory to the antiviral activity of these cytokines. *J Clin Invest*. 1997;100(12):3154-3163. doi:10.1172/JCI119871

124. Simon CO, Seckert CK, Dreis D, Reddehase MJ, Grzimek NKA. Role for tumor necrosis factor alpha in murine cytomegalovirus transcriptional reactivation in latently infected lungs. *J Virol*. 2005;79(1):326-340. doi:10.1128/JVI.79.1.326-340.2005

125. van der Flier LG, Clevers H. Stem Cells, Self-Renewal, and Differentiation in the Intestinal Epithelium. *Annu Rev Physiol*. 2009;71(1):241-260. doi:10.1146/annurev.physiol.010908.163145

126. Allaire JM, Crowley SM, Law HT, Chang S-Y, Ko H-J, Vallance BA. The Intestinal Epithelium: Central Coordinator of Mucosal Immunity. *Trends Immunol*. 2018;39(9):677-696. doi:10.1016/j.it.2018.04.002

127. Gehart H, Clevers H. Tales from the crypt: new insights into intestinal stem cells. *Nat Rev Gastroenterol Hepatol*. 2019;16(1):19-34. doi:10.1038/s41575-018-0081-y

128. Chelakkot C, Ghim J, Ryu SH. Mechanisms regulating intestinal barrier integrity and its pathological implications. *Exp Mol Med*. 2018;50(8):1-9. doi:10.1038/s12276-018-0126-x

129. Rescigno M. The intestinal epithelial barrier in the control of homeostasis and immunity. *Trends Immunol*. 2011;32(6):256-264. doi:10.1016/j.it.2011.04.003

130. Peterson LW, Artis D. Intestinal epithelial cells: regulators of barrier function and immune homeostasis. *Nat Rev Immunol*. 2014;14(3):141-153. doi:10.1038/nri3608

131. Gribble FM, Reimann F. Enteroendocrine Cells: Chemosensors in the Intestinal Epithelium. *Annu Rev Physiol*. 2016;78(1):277-299. doi:10.1146/annurev-physiol-021115-105439

132. Abreu MT. Toll-like receptor signalling in the intestinal epithelium: how bacterial recognition shapes intestinal function. *Nat Rev Immunol*. 2010;10(2):131-144. doi:10.1038/nri2707

133. Schlee M, Wehkamp J, Altenhoefer A, Oelschlaeger TA, Stange EF, Fellermann K. Induction of Human β-Defensin 2 by the Probiotic Escherichia coli Nissle 1917 Is Mediated through Flagellin. *Infect Immun*. 2007;75(5):2399-2407. doi:10.1128/IAI.01563-06

134. Rakoff-Nahoum S, Paglino J, Eslami-Varzaneh F, Edberg S, Medzhitov R. Recognition of Commensal Microflora by Toll-Like Receptors Is Required for Intestinal Homeostasis. *Cell*. 2004;118(2):229-241. doi:10.1016/j.cell.2004.07.002

135. Tschurtschenthaler M, Adolph TE, Ashcroft JW, et al. Defective ATG16L1-mediated removal of IRE1α drives Crohn's disease–like ileitis. *J Exp Med*. 2017;214(2):401-422. doi:10.1084/jem.20160791

136. Homer CR, Richmond AL, Rebert NA, Achkar J-P, McDonald C. ATG16L1 and NOD2 interact in an autophagy-dependent antibacterial pathway implicated in Crohn's disease pathogenesis. *Gastroenterology*. 2010;139(5):1630-1641, 1641.e1-2. doi:10.1053/j.gastro.2010.07.006

137. Conway KL, Kuballa P, Song J, et al. Atg16l1 is Required for Autophagy in Intestinal Epithelial Cells and Protection of Mice From Salmonella Infection. *Gastroenterology*. 2013;145(6):1347-1357. doi:10.1053/j.gastro.2013.08.035

138. Mochida K, Oikawa Y, Kimura Y, et al. Receptor-mediated selective autophagy degrades the endoplasmic reticulum and the nucleus. *Nature*. 2015;522(7556):359-362. doi:10.1038/nature14506

139. Hanna RA, Quinsay MN, Orogo AM, Giang K, Rikka S, Gustafsson ÅB. Microtubule-associated Protein 1 Light Chain 3 (LC3) Interacts with Bnip3 Protein to Selectively Remove Endoplasmic Reticulum and Mitochondria via Autophagy. *J Biol Chem*. 2012;287(23):19094-19104. doi:10.1074/jbc.M111.322933

140. Rogov V, Dötsch V, Johansen T, Kirkin V. Interactions between Autophagy Receptors and Ubiquitin-like Proteins Form the Molecular Basis for Selective Autophagy. *Mol Cell*. 2014;53(2):167-178. doi:10.1016/j.molcel.2013.12.014

141. Samie M, Lim J, Verschueren E, et al. Selective autophagy of the adaptor TRIF regulates innate inflammatory signaling. *Nat Immunol*. 2018;19(3):246-254. doi:10.1038/s41590-017-0042-6

142. Wang C-W, Klionsky DJ. The Molecular Mechanism of Autophagy. *Mol Med*. 2003;9(3-4):65-76.

143. Mizushima N. The role of the Atg1/ULK1 complex in autophagy regulation. *Curr Opin Cell Biol*. 2010;22(2):132-139. doi:10.1016/j.ceb.2009.12.004

144. Hayashi-Nishino M, Fujita N, Noda T, Yamaguchi A, Yoshimori T, Yamamoto A. A subdomain of the endoplasmic reticulum forms a cradle for autophagosome formation. *Nat Cell Biol*. 2009;11(12):1433-1437. doi:10.1038/ncb1991

145. Webber JL, Tooze SA. New insights into the function of Atg9. *FEBS Lett*. 2010;584(7):1319-1326. doi:10.1016/j.febslet.2010.01.020

146. Saitoh T, Fujita N, Hayashi T, et al. Atg9a controls dsDNA-driven dynamic translocation of STING and the innate immune response. *Proc Natl Acad Sci U S A*. 2009;106(49):20842-20846. doi:10.1073/pnas.0911267106

147. Itakura E, Mizushima N. Characterization of autophagosome formation site by a hierarchical analysis of mammalian Atg proteins. *Autophagy*. 2010;6(6):764-776. doi:10.4161/auto.6.6.12709

148. Axe EL, Walker SA, Manifava M, et al. Autophagosome formation from membrane compartments enriched in phosphatidylinositol 3-phosphate and dynamically connected to the endoplasmic reticulum. *J Cell Biol*. 2008;182(4):685-701. doi:10.1083/jcb.200803137

149. Tanida I, Ueno T, Kominami E. LC3 conjugation system in mammalian autophagy. *Int J Biochem Cell Biol*. 2004;36(12):2503-2518. doi:10.1016/j.biocel.2004.05.009

150. Fujita N, Itoh T, Omori H, Fukuda M, Noda T, Yoshimori T. The Atg16L complex specifies the site of LC3 lipidation for membrane biogenesis in autophagy. *Mol Biol Cell*. 2008;19(5):2092-2100. doi:10.1091/mbc.e07-12-1257
151. Mizushima N, Noda T, Yoshimori T, et al. A protein conjugation system essential for autophagy. *Nature*. 1998;395(6700):395-398. doi:10.1038/26506
152. Hanada T, Noda NN, Satomi Y, et al. The Atg12-Atg5 conjugate has a novel E3-like activity for protein lipidation in autophagy. *J Biol Chem*. 2007;282(52):37298-37302. doi:10.1074/jbc.C700195200
153. Kabeya Y, Mizushima N, Ueno T, et al. LC3, a mammalian homologue of yeast Apg8p, is localized in autophagosome membranes after processing. *EMBO J*. 2000;19(21):5720-5728. doi:10.1093/emboj/19.21.5720
154. Klionsky DJ, Abdelmohsen K, Abe A, et al. Guidelines for the use and interpretation of assays for monitoring autophagy (3rd edition). *Autophagy*. 2016;12(1):1-222. doi:10.1080/15548627.2015.1100356
155. Kraft C, Peter M, Hofmann K. Selective autophagy: ubiquitin-mediated recognition and beyond. *Nat Cell Biol*. 2010;12(9):836-841. doi:10.1038/ncb0910-836
156. Wurzer B, Zaffagnini G, Fracchiolla D, et al. Oligomerization of p62 allows for selection of ubiquitinated cargo and isolation membrane during selective autophagy. Schekman R, ed. *eLife*. 2015;4:e08941. doi:10.7554/eLife.08941
157. Pankiv S, Clausen TH, Lamark T, et al. p62/SQSTM1 binds directly to Atg8/LC3 to facilitate degradation of ubiquitinated protein aggregates by autophagy. *J Biol Chem*. 2007;282(33):24131-24145. doi:10.1074/jbc.M702824200
158. Stolz A, Ernst A, Dikic I. Cargo recognition and trafficking in selective autophagy. *Nat Cell Biol*. 2014;16(6):495-501. doi:10.1038/ncb2979
159. Kirkin V, McEwan DG, Novak I, Dikic I. A role for ubiquitin in selective autophagy. *Mol Cell*. 2009;34(3):259-269. doi:10.1016/j.molcel.2009.04.026
160. Fujita N, Morita E, Itoh T, et al. Recruitment of the autophagic machinery to endosomes during infection is mediated by ubiquitin. *J Cell Biol*. 2013;203(1):115-128. doi:10.1083/jcb.201304188
161. Johansen T, Lamark T. Selective autophagy mediated by autophagic adapter proteins. *Autophagy*. 2011;7(3):279-296. doi:10.4161/auto.7.3.14487
162. Bjørkøy G, Lamark T, Pankiv S, Øvervatn A, Brech A, Johansen T. Monitoring autophagic degradation of p62/SQSTM1. *Methods Enzymol*. 2009;452:181-197. doi:10.1016/S0076-6879(08)03612-4
163. Saitoh T, Akira S. Regulation of innate immune responses by autophagy-related proteins. *J Cell Biol*. 2010;189(6):925-935. doi:10.1083/jcb.201002021
164. Aden K, Tran F, Ito G, et al. ATG16L1 orchestrates interleukin-22 signaling in the intestinal epithelium via cGAS–STING. *J Exp Med*. 2018;215(11):2868-2886. doi:10.1084/jem.20171029
165. Deretic V, Levine B. Autophagy balances inflammation in innate immunity. *Autophagy*. 2018;14(2):243-251. doi:10.1080/15548627.2017.1402992
166. Chen M, Meng Q, Qin Y, et al. TRIM14 Inhibits cGAS Degradation Mediated by Selective Autophagy Receptor p62 to Promote Innate Immune Responses. *Mol Cell*. 2016;64(1):105-119. doi:10.1016/j.molcel.2016.08.025
167. Jin S, Tian S, Luo M, et al. Tetherin Suppresses Type I Interferon Signaling by Targeting MAVS for NDP52-Mediated Selective Autophagic Degradation in Human Cells. *Mol Cell*. 2017;68(2):308-322.e4. doi:10.1016/j.molcel.2017.09.005
168. Kimura T, Jain A, Choi SW, et al. TRIM-mediated precision autophagy targets cytoplasmic regulators of innate immunity. *J Cell Biol*. 2015;210(6):973-989. doi:10.1083/jcb.201503023
169. Harding SM, Benci JL, Irianto J, Discher DE, Minn AJ, Greenberg RA. Mitotic progression following DNA damage enables pattern recognition within micronuclei. *Nature*. 2017;548(7668):466-470. doi:10.1038/nature23470
170. Mackenzie KJ, Carroll P, Martin C-A, et al. cGAS surveillance of micronuclei links genome instability to innate immunity. *Nature*. 2017;548(7668):461-465. doi:10.1038/nature23449
171. Bartsch K, Knittler K, Borowski C, et al. Absence of RNase H2 triggers generation of immunogenic micronuclei removed by autophagy. *Hum Mol Genet*. 2017;26(20):3960-3972. doi:10.1093/hmg/ddx283
172. Smith MH, Ploegh HL, Weissman JS. Road to Ruin: Targeting Proteins for Degradation in the Endoplasmic Reticulum. *Science*. 2011;334(6059):1086-1090. doi:10.1126/science.1209235
173. Grootjans J, Kaser A, Kaufman RJ, Blumberg RS. The unfolded protein response in immunity and inflammation. *Nat Rev Immunol*. 2016;16(8):469-484. doi:10.1038/nri.2016.62
174. Hetz C, Martinon F, Rodriguez D, Glimcher LH. The Unfolded Protein Response: Integrating Stress Signals Through the Stress Sensor IRE1α. *Physiol Rev*. 2011;91(4):1219-1243. doi:10.1152/physrev.00001.2011
175. Harding HP, Zhang Y, Ron D. Protein translation and folding are coupled by an endoplasmic-reticulum-resident kinase. *Nature*. 1999;397(6716):271-274. doi:10.1038/16729
176. Harding HP, Novoa I, Zhang Y, et al. Regulated Translation Initiation Controls Stress-Induced Gene Expression in Mammalian Cells. *Mol Cell*. 2000;6(5):1099-1108. doi:10.1016/S1097-2765(00)00108-8

177. Haze K, Yoshida H, Yanagi H, Yura T, Mori K. Mammalian Transcription Factor ATF6 Is Synthesized as a Transmembrane Protein and Activated by Proteolysis in Response to Endoplasmic Reticulum Stress. *Mol Biol Cell*. 1999;10(11):3787-3799. doi:10.1091/mbc.10.11.3787

178. Gardner BM, Walter P. Unfolded Proteins Are Ire1-Activating Ligands That Directly Induce the Unfolded Protein Response. *Science*. 2011;333(6051):1891-1894. doi:10.1126/science.1209126

179. Scheuner D, Song B, McEwen E, et al. Translational Control Is Required for the Unfolded Protein Response and In Vivo Glucose Homeostasis. *Mol Cell*. 2001;7(6):1165-1176. doi:10.1016/S1097-2765(01)00265-9

180. Lee A-H, Iwakoshi NN, Glimcher LH. XBP-1 Regulates a Subset of Endoplasmic Reticulum Resident Chaperone Genes in the Unfolded Protein Response. *Mol Cell Biol*. 2003;23(21):7448-7459. doi:10.1128/MCB.23.21.7448-7459.2003

181. Lerner AG, Upton J-P, Praveen PVK, et al. IRE1α Induces Thioredoxin-Interacting Protein to Activate the NLRP3 Inflammasome and Promote Programmed Cell Death under Irremediable ER Stress. *Cell Metab*. 2012;16(2):250-264. doi:10.1016/j.cmet.2012.07.007

182. Oslowski CM, Hara T, O'Sullivan-Murphy B, et al. Thioredoxin-Interacting Protein Mediates ER Stress-Induced β Cell Death through Initiation of the Inflammasome. *Cell Metab*. 2012;16(2):265-273. doi:10.1016/j.cmet.2012.07.005

183. Tirasophon W, Welihinda AA, Kaufman RJ. A stress response pathway from the endoplasmic reticulum to the nucleus requires a novel bifunctional protein kinase/endoribonuclease (Ire1p) in mammalian cells. *Genes Dev*. 1998;12(12):1812-1824. doi:10.1101/gad.12.12.1812

184. Korennykh AV, Egea PF, Korostelev AA, et al. The unfolded protein response signals through high-order assembly of Ire1. *Nature*. 2009;457(7230):687-693. doi:10.1038/nature07661

185. Yoshida H, Matsui T, Yamamoto A, Okada T, Mori K. XBP1 mRNA Is Induced by ATF6 and Spliced by IRE1 in Response to ER Stress to Produce a Highly Active Transcription Factor. *Cell*. 2001;107(7):881-891. doi:10.1016/S0092-8674(01)00611-0

186. Hassler JR, Scheuner DL, Wang S, et al. The IRE1α/XBP1s Pathway Is Essential for the Glucose Response and Protection of β Cells. *PLOS Biol*. 2015;13(10):e1002277. doi:10.1371/journal.pbio.1002277

187. Hollien J, Weissman JS. Decay of Endoplasmic Reticulum-Localized mRNAs During the Unfolded Protein Response. *Science*. 2006;313(5783):104-107. doi:10.1126/science.1129631

188. Upton J-P, Wang L, Han D, et al. IRE1α Cleaves Select microRNAs During ER Stress to Derepress Translation of Proapoptotic Caspase-2. *Science*. 2012;338(6108):818-822. doi:10.1126/science.1226191

189. Ghosh R, Wang L, Wang ES, et al. Allosteric Inhibition of the IRE1α RNase Preserves Cell Viability and Function during Endoplasmic Reticulum Stress. *Cell*. 2014;158(3):534-548. doi:10.1016/j.cell.2014.07.002

190. Vattem KM, Wek RC. Reinitiation involving upstream ORFs regulates ATF4 mRNA translation in mammalian cells. *Proc Natl Acad Sci*. 2004;101(31):11269-11274. doi:10.1073/pnas.0400541101

191. Palam LR, Baird TD, Wek RC. Phosphorylation of eIF2 Facilitates Ribosomal Bypass of an Inhibitory Upstream ORF to Enhance CHOP Translation. *J Biol Chem*. 2011;286(13):10939-10949. doi:10.1074/jbc.M110.216093

192. Marciniak SJ, Yun CY, Oyadomari S, et al. CHOP induces death by promoting protein synthesis and oxidation in the stressed endoplasmic reticulum. *Genes Dev*. 2004;18(24):3066-3077. doi:10.1101/gad.1250704

193. Rutkowski DT, Arnold SM, Miller CN, et al. Adaptation to ER Stress Is Mediated by Differential Stabilities of Pro-Survival and Pro-Apoptotic mRNAs and Proteins. *PLOS Biol*. 2006;4(11):e374. doi:10.1371/journal.pbio.0040374

194. Han J, Back SH, Hur J, et al. ER-stress-induced transcriptional regulation increases protein synthesis leading to cell death. *Nat Cell Biol*. 2013;15(5):481-490. doi:10.1038/ncb2738

195. Wu J, Rutkowski DT, Dubois M, et al. ATF6α Optimizes Long-Term Endoplasmic Reticulum Function to Protect Cells from Chronic Stress. *Dev Cell*. 2007;13(3):351-364. doi:10.1016/j.devcel.2007.07.005

196. Coleman OI, Lobner EM, Bierwirth S, et al. Activated ATF6 Induces Intestinal Dysbiosis and Innate Immune Response to Promote Colorectal Tumorigenesis. *Gastroenterology*. 2018;155(5):1539-1552.e12. doi:10.1053/j.gastro.2018.07.028

197. Stengel ST, Fazio A, Lipinski S, et al. Activating Transcription Factor 6 Mediates Inflammatory Signals in Intestinal Epithelial Cells Upon Endoplasmic Reticulum Stress. *Gastroenterology*. Published online July 2020:S0016508520349246. doi:10.1053/j.gastro.2020.06.088

198. Bernales S, Schuck S, Walter P. ER-Phagy: Selective Autophagy of the Endoplasmic Reticulum. *Autophagy*. 2007;3(3):285-287. doi:10.4161/auto.3930

199. Khaminets A, Heinrich T, Mari M, et al. Regulation of endoplasmic reticulum turnover by selective autophagy. *Nature*. 2015;522(7556):354-358. doi:10.1038/nature14498

200. Qin L, Wang Z, Tao L, Wang Y. ER stress negatively regulates AKT/TSC/mTOR pathway to enhance autophagy. *Autophagy*. 2010;6(2):239-247. doi:10.4161/auto.6.2.11062

201. Kroemer G, Mariño G, Levine B. Autophagy and the Integrated Stress Response. *Mol Cell*. 2010;40(2):280-293. doi:10.1016/j.molcel.2010.09.023

202. B'chir W, Maurin A-C, Carraro V, et al. The eIF2α/ATF4 pathway is essential for stress-induced autophagy gene expression. *Nucleic Acids Res*. 2013;41(16):7683-7699. doi:10.1093/nar/gkt563

203. Salem M, Ammitzboell M, Nys K, Seidelin JB, Nielsen OH. ATG16L1: A multifunctional susceptibility factor in Crohn disease. *Autophagy*. 2015;11(4):585-594. doi:10.1080/15548627.2015.1017187

204. Nguyen HTT, Dalmasso G, Müller S, Carrière J, Seibold F, Darfeuille-Michaud A. Crohn's disease-associated adherent invasive Escherichia coli modulate levels of microRNAs in intestinal epithelial cells to reduce autophagy. *Gastroenterology*. 2014;146(2):508-519. doi:10.1053/j.gastro.2013.10.021

205. Yano T, Mita S, Ohmori H, et al. Autophagic control of listeria through intracellular innate immune recognition in drosophila. *Nat Immunol*. 2008;9(8):908-916. doi:10.1038/ni.1634

206. Barker N, van Es JH, Kuipers J, et al. Identification of stem cells in small intestine and colon by marker gene Lgr5. *Nature*. 2007;449(7165):1003-1007. doi:10.1038/nature06196

207. Tan X, Sun L, Chen J, Chen ZJ. Detection of Microbial Infections Through Innate Immune Sensing of Nucleic Acids. *Annu Rev Microbiol*. 2015;72(1):447-478. doi:10.1146/annurev-micro-102215-095605

208. Li T, Chen ZJ. The cGAS–cGAMP–STING pathway connects DNA damage to inflammation, senescence, and cancer. *J Exp Med*. 2018;215(5):1287-1299. doi:10.1084/jem.20180139

209. Hemmi H, Takeuchi O, Kawai T, et al. A Toll-like receptor recognizes bacterial DNA. *Nature*. 2000;408(6813):740-745. doi:10.1038/35047123

210. Kawai T, Akira S. The role of pattern-recognition receptors in innate immunity: update on Toll-like receptors. *Nat Immunol*. 2010;11(5):373-384. doi:10.1038/ni.1863

211. Fernandes-Alnemri T, Yu J-W, Datta P, Wu J, Alnemri ES. AIM2 activates the inflammasome and cell death in response to cytoplasmic DNA. *Nature*. 2009;458(7237):509-513. doi:10.1038/nature07710

212. Hornung V, Ablasser A, Charrel-Dennis M, et al. AIM2 recognizes cytosolic dsDNA and forms a caspase-1-activating inflammasome with ASC. *Nature*. 2009;458(7237):514-518. doi:10.1038/nature07725

213. Stetson DB, Medzhitov R. Recognition of Cytosolic DNA Activates an IRF3-Dependent Innate Immune Response. *Immunity*. 2006;24(1):93-103. doi:10.1016/j.immuni.2005.12.003

214. Ishii KJ, Coban C, Kato H, et al. A Toll-like receptor–independent antiviral response induced by double-stranded B-form DNA. *Nat Immunol*. 2006;7(1):40-48. doi:10.1038/ni1282

215. Ishikawa H, Barber GN. STING is an endoplasmic reticulum adaptor that facilitates innate immune signalling. *Nature*. 2008;455(7213):674-678. doi:10.1038/nature07317

216. Ishikawa H, Ma Z, Barber GN. STING regulates intracellular DNA-mediated, type I interferon-dependent innate immunity. *Nature*. 2009;461(7265):788-792. doi:10.1038/nature08476

217. Barber GN. STING: infection, inflammation and cancer. *Nat Rev Immunol*. 2015;15(12):760-770. doi:10.1038/nri3921

218. Wu J, Sun L, Chen X, et al. Cyclic GMP-AMP Is an Endogenous Second Messenger in Innate Immune Signaling by Cytosolic DNA. *Science*. 2013;339(6121):826-830. doi:10.1126/science.1229963

219. Sun L, Wu J, Du F, Chen X, Chen ZJ. Cyclic GMP-AMP Synthase Is a Cytosolic DNA Sensor That Activates the Type I Interferon Pathway. *Science*. 2013;339(6121):786-791. doi:10.1126/science.1232458

220. Ablasser A, Goldeck M, Cavlar T, et al. cGAS produces a 2'-5'-linked cyclic dinucleotide second messenger that activates STING. *Nature*. 2013;498(7454):380-384. doi:10.1038/nature12306

221. Diner EJ, Burdette DL, Wilson SC, et al. The Innate Immune DNA Sensor cGAS Produces a Noncanonical Cyclic Dinucleotide that Activates Human STING. *Cell Rep*. 2013;3(5):1355-1361. doi:10.1016/j.celrep.2013.05.009

222. Shang G, Zhang C, Chen ZJ, Bai X, Zhang X. Cryo-EM structures of STING reveal its mechanism of activation by cyclic GMP–AMP. *Nature*. 2019;567(7748):389-393. doi:10.1038/s41586-019-0998-5

223. Shu C, Yi G, Watts T, Kao CC, Li P. Structure of STING bound to cyclic di-GMP reveals the mechanism of cyclic dinucleotide recognition by the immune system. *Nat Struct Mol Biol*. 2012;19(7):722-724. doi:10.1038/nsmb.2331

224. Dobbs N, Burnaevskiy N, Chen D, Gonugunta VK, Alto NM, Yan N. STING Activation by Translocation from the ER Is Associated with Infection and Autoinflammatory Disease. *Cell Host Microbe*. 2015;18(2):157-168. doi:10.1016/j.chom.2015.07.001

225. Liu S, Cai X, Wu J, et al. Phosphorylation of innate immune adaptor proteins MAVS, STING, and TRIF induces IRF3 activation. *Science*. 2015;347(6227):aaa2630. doi:10.1126/science.aaa2630

226. Agalioti T, Lomvardas S, Parekh B, Yie J, Maniatis T, Thanos D. Ordered Recruitment of Chromatin Modifying and General Transcription Factors to the IFN-β Promoter. *Cell*. 2000;103(4):667-678. doi:10.1016/S0092-8674(00)00169-0

227. Konno H, Konno K, Barber GN. Cyclic Dinucleotides Trigger ULK1 (ATG1) Phosphorylation of STING to Prevent Sustained Innate Immune Signaling. *Cell*. 2013;155(3):688-698. doi:10.1016/j.cell.2013.09.049

228. Prabakaran T, Bodda C, Krapp C, et al. Attenuation of cGAS-STING signaling is mediated by a p62/SQSTM1-dependent autophagy pathway activated by TBK1. *EMBO J*. 2018;37(8). doi:10.15252/embj.201797858

229. Motwani M, Pesiridis S, Fitzgerald KA. DNA sensing by the cGAS–STING pathway in health and disease. *Nat Rev Genet*. Published online July 29, 2019:1-18. doi:10.1038/s41576-019-0151-1

230. Schneider WM, Chevillotte MD, Rice CM. Interferon-Stimulated Genes: A Complex Web of Host Defenses. *Annu Rev Immunol*. 2014;32(1):513-545. doi:10.1146/annurev-immunol-032713-120231

231. Schoggins JW, Wilson SJ, Panis M, et al. A diverse range of gene products are effectors of the type I interferon antiviral response. *Nature*. 2011;472(7344):481-485. doi:10.1038/nature09907

232. Abe T, Barber GN. Cytosolic-DNA-Mediated, STING-Dependent Proinflammatory Gene Induction Necessitates Canonical NF-κB Activation through TBK1. *J Virol*. 2014;88(10):5328-5341. doi:10.1128/JVI.00037-14

233. Fitzgerald KA, McWhirter SM, Faia KL, et al. IKKε and TBK1 are essential components of the IRF3 signaling pathway. *Nat Immunol*. 2003;4(5):491-496. doi:10.1038/ni921

234. Fang R, Wang C, Jiang Q, et al. NEMO–IKKβ Are Essential for IRF3 and NF-κB Activation in the cGAS–STING Pathway. *J Immunol*. 2017;199(9):3222-3233. doi:10.4049/jimmunol.1700699

235. Ahn J, Barber GN. Self-DNA, STING-dependent signaling and the origins of autoinflammatory disease. *Curr Opin Immunol*. 2014;31:121-126. doi:10.1016/j.coi.2014.10.009

236. Gao D, Wu J, Wu Y-T, et al. Cyclic GMP-AMP Synthase Is an Innate Immune Sensor of HIV and Other Retroviruses. *Science*. 2013;341(6148):903-906. doi:10.1126/science.1240933

237. Li X-D, Wu J, Gao D, Wang H, Sun L, Chen ZJ. Pivotal Roles of cGAS-cGAMP Signaling in Antiviral Defense and Immune Adjuvant Effects. *Science*. 2013;341(6152):1390-1394. doi:10.1126/science.1244040

238. Lahaye X, Satoh T, Gentili M, et al. The Capsids of HIV-1 and HIV-2 Determine Immune Detection of the Viral cDNA by the Innate Sensor cGAS in Dendritic Cells. *Immunity*. 2013;39(6):1132-1142. doi:10.1016/j.immuni.2013.11.002

239. Schoggins JW, MacDuff DA, Imanaka N, et al. Pan-viral specificity of IFN-induced genes reveals new roles for cGAS in innate immunity. *Nature*. 2014;505(7485):691-695. doi:10.1038/nature12862

240. Burdette DL, Monroe KM, Sotelo-Troha K, et al. STING is a direct innate immune sensor of cyclic di-GMP. *Nature*. 2011;478(7370):515-518. doi:10.1038/nature10429

241. Woodward JJ, Iavarone AT, Portnoy DA. c-di-AMP Secreted by Intracellular Listeria monocytogenes Activates a Host Type I Interferon Response. *Science*. 2010;328(5986):1703-1705. doi:10.1126/science.1189801

242. Guimarães ES, Gomes MTR, Campos PC, et al. *Brucella abortus* Cyclic Dinucleotides Trigger STING-Dependent Unfolded Protein Response That Favors Bacterial Replication. *J Immunol*. 2019;202(9):2671-2681. doi:10.4049/jimmunol.1801233

243. Barker JR, Koestler BJ, Carpenter VK, et al. STING-Dependent Recognition of Cyclic di-AMP Mediates Type I Interferon Responses during Chlamydia trachomatis Infection. *mBio*. 2013;4(3):e00018-13. doi:10.1128/mBio.00018-13

244. Schwartz KT, Carleton JD, Quillin SJ, Rollins SD, Portnoy DA, Leber JH. Hyperinduction of Host Beta Interferon by a Listeria monocytogenes Strain Naturally Overexpressing the Multidrug Efflux Pump MdrT. *Infect Immun*. 2012;80(4):1537-1545. doi:10.1128/IAI.06286-11

245. Hansen K, Prabakaran T, Laustsen A, et al. Listeria monocytogenes induces IFNβ expression through an IFI16-, cGAS- and STING-dependent pathway. *EMBO J*. 2014;33(15):1654-1666. doi:10.15252/embj.201488029

246. Sauer J-D, Sotelo-Troha K, Moltke J von, et al. The N-Ethyl-N-Nitrosourea-Induced Goldenticket Mouse Mutant Reveals an Essential Function of Sting in the In Vivo Interferon Response to Listeria monocytogenes and Cyclic Dinucleotides. *Infect Immun*. 2011;79(2):688-694. doi:10.1128/IAI.00999-10

247. Gaidt MM, Ebert TS, Chauhan D, et al. The DNA Inflammasome in Human Myeloid Cells Is Initiated by a STING-Cell Death Program Upstream of NLRP3. *Cell*. 2017;171(5):1110-1124.e18. doi:10.1016/j.cell.2017.09.039

248. Gulen MF, Koch U, Haag SM, et al. Signalling strength determines proapoptotic functions of STING. *Nat Commun*. 2017;8(1):1-10. doi:10.1038/s41467-017-00573-w

249. Cerboni S, Jeremiah N, Gentili M, et al. Intrinsic antiproliferative activity of the innate sensor STING in T lymphocytes. *J Exp Med*. 2017;214(6):1769-1785. doi:10.1084/jem.20161674

250. Tang C-HA, Zundell JA, Ranatunga S, et al. Agonist-Mediated Activation of STING Induces Apoptosis in Malignant B Cells. *Cancer Res*. 2016;76(8):2137-2152. doi:10.1158/0008-5472.CAN-15-1885

251. Larkin B, Ilyukha V, Sorokin M, Buzdin A, Vannier E, Poltorak A. Cutting Edge: Activation of STING in T Cells Induces Type I IFN Responses and Cell Death. *J Immunol Baltim Md 1950*. 2017;199(2):397-402. doi:10.4049/jimmunol.1601999

252. Wu J, Chen Y-J, Dobbs N, et al. STING-mediated disruption of calcium homeostasis chronically activates ER stress and primes T cell death. *J Exp Med*. 2019;216(4):867-883. doi:10.1084/jem.20182192

253. Brault M, Olsen TM, Martinez J, Stetson DB, Oberst A. Intracellular Nucleic Acid Sensing Triggers Necroptosis through Synergistic Type I IFN and TNF Signaling. *J Immunol*. 2018;200(8):2748-2756. doi:10.4049/jimmunol.1701492

254. Sarhan J, Liu BC, Muendlein HI, et al. Constitutive interferon signaling maintains critical threshold of MLKL expression to license necroptosis. *Cell Death Differ*. 2019;26(2):332-347. doi:10.1038/s41418-018-0122-7

255. Zeng L, Liu Y-P, Sha H, Chen H, Qi L, Smith JA. XBP-1 Couples Endoplasmic Reticulum Stress to Augmented IFN-β Induction via a cis-Acting Enhancer in Macrophages. *J Immunol*. 2010;185(4):2324-2330. doi:10.4049/jimmunol.0903052

256. Liu Y-P, Zeng L, Tian A, et al. Endoplasmic Reticulum Stress Regulates the Innate Immunity Critical Transcription Factor IRF3. *J Immunol*. 2012;189(9):4630-4639. doi:10.4049/jimmunol.1102737

257. Petrasek J, Iracheta-Vellve A, Csak T, et al. STING-IRF3 pathway links endoplasmic reticulum stress with hepatocyte apoptosis in early alcoholic liver disease. *Proc Natl Acad Sci*. 2013;110(41):16544-16549. doi:10.1073/pnas.1308331110

258. Gui X, Yang H, Li T, et al. Autophagy induction via STING trafficking is a primordial function of the cGAS pathway. *Nature*. 2019;567(7747):262-266. doi:10.1038/s41586-019-1006-9

259. Watson RO, Bell SL, MacDuff DA, et al. The Cytosolic Sensor cGAS Detects Mycobacterium tuberculosis DNA to Induce Type I Interferons and Activate Autophagy. *Cell Host Microbe*. 2015;17(6):811-819. doi:10.1016/j.chom.2015.05.004

260. Watson RO, Manzanillo PS, Cox JS. Extracellular M. tuberculosis DNA Targets Bacteria for Autophagy by Activating the Host DNA-Sensing Pathway. *Cell*. 2012;150(4):803-815. doi:10.1016/j.cell.2012.06.040

261. Henault J, Martinez J, Riggs JM, et al. Noncanonical Autophagy Is Required for Type I Interferon Secretion in Response to DNA-Immune Complexes. *Immunity*. 2012;37(6):986-997. doi:10.1016/j.immuni.2012.09.014

262. Gonugunta VK, Sakai T, Pokatayev V, et al. Trafficking-Mediated STING Degradation Requires Sorting to Acidified Endolysosomes and Can Be Targeted to Enhance Anti-tumor Response. *Cell Rep*. 2017;21(11):3234-3242. doi:10.1016/j.celrep.2017.11.061

263. Crow YJ. Type I interferonopathies: a novel set of inborn errors of immunity. *Ann N Y Acad Sci*. 2011;1238(1):91-98. doi:10.1111/j.1749-6632.2011.06220.x

264. Jeremiah N, Neven B, Gentili M, et al. Inherited STING-activating mutation underlies a familial inflammatory syndrome with lupus-like manifestations. *J Clin Invest*. 2014;124(12):5516-5520. doi:10.1172/JCI79100

265. Liu Y, Jesus AA, Marrero B, et al. Activated STING in a Vascular and Pulmonary Syndrome. *N Engl J Med*. 2014;371(6):507-518. doi:10.1056/NEJMoa1312625

266. Clarke SLN, Pellowe EJ, de Jesus AA, Goldbach-Mansky R, Hilliard TN, Ramanan AV. Interstitial Lung Disease Caused by STING-associated Vasculopathy with Onset in Infancy. *Am J Respir Crit Care Med*. 2016;194(5):639-642. doi:10.1164/rccm.201510-2102LE

267. Picard C, Thouvenin G, Kannengiesser C, et al. Severe Pulmonary Fibrosis as the First Manifestation of Interferonopathy (TMEM173 Mutation). *Chest*. 2016;150(3):e65-e71. doi:10.1016/j.chest.2016.02.682

268. König N, Fiehn C, Wolf C, et al. Familial chilblain lupus due to a gain-of-function mutation in STING. *Ann Rheum Dis*. 2017;76(2):468-472. doi:10.1136/annrheumdis-2016-209841

269. Rodero MP, Crow YJ. Type I interferon–mediated monogenic autoinflammation: The type I interferonopathies, a conceptual overview. *J Exp Med*. 2016;213(12):2527-2538. doi:10.1084/jem.20161596

270. Gray EE, Treuting PM, Woodward JJ, Stetson DB. Cutting Edge: cGAS Is Required for Lethal Autoimmune Disease in the Trex1-Deficient Mouse Model of Aicardi–Goutières Syndrome. *J Immunol*. 2015;195(5):1939-1943. doi:10.4049/jimmunol.1500969

271. Gall A, Treuting P, Elkon KB, et al. Autoimmunity Initiates in Nonhematopoietic Cells and Progresses via Lymphocytes in an Interferon-Dependent Autoimmune Disease. *Immunity*. 2012;36(1):120-131. doi:10.1016/j.immuni.2011.11.018

272. Mackenzie KJ, Carroll P, Lettice L, et al. Ribonuclease H2 mutations induce a cGAS/STING-dependent innate immune response. *EMBO J*. 2016;35(8):831-844. doi:10.15252/embj.201593339

273. Pokatayev V, Hasin N, Chon H, et al. RNase H2 catalytic core Aicardi-Goutières syndrome–related mutant invokes cGAS–STING innate immune-sensing pathway in mice. *J Exp Med*. 2016;213(3):329-336. doi:10.1084/jem.20151464

274. Gao D, Li T, Li X-D, et al. Activation of cyclic GMP-AMP synthase by self-DNA causes autoimmune diseases. *Proc Natl Acad Sci U S A*. 2015;112(42):E5699-5705. doi:10.1073/pnas.1516465112

275. Munoz J, Rodière M, Jeremiah N, et al. Stimulator of Interferon Genes-Associated Vasculopathy With Onset in Infancy: A Mimic of Childhood Granulomatosis With Polyangiitis. *JAMA Dermatol*. 2015;151(8):872-877. doi:10.1001/jamadermatol.2015.0251

276. Muller U, Steinhoff U, Reis LF, et al. Functional role of type I and type II interferons in antiviral defense. *Science*. 1994;264(5167):1918-1921. doi:10.1126/science.8009221

277. Bekisz J, Baron S, Balinsky C, Morrow A, Zoon KC. Antiproliferative Properties of Type I and Type II Interferon. *Pharm Basel Switz*. 2010;3(4):994-1015. doi:10.3390/ph3040994

278. González-Navajas JM, Lee J, David M, Raz E. Immunomodulatory functions of type I interferons. *Nat Rev Immunol*. 2012;12(2):125-135. doi:10.1038/nri3133

279. Tschurtschenthaler M, Wang J, Fricke C, et al. Type I interferon signalling in the intestinal epithelium affects Paneth cells, microbial ecology and epithelial regeneration. *Gut*. 2014;63(12):1921-1931. doi:10.1136/gutjnl-2013-305863

280. Katakura K, Lee J, Rachmilewitz D, Li G, Eckmann L, Raz E. Toll-like receptor 9-induced type I IFN protects mice from experimental colitis. *J Clin Invest*. 2005;115(3):695-702. doi:10.1172/JCI22996

281. Howell KJ, Kraiczy J, Nayak KM, et al. DNA Methylation and Transcription Patterns in Intestinal Epithelial Cells From Pediatric Patients With Inflammatory Bowel Diseases Differentiate Disease Subtypes and Associate With Outcome. *Gastroenterology*. 2018;154(3):585-598. doi:10.1053/j.gastro.2017.10.007

282. Ahn J, Son S, Oliveira SC, Barber GN. STING-Dependent Signaling Underlies IL-10 Controlled Inflammatory Colitis. *Cell Rep*. 2017;21(13):3873-3884. doi:10.1016/j.celrep.2017.11.101

283. Canesso MCC, Lemos L, Neves TC, et al. The cytosolic sensor STING is required for intestinal homeostasis and control of inflammation. *Mucosal Immunol*. 2018;11(3):820-834. doi:10.1038/mi.2017.88

284. Hu Q, Ren H, Li G, et al. STING-mediated intestinal barrier dysfunction contributes to lethal sepsis. *EBioMedicine*. 2019;41:497-508. doi:10.1016/j.ebiom.2019.02.055

285. Vidal K, Grosjean I, evillard JP, Gespach C, Kaiserlian D. Immortalization of mouse intestinal epithelial cells by the SV40-large T gene. Phenotypic and immune characterization of the MODE-K cell line. *J Immunol Methods*. 1993;166(1):63-73. doi:10.1016/0022-1759(93)90329-6

286. Lee A-H, Iwakoshi NN, Anderson KC, Glimcher LH. Proteasome inhibitors disrupt the unfolded protein response in myeloma cells. *Proc Natl Acad Sci*. 2003;100(17):9946-9951. doi:10.1073/pnas.1334037100

287. Sato T, Vries RG, Snippert HJ, et al. Single Lgr5 stem cells build crypt-villus structures in vitro without a mesenchymal niche. *Nature*. 2009;459(7244):262-265. doi:10.1038/nature07935

288. Sato T, Clevers H. Growing Self-Organizing Mini-Guts from a Single Intestinal Stem Cell: Mechanism and Applications. *Science*. 2013;340(6137):1190-1194. doi:10.1126/science.1234852

289. Yin X, Farin HF, van Es JH, Clevers H, Langer R, Karp JM. Niche-independent high-purity cultures of Lgr5+ intestinal stem cells and their progeny. *Nat Methods*. 2014;11(1):106-112. doi:10.1038/nmeth.2737

290. Fujii S, Suzuki K, Kawamoto A, et al. PGE2 is a direct and robust mediator of anion/fluid secretion by human intestinal epithelial cells. *Sci Rep*. 2016;6:36795. doi:10.1038/srep36795

291. Miyoshi H, Stappenbeck TS. In vitro expansion and genetic modification of gastrointestinal stem cells in spheroid culture. *Nat Protoc*. 2013;8(12):2471-2482. doi:10.1038/nprot.2013.153

292. Flowing Software. Accessed October 10, 2019. http://flowingsoftware.btk.fi/index.php?page=1

293. Lowry OH, Rosebrough NJ, Farr AL, Randall RJ. Protein measurement with the Folin phenol reagent. *J Biol Chem*. 1951;193(1):265-275.

294. Sorbara MT, Ellison LK, Ramjeet M, et al. The Protein ATG16L1 Suppresses Inflammatory Cytokines Induced by the Intracellular Sensors Nod1 and Nod2 in an Autophagy-Independent Manner. *Immunity*. 2013;39(5):858-873. doi:10.1016/j.immuni.2013.10.013

295. Chan B, Magalhães VG, Lemmermann NAW, et al. The murine cytomegalovirus M35 protein antagonizes type I IFN induction downstream of pattern recognition receptors by targeting NF-κB mediated transcription. *PLOS Pathog*. 2017;13(5):e1006382. doi:10.1371/journal.ppat.1006382

296. Brugiroux S, Beutler M, Pfann C, et al. Genome-guided design of a defined mouse microbiota that confers colonization resistance against Salmonella enterica serovar Typhimurium. *Nat Microbiol*. 2016;2(2):1-12. doi:10.1038/nmicrobiol.2016.215

297. Böck J. The role of ATG16L1 in chronic inflammatory bowel disease. Published online July 6, 2012. Accessed October 11, 2019. https://macau.uni-kiel.de/receive/dissertation_diss_00009057

298. Wirtz S, Neufert C, Weigmann B, Neurath MF. Chemically induced mouse models of intestinal inflammation. *Nat Protoc*. 2007;2(3):541-546. doi:10.1038/nprot.2007.41

299. Martin M. Cutadapt removes adapter sequences from high-throughput sequencing reads. *EMBnet.journal*. 2011;17(1):10-12. doi:10.14806/ej.17.1.200

300. Trapnell C, Roberts A, Goff L, et al. Differential gene and transcript expression analysis of RNA-seq experiments with TopHat and Cufflinks. *Nat Protoc*. 2012;7(3):562-578. doi:10.1038/nprot.2012.016

301. Anders S, Pyl PT, Huber W. HTSeq--a Python framework to work with high-throughput sequencing data. *Bioinforma Oxf Engl*. 2015;31(2):166-169. doi:10.1093/bioinformatics/btu638

302. Love MI, Huber W, Anders S. Moderated estimation of fold change and dispersion for RNA-seq data with DESeq2. *Genome Biol*. 2014;15(12):550. doi:10.1186/s13059-014-0550-8

303. Lu X, Masic A, Liu Q, Zhou Y. Regulation of influenza A virus induced CXCL-10 gene expression requires PI3K/Akt pathway and IRF3 transcription factor. *Mol Immunol*. 2011;48(12-13):1417-1423. doi:10.1016/j.molimm.2011.03.017

304. Foufelle F, Fromenty B. Role of endoplasmic reticulum stress in drug-induced toxicity. *Pharmacol Res Perspect*. 2016;4(1):e00211. doi:10.1002/prp2.211

305. Häsler R, Sheibani-Tezerji R, Sinha A, et al. Uncoupling of mucosal gene regulation, mRNA splicing and adherent microbiota signatures in inflammatory bowel disease. *Gut*. 2017;66(12):2087-2097. doi:10.1136/gutjnl-2016-311651

306. Martinon F, Chen X, Lee A-H, Glimcher LH. TLR activation of the transcription factor XBP1 regulates innate immune responses in macrophages. *Nat Immunol*. 2010;11(5):411-418. doi:10.1038/ni.1857

307. Marinho FV, Benmerzoug S, Oliveira SC, Ryffel B, Quesniaux VFJ. The Emerging Roles of STING in Bacterial Infections. *Trends Microbiol*. 2017;25(11):906-918. doi:10.1016/j.tim.2017.05.008

308. Cavlar T, Deimling T, Ablasser A, Hopfner K-P, Hornung V. Species-specific detection of the antiviral small-molecule compound CMA by STING. *EMBO J*. 2013;32(10):1440-1450. doi:10.1038/emboj.2013.86

309. Radoshevich L, Cossart P. *Listeria monocytogenes*: towards a complete picture of its physiology and pathogenesis. *Nat Rev Microbiol*. 2018;16(1):32-46. doi:10.1038/nrmicro.2017.126

310. Hu M-M, Yang Q, Xie X-Q, et al. Sumoylation Promotes the Stability of the DNA Sensor cGAS and the Adaptor STING to Regulate the Kinetics of Response to DNA Virus. *Immunity*. 2016;45(3):555-569. doi:10.1016/j.immuni.2016.08.014

311. Wang Y, Lian Q, Yang B, et al. TRIM30α Is a Negative-Feedback Regulator of the Intracellular DNA and DNA Virus-Triggered Response by Targeting STING. *PLOS Pathog*. 2015;11(6):e1005012. doi:10.1371/journal.ppat.1005012

312. Johansson MEV, Sjövall H, Hansson GC. The gastrointestinal mucus system in health and disease. *Nat Rev Gastroenterol Hepatol*. 2013;10(6):352-361. doi:10.1038/nrgastro.2013.35

313. Sato T, van Es JH, Snippert HJ, et al. Paneth cells constitute the niche for Lgr5 stem cells in intestinal crypts. *Nature*. 2011;469(7330):415-418. doi:10.1038/nature09637

314. Aden K, Bartsch K, Dahl J, et al. Epithelial RNase H2 Maintains Genome Integrity and Prevents Intestinal Tumorigenesis in Mice. *Gastroenterology*. 2019;156(1):145-159.e19. doi:10.1053/j.gastro.2018.09.047

315. Kotredes KP, Thomas B, Gamero AM. The Protective Role of Type I Interferons in the Gastrointestinal Tract. *Front Immunol*. 2017;8. doi:10.3389/fimmu.2017.00410

316. Wottawa F, Bordoni D, Baran N, Rosenstiel P, Aden K. The role of cGAS/STING in intestinal immunity. *Eur J Immunol*. 2021;51(4):785-797. doi:https://doi.org/10.1002/eji.202048777

317. King AP, Wilson JJ. Endoplasmic reticulum stress: an arising target for metal-based anticancer agents. *Chem Soc Rev*. Published online June 29, 2020. doi:10.1039/D0CS00259C

318. Cubillos-Ruiz JR, Bettigole SE, Glimcher LH. Tumorigenic and Immunosuppressive Effects of Endoplasmic Reticulum Stress in Cancer. *Cell*. 2017;168(4):692-706. doi:10.1016/j.cell.2016.12.004

319. Kubra K-T, Akhter MS, Uddin MA, Barabutis N. Unfolded protein response in cardiovascular disease. *Cell Signal*. 2020;73:109699. doi:10.1016/j.cellsig.2020.109699

320. Dandekar A, Mendez R, Zhang K. Cross Talk Between ER Stress, Oxidative Stress, and Inflammation in Health and Disease. In: Oslowski CM, ed. *Stress Responses: Methods and Protocols*. Methods in Molecular Biology. Springer; 2015:205-214. doi:10.1007/978-1-4939-2522-3_15

321. Engin F. ER stress and development of type 1 diabetes. *J Investig Med Off Publ Am Fed Clin Res*. 2016;64(1):2-6. doi:10.1097/JIM.0000000000000229

322. Schindler AJ, Schekman R. In vitro reconstitution of ER-stress induced ATF6 transport in COPII vesicles. *Proc Natl Acad Sci U S A*. 2009;106(42):17775-17780. doi:10.1073/pnas.0910342106

323. Zhang B, Nandakumar R, Reinert LS, et al. STEEP mediates STING ER exit and activation of signaling. *Nat Immunol*. 2020;21(8):868-879. doi:10.1038/s41590-020-0730-5

324. Lio C-WJ, McDonald B, Takahashi M, et al. cGAS-STING Signaling Regulates Initial Innate Control of Cytomegalovirus Infection. *J Virol*. 2016;90(17):7789-7797. doi:10.1128/JVI.01040-16

325. Piersma SJ, Poursine-Laurent J, Yang L, Barber GN, Parikh BA, Yokoyama WM. Virus infection is controlled by hematopoietic and stromal cell sensing of murine cytomegalovirus through STING. *eLife*. 2020;9. doi:10.7554/eLife.56882

326. Hoong BYD, Gan YH, Liu H, Chen ES. cGAS-STING pathway in oncogenesis and cancer therapeutics. *Oncotarget*. 2020;11(30):2930-2955. doi:10.18632/oncotarget.27673

327. Conlon J, Burdette DL, Sharma S, et al. Mouse, but not Human STING, Binds and Signals in Response to the Vascular Disrupting Agent 5,6-Dimethylxanthenone-4-Acetic Acid. *J Immunol*. 2013;190(10):5216-5225. doi:10.4049/jimmunol.1300097

328. Shih AY, Damm-Ganamet KL, Mirzadegan T. Dynamic Structural Differences between Human and Mouse STING Lead to Differing Sensitivity to DMXAA. *Biophys J*. 2018;114(1):32-39. doi:10.1016/j.bpj.2017.10.027

329. Ogawa E, Mukai K, Saito K, Arai H, Taguchi T. The binding of TBK1 to STING requires exocytic membrane traffic from the ER. *Biochem Biophys Res Commun*. 2018;503(1):138-145. doi:10.1016/j.bbrc.2018.05.199

330. NHS England, Medical Directorate. Medicines, Diagnostics and Personalised Medicine Unit, Graham E. Improving Outcomes through Personalised Medicine. Published online September 7, 2016. https://www.england.nhs.uk/wp-content/uploads/2016/09/improving-outcomes-personalised-medicine.pdf

331. Denson LA, Curran M, McGovern DPB, et al. Challenges in IBD Research: Precision Medicine. *Inflamm Bowel Dis*. 2019;25(Supplement_2):S31-S39. doi:10.1093/ibd/izz078